Novel functions of the cohesin accessory factor dPDS5 uncover a new meiotic checkpoint.

Raquel Alexandra Martinho dos Santos

Dissertation presented to obtain the Ph.D. degree in Biology

Instituto de Tecnologia Química e Biológica | Universidade Nova de Lisboa

Oeiras,
February, 2014

INSTITUTO
DE TECNOLOGIA
QUÍMICA E BIOLÓGICA
/UNL

Knowledge Creation

ITQB-UNL | Av. da República, 2780-157 Oeiras, Portugal
Tel (+351) 214 469 100 | Fax (+351) 214 411 277

www.itqb.unl.pt

Novel functions of the cohesin accessory factor dPDS5 uncover a new meiotic checkpoint.

Raquel Alexandra Martinho dos Santos

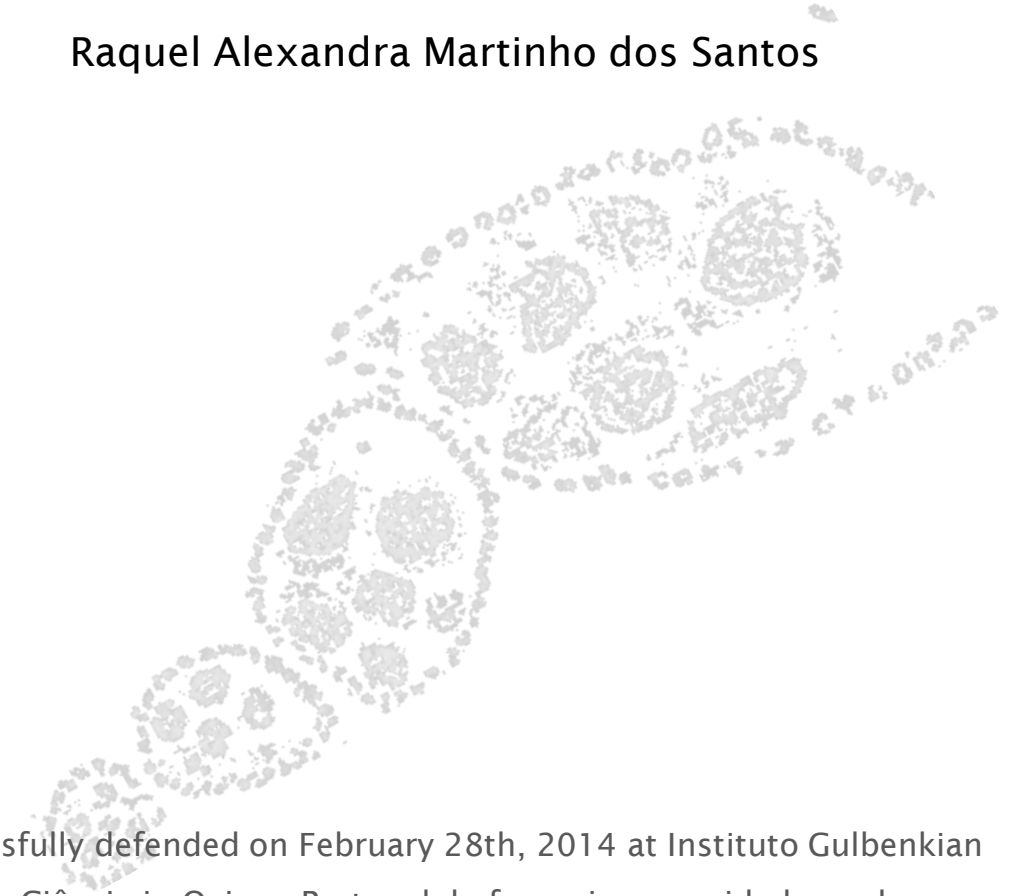

Sucessfully defended on February 28th, 2014 at Instituto Gulbenkian de Ciência in Oeiras, Portugal, before a jury presided over by:

Prof. Dr. Maria Arménia Abreu Fonseca de Carvalho Teixeira Carrondo

And Consisting of:

Dr. Rui Gonçalo Martinho
Dr. Catarina Cértima Homem
Dr. Florence Janody
Dr. Alisson Gontijo
Dr. J Élio Sucena
Dr. Vítor Barbosa

Declaração/Declaration

Esta dissertação é o resultado do meu próprio trabalho desenvolvido entre Março de 2010 e Setembro de 2013 no laboratório do Dr. Vítor Barbosa, Instituto Gulbenkian de Ciência em Oeiras, Portugal, no âmbito do Programa Gulbenkian de Doutoramento (edição 2009-2010). Parte deste trabalho encontra-se em preparação para ser publicado.

This dissertation is the result of my own research, carried out between March 2010 and September 2013 in the laboratory of Dr. Vítor Barbosa, Instituto Gulbenkian de Ciência in Oeiras, Portugal, under the Gulbenkian Doctoral Programme (2009-2010 edition). Part of this work in being prepared for publication.

Apoio Financeiro/Financial Support

Apoio financeiro da FCT e do FSE no âmbito do Quadro Comunitário de Apoio, bolsa de doutoramento #SFRH/BD/51183/2010, e projecto #FCT-PTDC/SAU-OBD/104522/2008.

Financial support for this thesis was provideed by the FCT and FSE through the *Quadro Comunitário de Apoio*, doctoral fellowship #SFRH/BD/51183/2010 and project grant #FCT-PTDC/SAU-OBD/104522/2008.

All images were treated in FIJI, and figures were made with Gimp and Inkscape. Statistical analysis were performed using R Software, unless otherwise stated.

Novel functions of the cohesin accessory factor dPDS5 uncover a new meiotic checkpoint.

Raquel Alexandra Martinho dos Santos

Dissertation presented to obtain the Ph.D. degree in Biology

Instituto de Tecnologia Química e Biológica | Universidade Nova de Lisboa

Research work coordinated by:

FUNDAÇÃO CALOUSTE GULBENKIAN
Instituto Gulbenkian de Ciência

Oeiras,
February, 2014

INSTITUTO
DE TECNOLOGIA
QUÍMICA E BIOLÓGICA
/UNL

Knowledge Creation

Acknowledgements

First and foremost, I would like to thank my family for their never ending support, guidance and love throughout, not only these last 4 years, but all of my life. Mom, Dad, Guida and Joana, no words can describe how proud and thankful I am to be part of our family, no matter how far apart we are.

To the IGC and the PIBS organizers for giving me the opportunity to continue my graduate studies. Since I started my Ph.D. until now the PIBS program has had two directors, Thiago Carvalho and Élio Sucena, without their support and guidance this journey would have been a bigger challenge. Also a big thank you is owed to Manuela Carvalho, for always being available to help us out with the bureaucracy and for much needed talks.

To everyone at the Meiosis and Development Lab, this was certainly an interesting ride. To my supervisor, Vítor Barbosa, I am grateful that he accepted me in his lab and for introducing me to the whole new world of *Drosophila* genetics. Also, for all the challenges that were set before me and that have helped me to evolve, both as a person and as a professional. To Patrícia Silva for the support, the long conversations and being a tireless companion in the dPDS5 project. To Triin Laos, who stayed the longest with me in the lab, for our philosophical conversations at lunch time, for our music mixes and volleyball afternoons, for the laughs and, above all, for the friendship and not thinking I was crazy. To Carla Morais and Basia Jezowska, for being awesome lab partners.

To my thesis committee, Miguel Godinho and Vasco Barreto, for the great advices and ideas they gave me, for listening to me and helping me keep my cool.

To Gastón Guilgur, Pedro Prudêncio and Paulo Navarro-Costa, for our "lab" meetings that were full of great science, sense of humour and food. You guys are the best! ☺

To the ladies, Tânia Ferreira, Marisa Oliveira, Catarina Brás-Pereira and Christen Mirth… thank you for all the support. You made it easier and kept me grounded.

To my favourite dorks for keeping me laughing and dancing.

To everyone at the Vasco da Gama Wing for providing a cool working environment. To all the participants of the Cell Cycle Club, the Fly Club and Chromatin Club for very profitable discussions. To the Fly Facility people, for helping me keep my flies alive. To my friends from my previous "lives", to whom I barely keep in touch with but that still support me.

A special shout-out to the two persons that read this Thesis from beginning to end: Paulo Navarro-Costa, for the constructive criticisms and dealing with my stressed out person, and my little sis that, for the second time, has read a thesis in a subject not at all similar to her own interests.

A sincere and heartfelt Thank You!!

Summary

Meiosis is a highly specialized type of cell division that is essential for sexual reproduction in all Eukaryotic species, where in two rounds of chromosome segregation take place without an intervening DNA replication phase (Petronczki et al., 2003). Genetic recombination during meiosis allows for the increase of genetic variability; furthermore, it is known that, at least in males, some level of chromatin reorganization occurs, such as histone displacement (White-Cooper and Davidson, 2011). Recombination requires the induction of endogenous Double Strand Breaks (DSBs), leading to the activation of a DNA Damage Response (DDR), that both recruits repair proteins and stalls the cell cycle until repair is completed (Harper and Elledge, 2007). Until now no surveillance pathway has been described that assures proper meiotic chromatin organization. In this work, we present evidence for the existence of such a surveying mechanism.

In the female germline of *Drosophila melanogaster*, induction of endogenous DSBs leads to the activation of the transducer kinase dATR. Persistent dATR activation, due to unrepaired DSBs, results in developmental defects, such as, defective condensation of the meiotic chromatin (karyosome) and loss of the dorsal-ventral polarity of the eggshell (Ghabrial and Schüpbach, 1999). Such phenotypes can be found in *dPds5* mutants, a cohesin accessory factor, and suggest a role for this protein during oogenesis (Barbosa et al., 2007). We show that these phenotypes are not dependent on dATR but instead dependent on dATM.

Using several dPDS5 transgenic lines, we show that this protein has a dynamic localization during the Prophase I arrest. dPDS5 nuclear foci are

present from stage 4 to stage 10 of oogenesis, do not co-localize with other cohesin related proteins, but with insulator protein foci. This co-localization is shown with three different insulator proteins, the accessory proteins CP190 and MOD(mdg4)2.2 and the DNA-binding protein BEAF32. Additionally, it is known that the clustering of different insulator proteins only happens in the presence of DNA and that it requires CP190 (Pai et al., 2004). Our work also shows that dPDS5 is differently required for the presence of CP190 and BEAF32 in the oocyte nucleus, which might imply a role for dPDS5 in nuclear organization. This CP190 phenotype is not checkpoint dependent, since it is not rescued in double mutants with the checkpoint effector protein *dChk2*.

The interaction between dPDS5 and insulator proteins raises the possibility that this protein could also regulate gene expression in the oocyte. By looking at the incorporation of an Uracil analogue, we show that the oocyte actively transcribes throughout mid-oogenesis, with a quiescent period during stage 5. This quiescent period corresponds to the appearance of insulator bodies and separates two phases of morphologically different transcription phases. Moreover, checkpoint activation delays the start of the second transcriptional phase.

Our results lead us to propose: 1) the existence of a new meiotic checkpoint that is dATM-dependent, and monitors chromatin dynamics; 2) that the Prophase I arrest is a dynamic process, due to the dynamics observed for the chromatin related proteins and for transcription; 3) the presence of additional genomic material aside from the hollow sphere of condensed chromatin (karyosome).

Sumário

A Meiose é um tipo de divisão celular especializada que é essencial para a reprodução sexuada de todas as espécies Eucarióticas, em que duas rondas de segregação cromossómica ocorrem sem uma fase de replicação de DNA interveniente (Petronczki et al., 2003) e que permite o aumento da variabilidade genética através da recombinação genética. Além disso, sabe-se que algum nível de reorganização da cromatina ocorre, pelo menos em machos com a substituição das histonas (White-Cooper and Davidson, 2011). Para que se dê recombinação é necessária a indução de quebras nos cromossomas emparelhados (*Double Strand Breaks* – DSBs), que levam à activação de uma resposta a danos no DNA (*DNA Damage Response* – DDR), que tanto recruta proteínas de reparação como bloqueia o ciclo celular até que o dano esteja reparado (Harper and Elledge, 2007). Até agora, não foi descrita nenhuma via que monitorize uma correcta organização da cromatina meiótica. Neste trabalho apresentamos evidências para existência de tal mecanismo de monitorização.

Na linha germinativa feminina de *Drosophila melanogaster*, a indução de DSBs endógenas leva à activação da quinase transdutora dATR. A activação persistente de dATR, devido a DBSs por reparar, resulta em defeitos no desenvolvimento, tais como uma condensação anormal da cromatina meiótica (cariossoma) e a perda da polaridade dorsoventral do ovo (Ghabrial et al., 1998). Mutantes de *dPds5*, uma proteína acessória do complexo das coesinas, apresentam estes fenótipos e sugerem uma função para esta proteína durante a oogénese (Barbosa et al., 2007). O nosso trabalho mostra que estes fenótipos não são dependentes de dATR, mas sim de dATM.

Através do uso de várias linhas transgénicas de dPDS5, mostramos que esta proteína tem uma localização dinâmica durante a pausa da Prófase I. Foci nucleares de dPDS5 são visiveís do estádio 4 a 10 da oogénese, não co-localizam com nenhuma outra proteína relacionada com as coesinas, mas com foci de proteínas isoladoras (*insulator proteins*). Esta co-localização é demonstrada para três proteínas isoladoras, as proteínas acessórias CP190 e MOD(mdg4)2.2 e a proteína de ligação ao DNA BEAF32. Sabe-se que o agrupamento de diferentes proteínas isoladoras apenas ocorre na presença de DNA e requere CP190 (Pai et al., 2004). O nosso trabalho revela que dPDS5 é necessário de modo diferente para o recrutamento de CP190 e BEAF32 no núcleo do oócito. O fenótipo de CP190 não é dependente da activação da DDR, uma vez que não é resgatado em mutantes duplos com a quinase efectora *dChk2*.

A interacção de dPDS5 com as proteínas isoladoras levanta a possibilidade desta proteína também regular a expressão génetica do oócito. Usando a incorporação de um análogo de Uracilo, demonstramos que o oócito transcreve durante a oogénese com um periodo quiescente no estádio 5. Este período quiescente corresponde ao aparecimento dos *insulator bodies* e separa dois períodos de transcrição morfológicamente diferentes. Além do mais, o início do segundo período de transcrição é atrasado devido à activação da DDR.

Os nossos resultados levam-nos a propôr: 1) a existência de uma nova DDR meiótica que depende de dATM e monitoriza a dinâmica da cromatina; 2) que a pausa da Prófase I é, de facto, um evento dinâmico, devido à dinâmica observada para proteínas relacionadas com a cromatina e da própria transcrição; 3) a presença de material genómico além esfera oca de cromatina condensada (cariossoma).

Table of Contents

Acknowledgements V

Summary VII

Sumário IX

Table of Contents XI

1 Introduction 1

1.1 Meiosis, the foundation of sexual reproduction 1

1.2 Drosophila oogenesis, a model to study meiosis 7

1.3 The Cohesin Accessory Protein PDS5 11

1.4 The DNA Damage Response during Drosophila oogenesis 12

1.5 The Cohesin Complex 14

1.6 Drosophila Chromatin Insulators 19

1.7 Objectives of this work 21

2 dPDS5 is an insulator protein 23

Summary 23

2.1 Introduction 24

2.2 Material and Methods 26

2.3 Results 30

2.4 Discussion 39

2.5 Supplemental Material 43

3 dPDS5 is required for insulator body assembly in the oocyte nucleus 45

Summary 45

3.1 Introduction 46

3.2 Material and Methods 49

3.3 Results 53

3.4 Discussion 66
3.5 Supplemental Material 70
4 A new dATM-dependent checkpoint monitors dPDS5 during oogenesis 77
Summary 77
4.1 Introduction 78
4.2 Material and Methods 80
4.3 Results 82
4.4 Discussion 86
4.5 Supplemental Material 92
5 Final Discussion and Concluding Remarks 93
5.1 dPDS5 is required for nuclear organization during oogenesis 93
5.2 A new meiotic dATM-dependent checkpoint 97
5.3 Concluding Remarks 100
References 101
Abbreviation List 111

1 Introduction

1.1 Meiosis, the foundation of sexual reproduction

The advent of sexual reproduction, is likely to have played fundamental role in the success of the Eukaryotes. At its core is a specialized type of cell division known as Meiosis, where one round of DNA replication is followed by two rounds of chromosome segregation without an intervening S-phase (Figure 1.1) (Petronczki et al., 2003; Tsai and McKee, 2011). This results in the production of haploid gametes, thereby allowing for ploidy maintenance across generations. In addition, it also promotes the increase of offspring diversity through the random segregation of chromosomes and, mainly, by the occurrence of genetic recombination between parental homologous chromosomes (Figure 1.1) (Yanowitz, 2010).

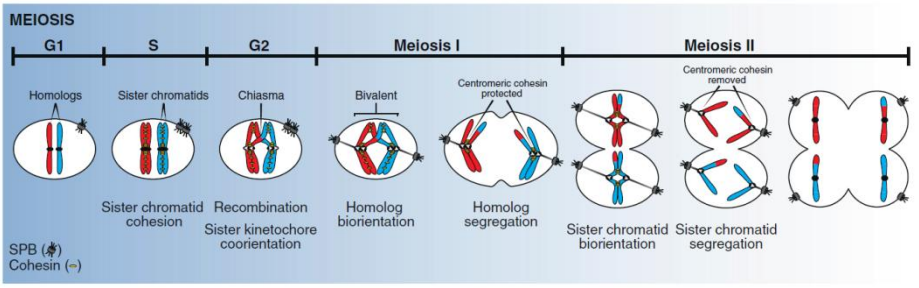

Figure 1.1 – General scheme of meiosis. During the pre-meiotic S-phase cohesin complexes are loaded onto chromosomes, allowing for synaptonemal complex (SC) assembly between homologous chromosomes, later during prophase I. Recombination also occurs during prophase I, leading to the formation of chiasmata. These will maintain the homologous chromosomes physically linked upon SC disassembly. During meiosis I, the homologous chromosomes bi-orient, in such a way that the pairs of sister kinetochores attach to microtubules emanating from the same pole. Also during meiosis I, cohesin is removed from the chromosome arms, while centromeric cohesin is protected, leading to the segregation of the homologous chromosomes. During meiosis II, centromeric cohesin is removed and sister chromatids segregate as in mitosis.

Meiosis can be seen as a two-step process. In the first one, commonly designated meiosis I (reductional division), homologous chromosomes separate and in the second step, meiosis II (equational division), the sister chromatids segregate in a manner similar to mitosis (Figure 1.1 and Figure 1.2) (Ivanovska and Orr-Weaver, 2006). Meiosis initiates with prophase I, which encompasses several events namely, homologous chromosome pairing, synapsis, Double Strand Break (DSB) induction and repair, chiasmata formation and chromosome condensation (Tsai and McKee, 2011). Prophase I can be divided into five stages based on chromosome morphology and the extent of their pairing and synapses: (1) Leptotene: the individual chromosome can be seen as thin strands that initially are not aligned; (2) Zygotene: the homologous chromosomes are paired, Synaptonemal Complex (SC) assembly and recombination are initiated; (3) Pachytene: SC assembly is complete, recombination is resolved and the chromosomes are synapsed; (4) Diplotene: the SC disassembles and the chiasmata, the physical linkages between the chromosomes, become visible, the individual chromosomes start to become perceptible; (5) Diakinesis: the chromosomes undergo a final stage of de-condensation (Figure 1.2) (Ivanovska and Orr-Weaver, 2006; Tsai and McKee, 2011).

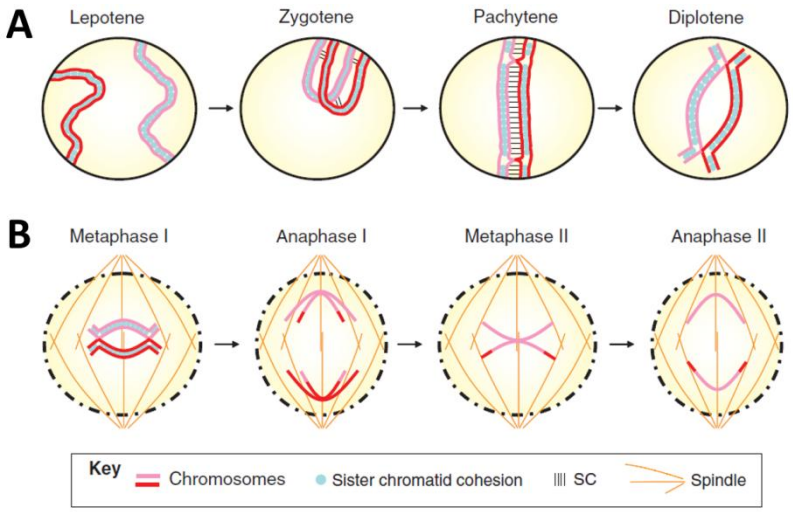

Figure 1.2 – Schematic representation of meiosis. (A) Initial stages of prophase I: during leptotene, the telomeres of the individual chromosomes bind to the nuclear envelope and the chromosomes initiate pairing through their homologous sequences; in zygotene, chromosomes initiate synapsis, taking a typical bouquet conformation (that is absent in *Drosophila melanogaster*); in pachytene, mature bivalents are obtained when the chromosomes become fully synapsed; during diplotene, upon the completion of recombination the SC is disassembled. (B) Representation of the two chromosome segregation steps that take place during meiosis: during metaphase I the paired homologous chromosomes align at the metaphase plate, being segregated during anaphase I; during metaphase II the sister chromatids line up at the metaphase plate and segregate to opposite poles with the onset of anaphase II (for simplicity only one pair of sister chromatids is showed). Where: one pair of homologous chromosomes is represented in pink and red lines. Taken from: (Tsai and McKee, 2011).

1.1.1 The Synaptonemal Complex and Genetic Recombination

Proper segregation of the homologous chromosomes after meiosis I, but not of sister chromatids after meiosis I, requires that the chromosomes are properly paired with their respective homologue. This process is initiated at zygotene of prophase I when Synaptonemal Complex (SC) assembly between homologous begins. The SC is a tripartite proteinaceous complex that forms an elaborate zipper-like structure that connects the aligned chromosomes along

their entire length (Carpenter, 1975; Manheim and McKim, 2003; Tsai and McKee, 2011). The SC allows the homologous chromosomes to stabilize their association during the initial stages of meiosis until diplotene, when SC disassembles and the chromosomes are joined only by the chiasmata (Lake and Hawley, 2012). The structure of this complex is fairly conserved between species, although sequence similarity of its components is low between organisms. It consists of two lateral elements (LEs) and a central region (CR), which contains the central element (CE) and the transverse filament (TF). The CE is connected to the LEs by the TF, which runs perpendicularly to the LEs (Figure 1.3) (Lake and Hawley, 2012; Tsai and McKee, 2011). LEs formation initiates once pre-meiotic DNA replication is completed with the loading of the Axial Elements (AEs) onto the chromosome cores (the scaffold established by the shortening of paired sister chromatids along their longitudinal axes) (Lake and Hawley, 2012). During *Drosophila melanogaster* (*Drosophila*) oogenesis, the AEs load onto sister chromatids through their localization with the cohesin proteins dSMC1 and dSMC3. Furthermore, AEs formation also depends on non-SMC proteins such as the Orientation Disruptor (ORD) and Crossover Suppressor on 2 of Manheim (C(2)M) AEs/LEs proteins and the cohesin-loading factor NIPPED-B, since mutations in any of these proteins either results in the inability to form chromosome cores or even to assemble the SC (Lake and Hawley, 2012).

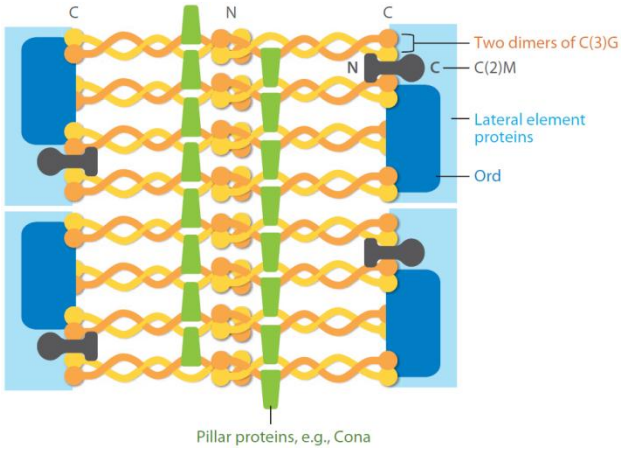

Figure 1.3 – Schematic representation of the Synaptonemal Complex in *Drosophila melanogaster* oocytes. The SC is composed of two LEs (C(2)M and ORD) and a CR containing both the TFs (C(3)G) and the CE (Corona/CONA). The chromosome core is formed after completion of pre-meiotic DNA replication and loading of the protein Orientation Disruptor (ORD) together with the cohesin complex core proteins dSMC1 and dSMC3 and the cohesion accessory protein NIPPED-B (not shown). Chromosome core formation requires the AE/L element C(2)M. Taken from: (Lake and Hawley, 2012).

In addition to stabilizing homologous chromosome pairing, the SC appears to be required for the maturation of DSBs into crossovers (Carpenter, 1975; Manheim and McKim, 2003). In mutants for SC components, either homologous pairing is affected such as upon loss of *ord* and *c(3)g*, or the number of occurring crossovers is greatly reduced as in *c(2)m* and *cona* mutants (Lake and Hawley, 2012; Yanowitz, 2010). These data imply a role for the SC in homologous recombination. This distinctive feature of meiosis takes place during pachytene and is dependent on the induction and subsequent repair of DSBs, through the activity of the highly conserved Sporulation-Specific Protein 11 (SPO11), a type II topoisomerase-like protein (Keeney, 2008; Lake and Hawley, 2012). In all species studied, DSB induction is considered to be a highly regulated process both in terms of timing and

number, and in addition to SPO11, appears to require the action of other proteins. However, very little is known about the actual mechanism that controls DSB formation (Lake and Hawley, 2012). Upon DSB induction, SPO11 is removed and breaks are resected by the MRE11-RAD50-NBS1 (MRN) complex, which forms 3'-single-stranded overhangs of approximately 300 nucleotides long. These overhangs are then coated with proteins from the RecA family, forming nucleoprotein filaments that will catalyze strand invasion to find a repair template. Meiotic DSBs can be repaired either through the formation of crossovers, in which a reciprocal exchange between the two chromosome arms surrounding the break occurs taking the appearance of a chiasma, or of non-crossovers, without the occurrence of exchange (Figure 1.4) (Keeney, 2008; Tsai and McKee, 2011).

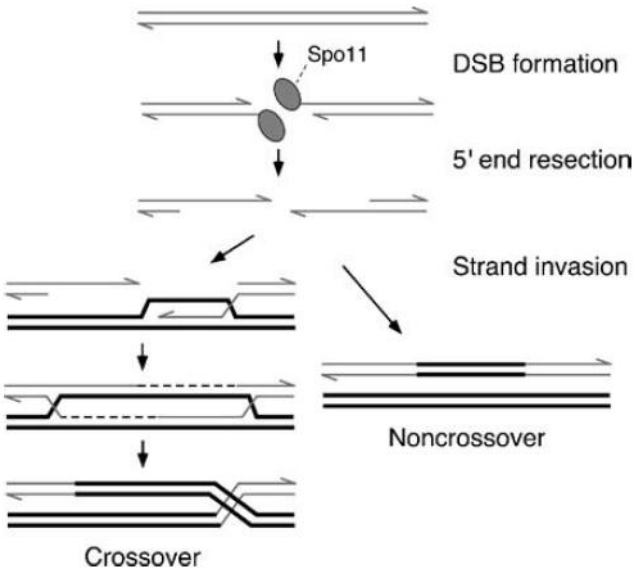

Figure 1.4 – Overview of meiotic recombination in *Saccharomyces cerevisae*. Only two sister chromatids from each homolog are shown and all proteins with the exception of SPO11 are omitted. Taken from: (Keeney, 2008).

As a crucial developmental program for all sexually reproducing species, meiosis is a tightly regulated cellular event under the surveillance of several checkpoint pathways. The work presented in this thesis aimed at increasing our understanding of the proteins and monitoring mechanisms that control meiosis.

1.2 Drosophila *oogenesis, a model to study meiosis*

The *Drosophila* ovary is composed of 16 to 20 ovarioles, each consisting of a chain of sequentially more mature egg chambers (ovarian follicles), making it an ideal model to study egg development and meiosis (Figure 1.5A) (Ashburner et al., 2005; Lake and Hawley, 2012; Spradling, 1993).

Oogenesis is initiated in the germarium, located at the anterior of the ovariole. The germarium can be divided into four regions from anterior to posterior: region 1, at the anterior-most, comprises the germline stem cells and the initial stages of germ cell differentiation; in region 2A, oocyte fate starts to be determined and meiosis is initiated; in region 2B, the oocyte is fully specified and the somatic covering of the egg chamber begins to be assembled; and in region 3 the egg chamber is fully formed (Figure 1.5B).

At the anterior of the germarium, a germline stem cell (GSC) suffers an asymmetric mitotic division, giving rise to another GSC and a cystoblast that will progress through germ cell differentiation. The cystoblast undergoes four synchronized mitotic divisions with incomplete cytokinesis, producing a cyst of sixteen interconnected germ cells (GCs). These sixteen GCs share the same cytoplasm and go through pre-meiotic S-phase synchronously. In region 2A, up to four GCs initiate SC assembly entering zygotene of prophase I. Of the four

GCs that initiate meiosis only two complete SC assembly (pro-oocytes) and enter pachytene. It is also in region 2A that the endogenous DSBs are induced and repaired, promoting genetic recombination (Figure 1.5BC). By region 2B, one of the pro-oocytes has already been selected as the female gametogenic cell (the oocyte) and the remaining fifteen GCs acquire a supporting role for oocyte development [nurse cells (NCs)]. In this region, the germ cell cyst begins to be enveloped by a monolayer of somatic cells [follicle cells (FCs)] via the action of the follicle stem cells. In region 3, the oocyte is in mid-pachytene and all sixteen GCs of a cyst have been completely surrounded by FCs, thus forming a spherical egg chamber (stage 1 egg chamber) (Figure 1.5B) (Ashburner et al., 2005; Spradling, 1993).

Based on morphological characteristics, egg chamber development has been divided into 14 stages, with stage 1 corresponding to region 3 of the germarium and stage 14 to mature oocytes (King, 1970). As the egg chamber leaves the germarium and progresses through development, the oocyte chromosomes condense into a sphere of meiotic chromatin known as the karyosome. This structure forms at stages 3-4, concomitantly with the disassembly of the SC that eventually disappears by stages 6-7. At these stages the oocyte nucleus is already arrested in a diplotene-like state, also known as the prophase I arrest (Figure 1.5A) (Ashburner et al., 2005; Spradling, 1993). While this dramatic remodelling of the oocyte's chromatin occurs, the NCs enter an endoreplicative cell cycle, suffering several rounds of DNA replication without an intervening M-phase (thus becoming polyploid). Starting at stage 10, proteins and mRNAs produced in the NCs start to be actively transferred into the oocyte, in a process known as "dumping". The oocyte remains arrested in prophase I until stage 13, when it goes through prometaphase I. This results in nuclear envelope breakdown and in the assembly of the meiotic

spindle. Once metaphase I is achieved at stage 14, oocyte development arrests for a second time. This arrest is lifted and meiosis is completed once the mature egg goes through the oviduct (Ashburner et al., 2005; Spradling, 1993).

An important step of egg development is the establishment of the dorsal-ventral polarity of the eggshell. This developmental process depends on the activity of the GURKEN (GRK) protein and takes place between stage 9 to 12 of oogenesis (Cooperstock and Lipshitz, 2001; Spradling, 1993). GRK is a transforming factor growth factor-α (TGF-α) homolog that acts as a ligand for the Epidermal Growth Factor Receptor (EGFR), which is present on the FCs that surround the oocyte (Cooperstock and Lipshitz, 2001). During stage 7/8 of oogenesis the oocyte localizes to the anterior-dorsal end of the oocyte and starts to synthesize Grk mRNA. From stage 9 to stage 12, the GRK protein is translated in the cytoplasmatic region proximal to the oocyte, allowing for the establishment of the dorsal region of the future egg. Proper establishment of the dorsal-ventral axis of the egg results in the appearance of two dorsal appendages in the eggshell. In previous stages (1 to 7) this protein is also required to specify the anterior-posterior axis of the egg (Cooperstock and Lipshitz, 2001; Spradling, 1993).

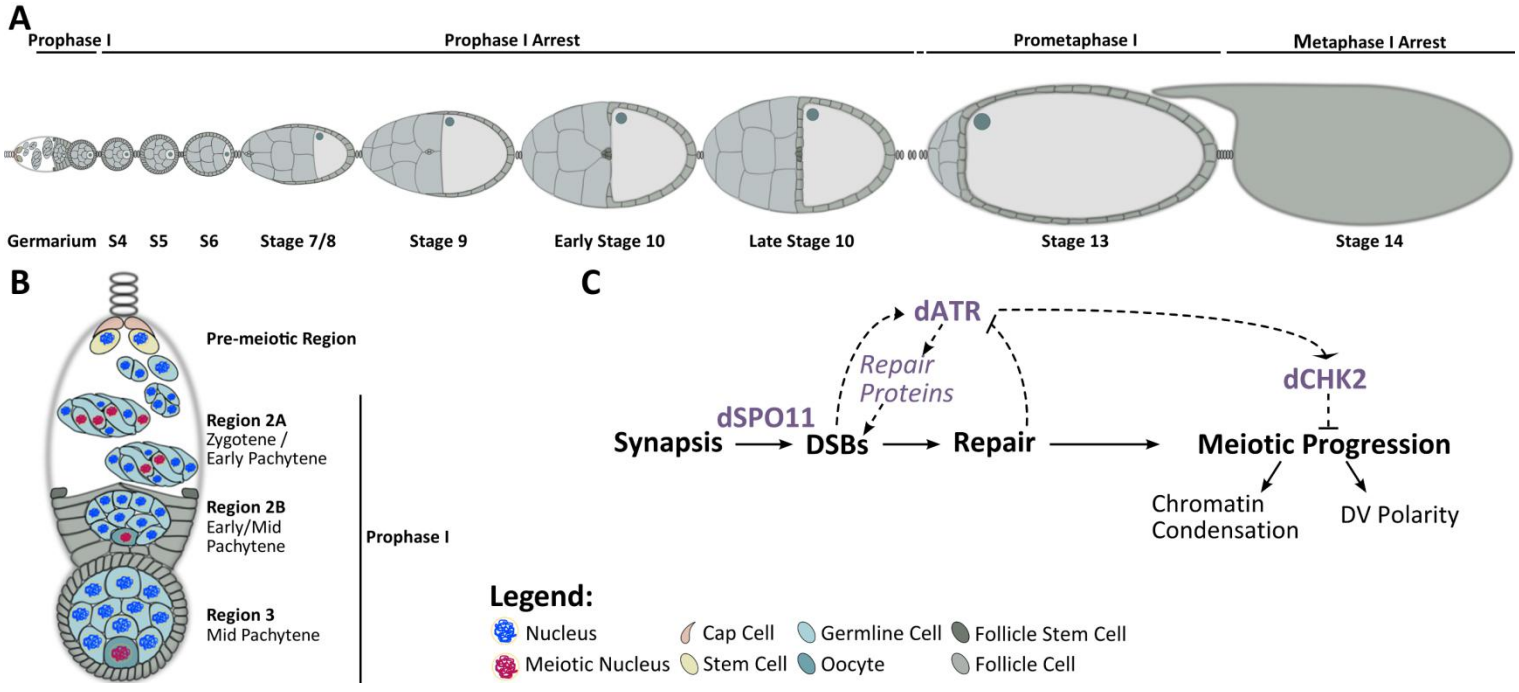

Figure 1.5 – *Drosophila* oogenesis.(A) Schematic representation of an ovariole with a germarium at the anterior (left) and a mature egg, stage 14, at the posterior (right), (Ashburner et al., 2005). Above the ovariole are indicated the corresponding stages of meiosis at which the oocyte is in given egg chamber development. (B) A detailed scheme of the germarium, with special emphasis on the process of oocyte specification. (C) Schematic representation of the canonical meiotic checkpoint that depends on dATR and takes place between region 2A and 2B of the germarium.

1.3 The Cohesin Accessory Protein PDS5

PDS5 is a highly conserved cohesin complex (section 1.5) accessory protein composed mostly of HEAT repeats (Figure 3.1) that, depending on the cell cycle stage, can either be involved in the unloading of cohesin from chromatin or be required for cohesion establishment and/or maintenance. PDS5 has been shown to be recruited to the cohesin complex through the interaction with the N-terminus of its α-kleisin subunit, in close proximity to the interacting sites between RAD21 and SMC3 (Chan et al., 2013). By interacting with RAD21 at its N-terminus, PDS5 promotes both SMC3 acetylation by ECO1 and protects SMC3 from de-acetylation by HDAC8, effectively promoting cohesion maintenance (Chan et al., 2012; Nasmyth and Haering, 2009; Vaur et al., 2012). Also, by docking to cohesin in proximity to the RAD21-SMC3 interface, PDS5 promotes cohesin release from chromatin, since the turnover of this complex increases in mutants unable to bind PDS5 to RAD21 (Chan et al., 2013). This latter function of PDS5 in cohesion "anti-establishment" requires the interaction of PDS5 with WAPL (Kueng et al., 2006; Remeseiro et al., 2013).

PDS5 has also been found to have functions during meiosis in yeast, where it co-localizes to chromosomes with the meiotic specific α-kleisin subunit REC8. However, REC8 loading does not depend on PDS5 and sister chromatid cohesion is weakly affected in *pds5* mutants (Jin et al., 2009). Nonetheless, meiotic phenotypes are present in *pds5* mutants, namely the occurrence of synapsis between sister chromatids instead of homologous chromosomes, inefficient repair of endogenous DSBs and meiotic chromosome hypercondensation (Jin et al., 2009).

In *Drosophila*, dPDS5 has been shown to co-localize with cohesin on chromosomes and to be required for sister chromatid cohesion (Dorsett et al.,

2005; Gause et al., 2008). Furthermore, dPDS5 is involved in gene expression regulation, since a null *dPds5* mutant presents a slight decrease in the expression of *cut* at the wing margin (Dorsett et al., 2005). Moreover, dPDS5 appears to also have meiotic functions since mutation in these genes where found in a screen designed to identify genes involved in meiotic progression (Barbosa et al., 2007). This screen used has readouts two phenotypes associated to persistent meiotic checkpoint activation, defective GRK expression and/or localization with consequent eggshell ventralization, and karyosome fragmentation (Barbosa et al., 2007). By looking at C(3)G staining, the authors show that *dPds5* alleles effectively delay meiotic progression, since a percentage of stage 2 egg chambers still presented two C(3)G positive cells (Barbosa et al., 2007). In addition, dPDS5 was shown to be required upon DSBs, since double mutants for *dPds5* and *dSpo11* rescued the ventralization phenotype. However, this phenotype was not rescued in *dAtr; dPds5* double mutants. These results suggest that *dPds5* mutants are sensitive to DSBs but that they do not activate the dATR-dependent meiotic checkpoint (Barbosa et al., 2007).

1.4 The DNA Damage Response during Drosophila oogenesis

During *Drosophila* oogenesis, genetic recombination is initiated in region 2A of the germarium, after SC assembly, with the induction of programmed DSBs by dSPO11 (MEI-W68) (Ashburner et al., 2005; Lake and Hawley, 2012). The presence of DSBs leads to the activation of a DNA damage response (DDR), a signalling pathway that will both recruit repair proteins to the damaged sites and stall cell cycle progression until DNA repair is completed (Harper and Elledge, 2007).

Two main transducer kinases that belong to the PI3-like protein family have been described to participate in DSB repair related DNA Damage Responses (DDRs), namely Ataxia-Telangiectasia Mutated (ATM) and Ataxia Telangiectasia-Related (ATR) (Gospodinov and Herceg, 2013; Wood and Chen, 2008). These two proteins appear to share substrates, such as the histone variant H2 (H2A in yeast, H2Ax in mammals and H2Av in *Drosophila*), that is phosphorylated upon damage. This post-translational modification is important both for the recruitment/docking of repair proteins to the DSBs and for signalling of incomplete repair (Gospodinov and Herceg, 2013; Polo and Jackson, 2011). H2Ax is rapidly phosphorylated (γH2Ax) upon DNA damage, initially by the ATM and later by the ATR transducer kinases, appearing as nuclear foci at DSB sites (Price and D'Andrea, 2013; Wood and Chen, 2008). Consequently, the phosphorylation of the *Drosophila* homologue H2Av (γH2Av) has traditionally been used as a marker for DSBs. Using an antibody against γH2Av and counting the visible foci, DSBs have been shown to be induced in region 2A and to increase in number as the cysts progress through it; in region 2B, the number of DSBs starts to diminish and these eventually disappear when the cyst reaches region 3. Consequently, the dynamic behaviour of the γH2Av foci has been considered to likely represent the process of DSB induction and subsequent repair (Lake and Hawley, 2012; Mehrotra and McKim, 2006).

In order to ensure that the meiotic DNA lesions are repaired, a DDR is in place. This mechanism arrests meiotic progression until DSBs are resolved. The canonical meiotic DNA damage checkpoint is dependent on the activation of the transducer kinase dATR (MEI-41) and subsequent activation of the effector kinase dCHK2 (MNK) (Figure 1.5C) (Abdu et al., 2002; Ghabrial and Schüpbach, 1999). Inability to repair the meiotic DSBs results in the persistent activation

of these kinases, as can be seen in mutants for repair genes such has *dRad51 (spn-A)*, *dRad54 (okr)*, *spn-B* or *spn-D* (Ghabrial et al., 1998; Staeva-Vieira et al., 2003). This continual activation of dCHK2 leads to defects both in the organization of the meiotic chromatin (through the suppression of the activity of the kinase NHK-1), and in the establishment of the dorsal-ventral polarity of the eggshell (due to the inadequate redistribution and translation of the GRK morphogen) (Ghabrial and Schüpbach, 1999; Lancaster et al., 2010). Another marker of persistent checkpoint activation is the permanence of γH2Av foci beyond region 2B of the germarium (Mehrotra and McKim, 2006).

At the time this work was initiated, dATM (TEFU) had not been described to have functions during oogenesis. Nonetheless, recent work from the McKim lab has suggested that while dATM phosphorylates H2Av redundantly with dATR, the former kinase is not required for the activation of the meiotic checkpoint *per se*. However, it appears to be involved in the actual repair process through the regulation of occurring DSBs (Joyce et al., 2011).

1.5 The Cohesin Complex

The Cohesin Complex has been described to have important functions in sister chromatid cohesion, DNA repair and transcription regulation (Dorsett and Ström, 2012; Nasmyth and Haering, 2009).

At its core the cohesin complex is composed of two Structural Maintenance Chromosome proteins, SMC1 and SMC3, and two non-SMC proteins, the α-kleisin RAD21 (SCC1) and SCC3 (SA). The SMC subunits fold on themselves forming 50nm anti-parallel coiled coils, with the central aminoacids composing the “hinge” domain at one end and the N-terminal and C-terminal

aminoacids assembling in a globular ATPase "head" at the other end. SMC1 and SMC3 interact with each other through their hinge domains and their head domains are bridged by the interaction with the N-terminal and C-terminal domains of RAD21, creating a tripartite ring. SCC3 binds to the central region of RAD21 (Figure 1.6A). Taking into consideration this configuration, the most prevalent model for the establishment of sister chromatid cohesion is that the complex topologically encircles the chromatin fibers. The fact that the cohesin ring diameter can vary between 30 to 35nm and that its rupture by SEPARASE results in loss of sister chromatid cohesion further supports this model (Dorsett and Ström, 2012; Nasmyth and Haering, 2009; Remeseiro and Losada, 2013).

Cohesin loading/unloading onto chromatin, as well as, cohesion establishment require the assistance of additional proteins, usually known as cohesin accessory factors. Cohesin loading is initiated during telophase, but occurs in its earnest during interphase. It depends on ATP hydrolysis, on a complex composed of NIPPED-B (SCC2) and SCC4, known as the kollerin complex, and it appears to occur through the opening of the SMC1-SMC3 hinge domain. The sites where loading takes place are still not fully clear, however, in *Drosophila,* NIPPED-B and cohesin are found at active transcription sites (Dorsett and Ström, 2012; Nasmyth, 2011; Remeseiro and Losada, 2013). During G1-phase, cohesin is dynamically bound to DNA, being loaded by kollerin and released by WAPL together with PDS5 (that form the releasin complex). The destabilising action of the releasin complex has also been called "anti-establishment" (Kueng et al., 2006; Remeseiro and Losada, 2013). Cohesion establishment only occurs during S-phase, after DNA replication. For cohesin to become cohesive it requires the action of the cohesin acetyltransferase ECO1, that acetylates two lysine residues located at the head

domain of SMC3. Both in mammals and *Drosophila*, this acetylation leads to the recruitment of SORONIN (DALMATIAN), displacing WAPL from the releasin complex. This displacement is thought to be a consequence of the binding of SORONIN to PDS5, which helps to reconcile the findings that PDS5 protein is important for both cohesion anti-establishment and establishment. After S-phase, ECO1 is degraded in a CDK1 dependent manner and, with the exception of DNA damage occurrence, newly synthesized cohesin rings are unable to become cohesive even if they can be loaded onto chromatin (Dorsett and Ström, 2012; Nasmyth, 2011; Remeseiro and Losada, 2013) (Figure 1.6B).

In higher Eukaryotes, cohesin is removed in two steps during mitosis. From the beginning of prophase until metaphase, most of the cohesin is lost from the chromosome arms in a SEPARASE-independent manner. This step depends on AURORA B and involves the phosphorylation of both SCC3, by PLK, and SORONIN, by CDK1, leaving the latter protein unable to compete with WAPL for PDS5 binding. This step is known as the prophase pathway and depends on WAPL, since its loss completely abolishes it. Most of the pericentric and some of the arm's cohesins are protected by SHUGOSHIN, which recruits PP2A and appears to counteract the effects of the releasin complex activation and of SCC3 and SORONIN phosphorylations. These protected cohesins allow for the maintenance of sister chromatid association during prometaphase and metaphase. At the onset of anaphase, their α-kleisin subunit is cleaved by SEPARASE, which becomes active upon degradation of SECURIN and Cyclin B by the anaphase promoting complex-cyclosome (APC/C) (Dorsett and Ström, 2012; Nasmyth, 2011; Remeseiro and Losada, 2013) (Figure 1.6B).

After S-phase upon DNA damage, ECO1 is once again capable of stabilizing cohesin rings, allowing cohesin to become cohesive again. Furthermore, effective homologous-recombination mediated repair is facilitated by the

interaction of BRCA2 with cohesin through PDS5 (Dorsett and Ström, 2012; Remeseiro and Losada, 2013) (Figure 1.6B).

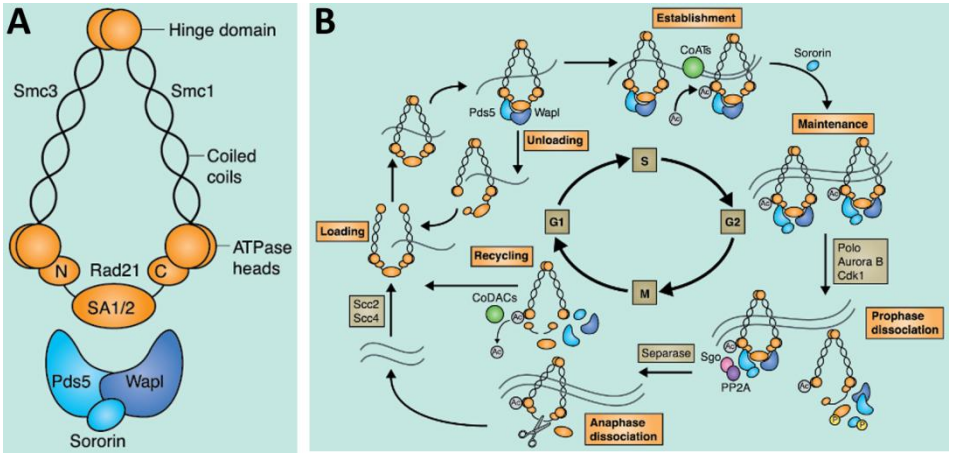

Figure 1.6 – The Cohesin Complex. (A) The Cohesin tripartite ring is composed of SMC1, SMC3 and RAD21, with SCC3 (SA1/2) binding to the central region of RAD21. The cohesion accessory factors PDS5 and WAPL are shown forming the releasing complex, with SORONIN also represented, showing that it can also interact with PDS5. (B) Regulation of the cohesion ring during the cell cycle. Abbreviation: Ac, acetylation; CoATS, Cohesin Acetyltransferases; CoDACs, Cohesin Deacetylases; P, phosphorylation. Taken from: (Remeseiro et al., 2013).

1.5.1 The Cohesin Complex during Meiosis

The cohesin complex is also required during meiosis, where it is essential both for the stabilization of chiasmata (allowing for the proper segregation of the homologous chromosomes during meiosis I), and for sister chromatid segregation during meiosis II (Ivanovska and Orr-Weaver, 2006). With the exception of the α-kleisin subunit, RAD21, the cohesin complex is thought to be similarly composed during meiosis. Both in mammalian and in yeast cells a meiosis specific α-kleisin subunit, REC8, has been identified. In *Drosophila*, C(2)M has been identified as a meiosis specific α-kleisin that interacts with dSMC3 and is needed for both SC assembly, and for the localization of

dSMC1/3 to chromosome cores, a proteinaceous structure that is thought to serve as the scaffold for SC formation. However, C(2)M is only expressed in cells that assemble the SC, it is not required for the binding of dSMC1 and dSMC3 to either the centromeres or the chromosome arms. Consequently, *c(2)m* mutants do not result in high levels of meiosis II segregation defects as it would be expected if it were a component of the meiotic cohesin complex (Heidmann et al., 2004; Khetani and Bickel, 2007; Manheim and McKim, 2003).

In *Drosophila* pre-meiotic cells, both dSMC1 and dSMC3 (dSMC1/3) localize along the chromosome arms and are enriched at the centromeres of all sixteen germline cells of a cyst. As the cyst enters region 2A, dSMC1/3 take a thread-like appearance in the cells that initiate SC assembly, a localization pattern similar to that of C(3)G, a component of the SC complex. This similar localization is maintained as the cysts progress along the germarium. In region 2B, only the two pro-oocytes maintain the thread-like pattern of dSMC1/3, while in the cell that reverts to NC fate, the signal starts to become fragmented. Once the oocyte fate has been fully determined, dSMC1/3 thread-like staining is restricted to that cell. Between stages 2 to 6 of egg chamber development, the dSMC1/3 signal continues to coincide with that of C(3)G and, similar to the SC, starts to fade. The signal becomes more nucleoplasmatic and eventually disappears around the latter stage (Khetani and Bickel, 2007). This pattern is followed by the meiosis-specific cohesin proteins ORD (Orientation Disruptor) and SOLO (Sisters On the Loose) (Webber et al., 2004; Yan and McKee, 2013). These proteins co-localize with dSMC1/3 and are also present at the chromosome cores. The localization of the two dSMCs to the centromeric region of oocytes, as well as chromosome segregation are affected in *ord* and in *solo* mutants (Webber et al., 2004; Yan and McKee, 2013). Despite the lack of sequence homology with other known cohesin complex components, both

ORD and SOLO have been proposed to be part of the meiosis specific cohesin complex in *Drosophila* (Yan and McKee, 2013).

1.6 Drosophila *Chromatin Insulators*

In mammals, the cohesin complex has been shown to co-localize with the insulator protein CTCF and to promote its function has an insulator (Nativio et al., 2009; Wendt et al., 2008).

Chromatin insulators were initially described in *Drosophila* and chicken as *cis*-regulatory elements that mediate enhancer-promoter interactions and that define boundaries between adjacent chromatin domains (Van Bortle and Corces, 2012; Vogelmann et al., 2011). In *Drosophila*, at least 5 different insulator sub-classes exist, characterized by specific DNA sequences that are recognized by different DNA-binding proteins, which might dictate their functional specificity: Supressor of Hairy-Wing (SuHw), *Drosophila* CCCTC-binding factor (dCTCF), Boundary-Element Associated Factor of 32 kDa (BEAF32), Zeste-White 5 (Zw5) and GAGA factor/Trithorax-like (GAGA/TRL) (Gurudatta and Corces, 2009; Vogelmann et al., 2011). In addition to DNA-binding proteins these DNA-protein complexes share common factors, such as the accessory proteins: Centrosomal Protein 190kDa (CP190), found to be present in all insulators with the exception of Zw5 (that needs to be studied in more detail), and an isoform of Modifier of Modg4 (MOD(mdg4)). Both of these proteins contain BTB/POZ domains, which are capable of forming multimers *in vivo*. These insulator accessory proteins are thought to not directly interact with chromatin but to facilitate the interaction between

different insulator complexes (Figure 1.2)(Van Bortle and Corces, 2012; Vogelmann et al., 2011).

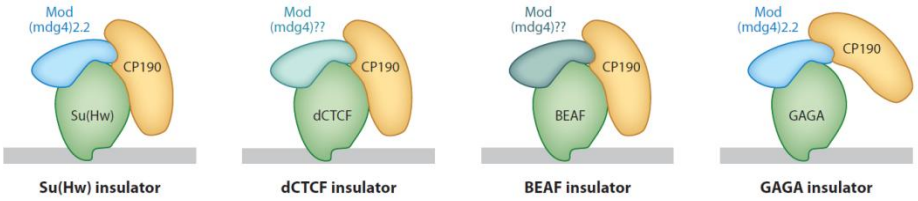

Figure 1.7 – Four of *Drosophila*'s insulator sub-classes, each containing a specific DNA-binding protein that might define their functional specificity. The protein CP190 is common to all insulators and these appear to possess also one of MOD(mdg4) isoforms, both Su(Hw) and GAGA/TRL interact with MOD(mdg4)2.2 and BEAF32 and dCTCF contain different variants. Taken from (Van Bortle and Corces, 2012).

Insulator subclasses have been shown to cluster together in *Drosophila* nuclei in sub-nuclear structures name "insulator bodies" (Ghosh et al., 2001), which require the presence of CP190 for their proper assembly (Pai et al., 2004). The fact that these proteins cluster together has raised the possibility that insulators might have functions in high order chromatin organization of the nucleus, mediating tri-dimensional chromatin interactions. Consistent with this hypothesis, the insulator DNA-binding proteins BEAF32 and Zw5 have the ability to directly interact both *in vitro* and *in vivo* (Blanton et al., 2003). In addition, sites occupied by CP190, Su(Hw), BEAF32 and/or dCTCF have been shown to cluster together within 100bp to 300bp genomic elements across the genome and named "aligned insulator elements" (Van Bortle and Corces, 2013).

Topologically associating domains (TADs) are highly self-interacting domains, whose boundaries appear to be enriched for insulator proteins (Hou et al., 2012; Sexton et al., 2012). These boundaries appear to define the regions where the chromatin interactions within adjacent TADs switch their

directionality (Hou et al., 2012; Sexton et al., 2012). In *Drosophila*, this boundaries appear to be enriched for CP190, BEAF32 and dCTCF but not Su(Hw) (Sexton et al., 2012) and to be enriched for "aligned insulator elements" containing two or more DNA-binding proteins together with CP190 (Hou et al., 2012). On the other hand, single-insulator sites seem to be enriched inside the TADs (Hou et al., 2012). Once again suggesting that insulator might be involved in the chromatin organization inside nuclei.

1.7 Objectives of this work

The fact that dPDS5 loss results in eggshell ventralization and karyosome fragmentation suggests that dPDS5 is required to limit defective endogenous DSB repair and persistent meiotic checkpoint activation. This hypothesis is further supported by data from yeast showing that its dPDS5 orthologue is required for homologous chromosome pairing and DSB repair in meiosis (Jin et al., 2009). This would imply: first, that dPDS5 is required upon DSBs; and second, that it is under dATR surveillance. While the first expectation holds, the same is not true for the second, since removing dATR in a *dPds5* mutant background does not rescue the checkpoint activation phenotypes (Barbosa et al., 2007). This result has, again, two main implications: first, the possible existence of either an additional branch of the meiotic checkpoint or of a parallel checkpoint that converges into the canonical one; and second, a possible function for dPDS5 during oogenesis that is not related to DSB repair, hence independent of sister chromatid cohesion.

In this context, during the course of my Ph.D., I have investigated which additional functions dPDS5 has during female meiosis in *Drosophila* to

determine whether dPDS5 is under the surveillance of another DNA Damage transducer kinase and if so, characterize this new meiotic DDR. With this work, I propose to contribute to a better understanding of meiosis, this crucial developmental program for all sexually reproducing species.

2 dPDS5 is an insulator protein

Summary

Mutations in the cohesin accessory factor *dPds5* result in the appearance of the "spindle" phenotype (Barbosa et al., 2007). This "spindle" phenotype implies a persistently active meiotic checkpoint (Ghabrial and Schüpbach, 1999; Joyce and McKim, 2011) and a possible function for dPDS5 during oogenesis. To understand this function, we analysed the expression of several dPDS5 transgenic lines that revealed that this protein has a punctuated dynamic expression pattern during mid-oogenesis, exclusively in the oocyte nucleus. Furthermore, these dPDS5 nuclear foci were identified as insulator bodies due to their co-localization with foci from the insulator proteins CP190, MOD(mdg4)2.2 and BEAF32. This localization to insulator foci is suggestive of the presence of additional chromatin in the oocyte nucleus aside from the karyosome, possibly as chromatin loops. Furthermore, we present evidence that the Prophase I arrest, in which the oocyte nucleus is postulated to be during mid-oogenesis, is actually a dynamic event.

2.1 Introduction

In *Drosophila melanogaster* (*Drosophila*) egg development is initiated in the germarium located at the anterior tip of the ovary. Once the egg chamber leaves the germarium, Pachytene is completed with the disassembly of the Synaptonemal Complex (SC), the meiotic chromatin condenses into a hollow sphere (karyosome), entering a diplotene-like state, where it arrests until stage 13. This Prophase I arrest is a conserved feature of egg development across animals, that allows for oocyte differentiation and the stockpiling of maternal material (Ashburner et al., 2005; Lake and Hawley, 2012; Spradling, 1993; Von Stetina and Orr-Weaver, 2011).

Prophase I is initiated in region 2A of the germarium with the induction of Double Strand Breaks (DSBs) and SC assembly (Ashburner et al., 2005; Lake and Hawley, 2012; Spradling, 1993). The presence of DSBs activates a DNA damage response (DDR), mediated by dATR (MEI-41), that recruits repair machinery to the damaged sites and delays cell cycle progression until DNA repair is complete (Ghabrial and Schüpbach, 1999; Joyce and McKim, 2011). In repair mutants, such as *dRad51* (*spn-A*) and *dRad54* (*okr*) where DSBs are not resolved, the meiotic checkpoint is persistently active. This results in developmental defects, namely at the level of karyosome condensation and in the establishment of the dorsal-ventral polarity of the eggshell (known as the "spindle" phenotype) (Ghabrial and Schüpbach, 1999; Ghabrial et al., 1998). Mutations in the cohesin accessory factor *dPds5* result in such phenotypes (Barbosa et al., 2007), suggesting a potential function during oogenesis.

PDS5 is known to interact with the cohesin complex and to be required both for cohesin release from chromatin, during the M and G1 phases (together with WAPL), and for the establishment and maintenance of cohesion

during the S and G2 phases (Nasmyth and Haering, 2009; Remeseiro and Losada, 2013). The cohesin complex was initially characterized for its role in cohesion establishment, essential for chromosome segregation both during mitosis and meiosis, and also for DNA repair (Dorsett and Ström, 2012; Nasmyth and Haering, 2009). In addition, recent work has revealed that cohesin also has functions in gene expression during development, probably through mechanisms that involve DNA loops (Dorsett and Merkenschlager, 2013; Remeseiro and Losada, 2013; Remeseiro et al., 2013). Furthermore, in mammals, cohesin has been shown to co-localize and be required for CTCF function as a transcriptional insulator, and to also be required for the maintenance of a CTCF-dependent higher-order chromatin organization (Nativio et al., 2009; Wendt et al., 2008).

Chromatin insulators are classically defined as DNA-protein complexes that mediate enhancer-promoter interactions, and might establish boundaries between heterochromatin and euchromatin (Vogelmann et al., 2011). Recent evidence suggests that these complexes might have additional functions in higher-order chromatin organization (Hou et al., 2012; Sexton et al., 2012), influencing nuclear events such as transcription (Yang et al., 2012) and replication (Gurudatta et al., 2013). In *Drosophila*, five different insulator types have been described, are characterized by a specific DNA sequence and their unique DNA binding protein: *Drosophila* CTCF (dCTCF), Suppressor of Hairy-wing (Su(Hw)), Boundary Element Associated Factor of 32kDa (BEAF32), GAGA binding factor (GAF/TRL) and Zeste-white 5 (Zw-5). The insulator proteins have been shown to have a punctuated nuclear distribution, forming nuclear foci. These nuclear foci, which have been designated insulator bodies, appear to accommodate several DNA sequences and are disrupted in insulator component mutants (Gurudatta and Corces, 2009). Centrosomal Protein 190

(CP190) and Modifier of mdg4 (MOD(mdg4)) are two known accessory insulator proteins, that include BTB/POZ protein interaction domains; and have been shown to either directly interact with several DNA-binding insulator proteins or to occupy the same genomic site (Bortle et al., 2012; Gerasimova et al., 2007; Ghosh et al., 2001; Melnikova et al., 2004; Pai et al., 2004).

In this chapter, we aimed at understanding what dPDS5 function is during oogenesis, by looking at its expression pattern and possible co-localization with other cohesin proteins and with insulator proteins, known to be involved in high-order chromatin organization and gene expression regulation.

2.2 Material and Methods

2.2.1 Fly Stock Maintenance

All *Drosophila* stocks were raised under standard conditions at 23°C. The *dPds5*^{2} and *dPds5*^{6} alleles were obtained in a screen for mutations that elicit the meiotic checkpoint (Barbosa et al., 2007) and are described in chapter 3 of this thesis, *cp190*^{1} and *cp190*^{2} alleles were obtained from William Whitfield (Butcher et al., 2004); the BEAF32$^{GFBF.3A}$ transgenic line was given by Craig Hart (Roy et al., 2007); dRAD21:GFP, dSMC1:GFP and dSMC3:GFP transgenic lines were provided by Raquel Oliveira (Eichinger et al., 2013) (Oliveira *et al.*, manuscript in preparation)

2.2.2 dPDS5 transgenic lines

To determine the localization of dPDS5 during oogenesis, several transgenic lines where constructed. Five candidate ESTs (GH01934; GH043388; GH12466; HL02802) that were obtained from the Berkeley Drosophila Genome Project (BDGP) fulfilled the following criteria: having the correct first five aminoacids from the dPDS5 protein sequence (MADIV) and the sequence upstream from the transcription starting site. The sequences of the candidate ESTs were aligned both with the available *dPds5* cDNA sequence from Flybase and with the *dPds5* sequence of our FRT42B control line. We selected the cDNAs that presented the highest similarity to our control line (GH01934; GH04388; GH12466; GH12788). These were introduced to the entry vector pENTR/D-TOPO (Molecular Probes, Eugene, OR), and recombined into four different destination vectors from the Drosophila Gateway™ Collection that carried the UASp GAL4-responsive promoter at the N-terminal and one of four different tags at its C-terminal module (EGFP - pPWG; 6xMyc – pPWM; Venus – pPWV and FLAG – pPWF). The obtained vectors were transfected to competent cells and amplified, the DNA was purified and then sent to be transfected to flies. For the EGFP and Venus tagged constructs, the DNA was transiently transfected to S2 cells to verify the correct expression of the tags and their nuclear localization. Only the fly lines that were able to rescue the lethality of the *dPds5* mutants were kept and used for further analysis.

2.2.3 Dissection of Drosophila *ovaries*

Ovaries were processed for immunofluorescence as described by Navarro and colleagues (Navarro et al., 2004). For each genotype five to six pairs of ovaries were dissected in 1xPBS. Fixation was performed at room temperature (RT) for 20 minutes in 1xPBS containing 3% to 6% of EM grade formaldehyde

and 0.5% of NP-40, in a 1:3 ratio with heptane. The samples were rinsed three times and washed three times for 5 minutes with 1xPBST (1xPBS with 0.2% Tween-20). Afterwards, the ovarioles were separated using a tungsten needle, and subsequently permeabilized and blocked for one hour in 1xPBST with 1% Triton X-100 and 1% BSA at RT. After washing the samples three times for 20 minutes with 1xPBST they were ready to be processed for immunofluorescence or DNA staining.

2.2.4 Immunoflourescence of Drosophila *ovaries*

Primary antibodies were used at the following dilutions: 1:1000 for α-WAPL[L] and α-WAPL[SL] (Cunningham et al., 2012); 1:20 for α-LaminC antibody LC 28-26 (Developmental Studies Hybridoma Bank); 1:1000 for α-CP190 antibody Rb188 (Whitfield et al., 1988); 1:1000 for α-MOD(mdg4)2.2 (Gerasimova et al., 1995) and 1:500 for α-Myc c-Myc antibody (9E10) (Santa Cruz Biotechnology, Inc.). Alexa 546-conjugated and Alexa 488-conjugated secondary antibodies (Molecular Probes, Eugene, OR) were used at a dilution of 1:500. DNA was stained either with TOTO-3® or DAPI (Molecular Probes, Eugene, OR) diluted 1:1000 or 0,3μM, respectively *as per* the company's instructions. Ovaries where mounted in Vectashield (Vector Labs, Burlingame, CA) and visualized in a Leica SP5 Live (Leica, Bannockburn, IL) or a Zeiss Meta 501 (Carl Zeiss Microscopy, Germany) confocal microscopes.

2.2.5 Immunoprecipitation Assays

For each immunoprecipitation, ovarian extracts were prepared with about 40 pairs of ovaries dissected in 1xPBS and suspended in 200µL of extraction buffer (1% Triton X-100 in 1xPBS, with 2 mM EDTA and EGTA) supplemented with protease inhibitors (Roche, Basel, Switzerland). Nuclear proteins were obtained by manually homogenizing the extracts 30 times with a pestle at 4°C and laying it to rest on ice for 30 minutes. The extracts were cleared by retrieving the supernatant after 10 minutes centrifugations at 13000rpm at 4°C, this step was repeated three times. Total protein was determined by the Standard Bradford assay (Bio-Rad, Hercules, CA) according to the manufacturer's instructions. Proteins were immunoprecipitated by addition of 15µL of Protein G Sepharose 4 Fast Flow (GE Healthcare, Little Chalfont, UK) to 1mg of protein extract that was pre-incubated with appropriate antibody: 1µL of Rb188 (Whitfield *et al.*, 1988) or 8µL of c-myc (Santa Cruz Biotechnology, sc-40). The mixture was incubated for a minimum of 3 hours at 4°C with gentle agitation. After the 4°C incubation the sepharose beads were washed three times with extraction buffer. The immunoprecipitate was eluted by addition of 30µL of 2x Laemmli sample buffer and incubation for 5 minutes at 100°C.

2.2.6 Western Blots

Protein extracts from larval brains, ovaries or immunoprecipitation samples were run in SDS-PAGE (8% polyacrylamide gels; Bio-Rad, Hercules, CA) and transferred to nitrocellulose membranes (Bio-Rad, Hercules, CA). The membranes where blocked overnight at 4°C in 5% milk and subsequently probed for 1 hour with the appropriate antibodies: 1:2000 α-CP190 antibody Rb188 (Whitfield *et al.*, 1988); 1:1000 of α-Myc c-myc (Santa Cruz Biotechnology, sc-40); 1:20 of a 1:1 mix of 1B11 and 4C2 Bicaudal-D antibodies

(Developmental Studies Hybridoma Bank), 1:200000 of α-tubulin (Sigma-Aldrich LLC, Co; B-5-1-2) or 1:2000 PKC-ζ (Santa Cruz Biotechnology, sc-216). The membranes were incubated for 1h with the secondary antibody α-HRP diluted 1:3000 (Jackson ImmunoResearch Laboratories) after which they were revealed using ECL plus (GE Healthcare), according to manufacturer's instructions and imaged with a Storm 860 PhosphorImager. The intensity of CP190 bands obtained in the immunoprecipitation assays was quantified using the FIJI software (Schindelin *et al.*, 2012; following the ImageJ user guide instructions) and compared with the intensities of the respective α-tubulin loading control bands acquired following the same methodology. Excel software was used for the graphic analysis and to run the *t*-student test.

2.3 Results

2.3.1 dPDS5:TAG transgenes have a dynamic expression pattern during mid-oogenesis

In order to determine dPDS5 function during *Drosophila* oogenesis several UASp>dPDS5:TAG transgenes, with either Myc, GFP, FLAG or Venus, were obtained using the Gateway® technology. Two different GAL4 drivers were used to drive their expression in adult flies: an ubiquitous driver, *actin*(*act)*>GAL4 (*act*GAL4), and a germline specific driver, *nanos(nos)*>GAL4 (*nos*GAL4). Preference was given to transgenes that were considered functional to be used in the work here presented. The transgenes were considered functional if, when expressed under the control of *act*GAL4, they were able to rescue the lethality associated with our *dPds5* mutants (Figure 2.1). Of the four dPDS5:TAG lines used only UASp>dPDS5:Myc does not completely rescue the lethality, nonetheless this line was also used (Table 2.1).

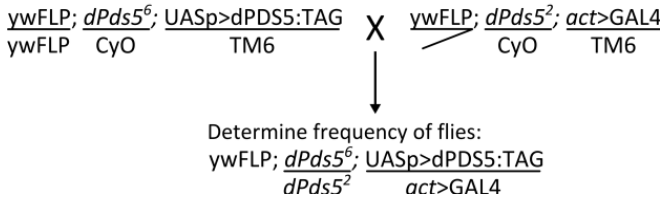

Figure 2.1 - Cross scheme for the functionality tests of the obtain UASp>dPDS:TAG transgenes.

Table 2.1 - Frequency of transheterozygous flies *dPds5*^{6}*/dPds5*^{2} rescued by the expression of UASp>dPDS5:TAG transgenes under the control of the *act*GAL4 driver. Expected survival frequency if lethality is rescued is 14,3%. Where: n, total number of scored flies.

Genotype	*dPds5*^{6}*/dPds5*^{2}; *act*>GAL4/UASp>dPDS5:TAG			
	GFP	Myc	VENUS	FLAG
Frequency (n)	15,5% (45)	5,0% (120)	13,3% (98)	18,9% (79)

The chosen lines were then used to determine dPDS5's expression pattern in the female germline. The observed pattern was consistent between all tested transgenes, independently of the used driver. dPDS5:TAG is present in the nucleus of all ovarian cell types throughout all egg development stages (Figure 2.2A-A' and Figure 2.3). Whereas in both the follicle and nurse cells dPDS5 appears diffuse on the chromatin, in the oocyte nuclear foci are present during a very specific time frame (from stage 4 or 5 to stage 10). Furthermore, these foci appear to be oocyte specific since expression of the UASp>dPDS5:TAG transgenes in an *egalitarian* (*egl*) mutant background (*elg*^{PR29}*/egl*^{3e}), where oocyte identity is lost (Navarro et al., 2004), results in the disappearance of these nuclear structures (Figure 2.2B-C).

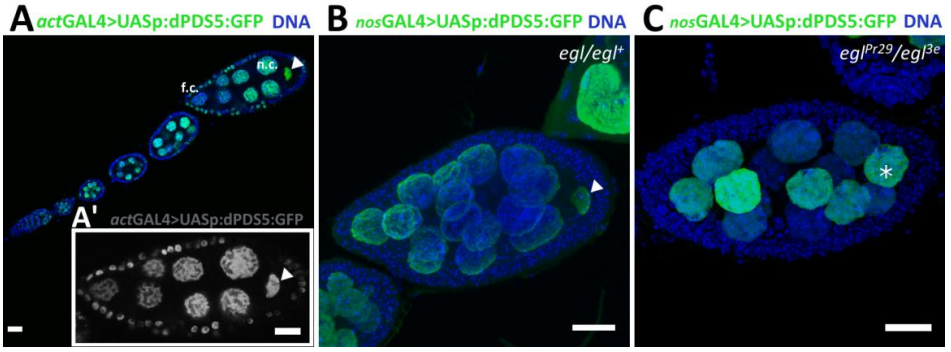

Figure 2.2 - dPDS5:GFP expression in the female germline. (A-A') dPDS5:GFP is expressed in all cell types and throughout all the stages of egg development. The inset (A') shows only the dPDS5 channel for the stage 6 egg chamber, allowing a better exemplification of the expression pattern of this protein. Foci can be seen uniquely in the oocyte nucleus. (B-C) dPDS5:GFP foci are oocyte specific. (B) Projection of a *egl/egl*$^{+}$ stage 6 egg chamber. (C) Projection of an *elg*^{PR29}*/egl*^{3e} mutant stage 6 egg chamber; the posterior most nucleus (asterisk) has acquired a nurse cell fate and no foci are present. In all images: arrowhead indicates foci in the oocyte nucleus; f.c., follicule cell; n.c., nurse cell; *act*GAL4>UASp:dPDS5:GFP is in green; DNA is in blue; anterior to the left and posterior to the right; scale bar = 20µm.

Until stage 4, dPDS5:TAG presents a diffuse nuclear expression with a clear avoidance of the meiotic chromatin (not shown). However, starting around late stage 4 or stage 5, a small number of nuclear foci (one to two) become visible close to the karyosome. These start to increase in number during stage 6, where they can be found both near the meiotic chromatin, and often appear to be interconnected, taking a string-like appearance ("collar"), and dispersed on the nucleoplasm. This "collar" structure usually disappears in stage 7/8, but the foci continue to increase in number until stage 9/early stage 10. By late stage 10, the foci become increasingly smaller, the nucleoplasmatic fraction gradually stronger and the foci eventually completely disappear (Figure 2.3).

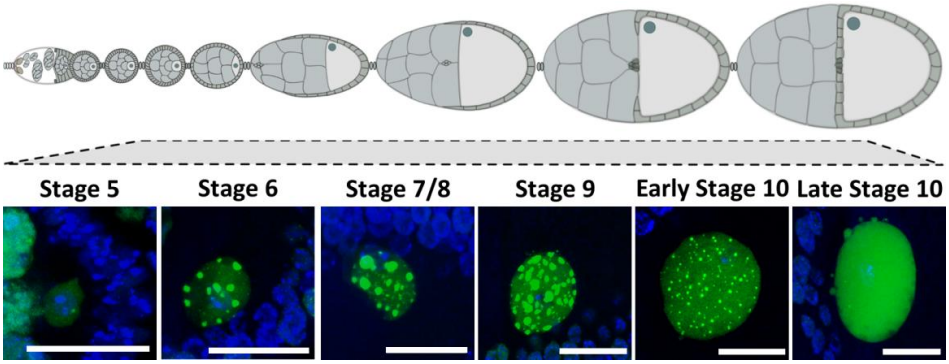

Figure 2.3 - dPDS5:TAG foci appear in the oocyte nucleus during mid-oogenesis from stage 4/5 until stage 10. In all images: *act*GAL4>UASp:dPDS5:GFP is in green; DNA is in blue; anterior to left, posterior to the right; scale bar = 20µm.

2.3.2 dPDS5:TAG and Cohesin core proteins show distinct localization in the oocyte nucleus

Taking into consideration the role of dPDS5 in cohesion establishment, we asked if other cohesin complex or cohesin accessory factors presented a similar oocyte-specific dynamic expression pattern.

To determine the localization of the cohesin core proteins (dSMC1, dSMC3 and dRAD21) during egg development, we looked at ovaries expressing functional transgenes tagged with GFP (Eichinger et al., 2013). During mid-oogenesis, the cohesin core proteins are either located on top of the meiotic chromatin or diffused in the oocyte nucleoplasm, as can be seen for dSMC1 and dSMC3 (Figure 2.4A-B). Alternatively, they are not present or are weakly nucleoplasmatic, as in the case of RAD21 (Figure 2.4C). These localization patterns are not at all similar to that presented by dPDS5:TAG.

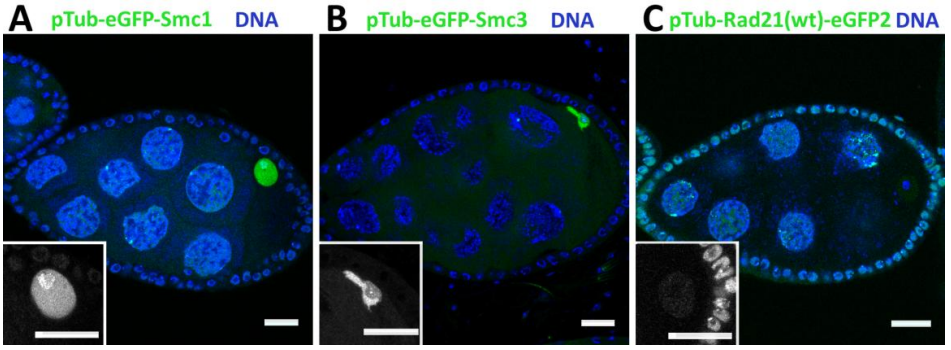

Figure 2.4 - The cohesin core complex proteins do not form foci during mid-oogenesis. For each cohesin protein a stage 6 egg chamber is presented, the inset is a detail of the oocyte nucleus in the green channel that refers uniquely to the protein of interest. In all images: anterior to left, posterior to the right; scale bar = 20µm.

We proceeded by looking at localization of the cohesin accessory factor WAPL, known to interact with dPDS5 forming a complex required for the unloading of cohesin from chromatin (Dorsett and Ström, 2012; Nasmyth and Haering, 2009). The *wapl* gene encodes two different transcripts of different sizes that result in the production of a long protein (WAPL-L) and a short protein (WAPL-S) (Vernì et al., 2000). The presence of both proteins in the ovary was determined by using two antibodies: one that was raised against the long isoform (α-WAPL[L]) and another that detects both isoforms (α-WAPL[SL]) (Cunningham et al., 2012). Immunofluorescence using the α-WAPL[L] antibody revealed that WAPL-L is present in nuclei from both follicle and nurse cells but is completely absent from the oocyte nucleus (Figure 2.5A-B''). However, the α-WAPL[SL] antibody revealed the presence of WAPL foci in the oocyte nucleus, in addition to a diffuse expression on the follicle and nurse cells. Bearing in mind the former result, we can assume that only WAPL-S is present in the oocyte nucleus. These WAPL-S foci do not co-localize with or follow the same dynamics has dPDS5 foci (Figure 2.5C-D'') and appear not to depend on

the presence of dPDS5 (preliminary data not shown). dPDS5:TAG foci do not appear to co-localize with other cohesin proteins during mid-oogenesis.

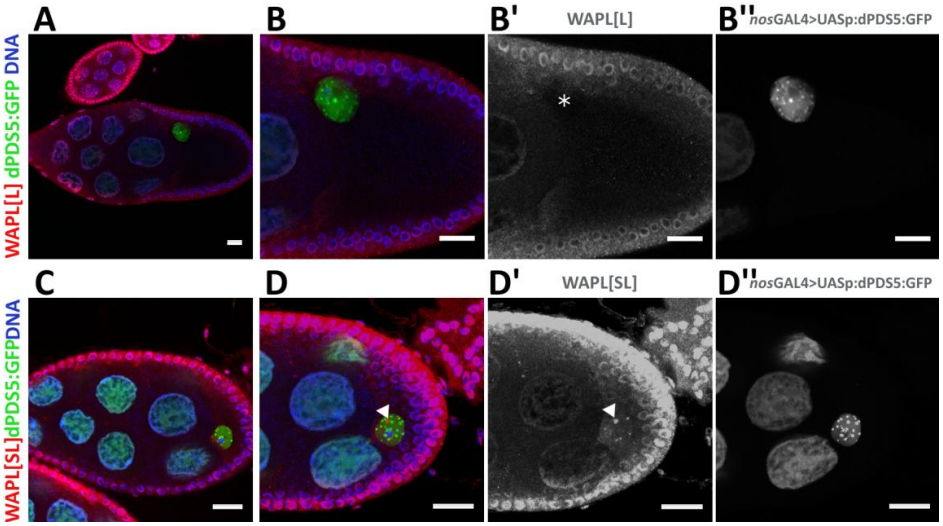

Figure 2.5 - WAPL-S foci are present in the oocyte nucleus and do not co-localize with dPDS5:GFP foci. (A-B'') α-WAPL[L] signal is present in the follicle cells and nurse cell nuclei, but is absent from the oocyte nucleus. (B-B'') Amplification of the oocyte presented in (A); where the α-WAPL[L] signal is absent from the oocyte nucleus (B', asterisk) while dPDS5:GFP foci are still present (B''). (C-D'') α-WAPL[SL] can be seen in nuclei from all three cell types, with the presence of foci in the oocyte nucleus. (D-D'') Amplification of the oocyte from (C); where, α-WAPL[SL] reveals the presence of WAPL foci (D') that do not co-localize with dPDS5:GFP foci (arrowhead in D and D'). In all images: anterior to left, posterior to the right; scale bar = 20µm.

2.3.3 dPDS5:TAG co-localizes with insulator protein foci during mid-oogenesis

To better understand the nature of the dPDS5 foci, we looked in the literature for proteins that either define nuclear regions and/or localize to specific nuclear regions. One such example is the nuclear envelope; dPDS5's localization to this specific structure was assessed by immunofluorescence against the nuclear lamina component LaminC (LamC) in an

actGAL4>UASp:dPDS5:GFP background, that revealed that the dPDS5 foci do not localize to the nuclear envelope (Figure 2.6).

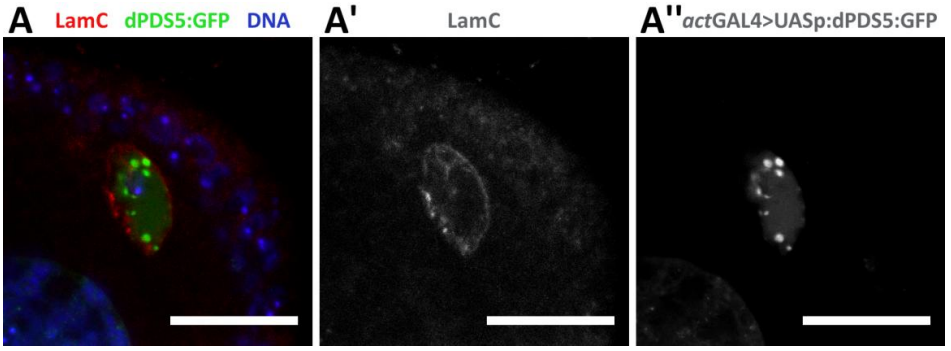

Figure 2.6 - (A) dPDS5:GFP foci, in a stage 6 egge chamber, do not localize to the nuclear membrane. In all images: anterior to left, posterior to the right; scale = 20µm.

Another example are the insulator proteins, that when co-localizing assemble in nuclear structures known as insulator bodies that take the appearance of foci (Gurudatta and Corces, 2009; Phillips-Cremins and Corces, 2013). Four different insulator proteins were studied to allow a better understanding of the oocyte's chromatin organization: two accessory insulator proteins, CP190 and MOD(mdg4)2.2 [an isoform know to be present in Su(Hw) and GAGA/TRL insulators (Gause et al., 2001; Ghosh et al., 2001; Melnikova et al., 2004)], and two DNA-binding insulator proteins, BEAF32 and Su(Hw). All these proteins were found to be present in follicle and nurse cells nuclei throughout oogenesis (Figure 2.7A-D); and also in the oocyte nucleus as foci that co-localize with dPDS5:TAG (Figure 2.7A-D) and follow the same dynamics (Figure S2.1), the only exception being Su(Hw), a result concordant with previous results by the Geyer lab (Baxley et al., 2011). Moreover, these foci are not a consequence of dPDS5 overexpression, since are still formed even in the absence of any GAL4 driver (Figure S2.1).

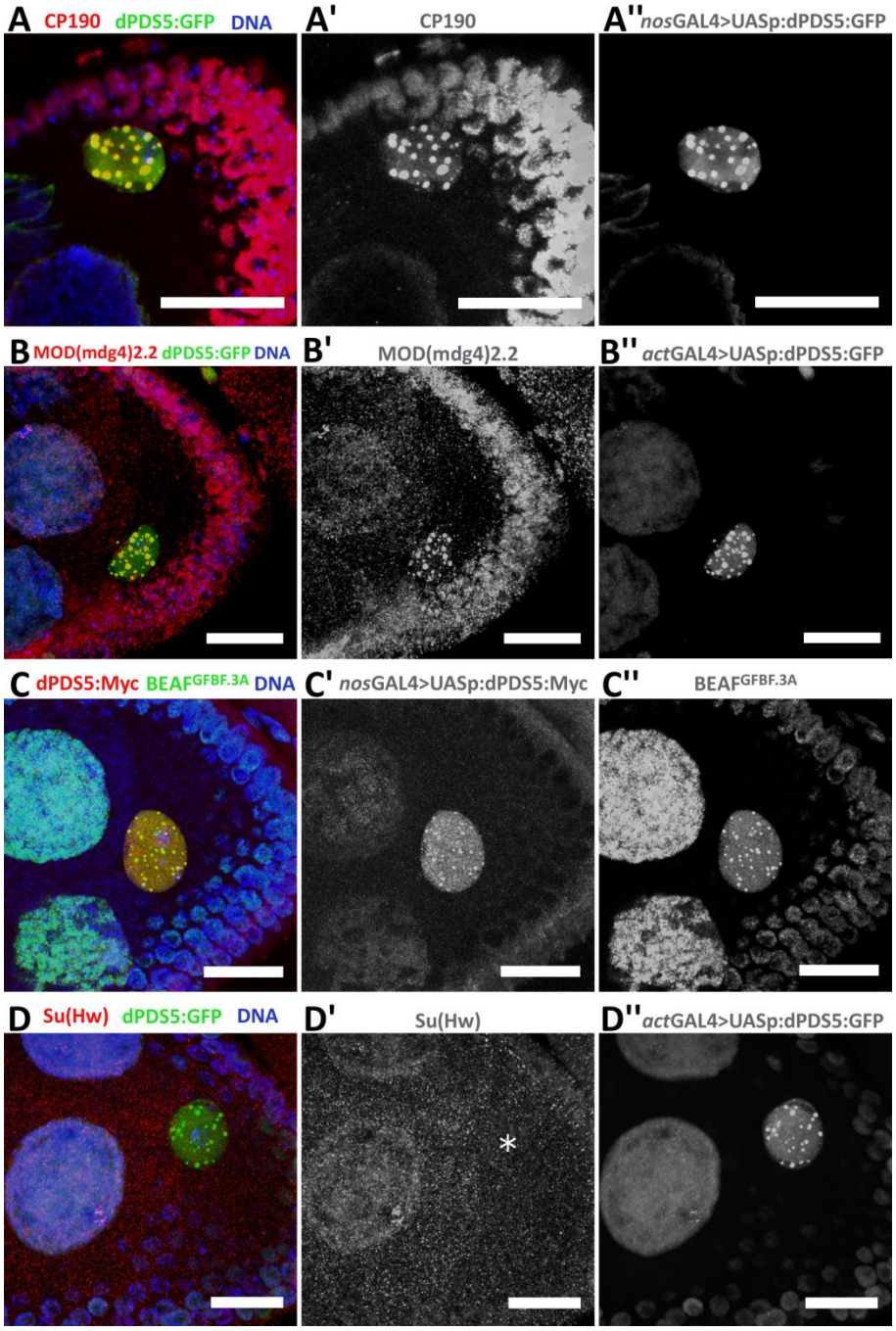

Figure 2.7 - Insulator proteins, with the exception of Su(Hw), form foci in the oocyte nucleus and co-localize with dPDS5:TAG. In D': asterisk, indicating where the oocyte nucleus is located. In all images: stage 6 egg chambers; scale bar = 20µm.

The previous results favour the hypothesis that dPDS5 is a component of insulator bodies, at least in the oocyte nucleus. However, the fact that two proteins co-localize in an immunofluorescence assay is not synonymous of a direct *in vivo* interaction. To determine if the dPDS5 and the insulator proteins could, at least, be part of the same complex, co-immunoprecipitation assays were performed using ovarian extracts from females expressing UASp:dPDS5:Myc, either under the control of the *actGAL4* or the *nosGAL4* driver, or from control females that do not possess neither of the drivers. From these ovarian extracts either dPDS5 or CP190 were immunoprecipitated using an α-Myc or an α-CP190 antibody, respectively; and when probed for the presence of either CP190 or dPDS5 both proteins were detected, a clear indication that these two proteins interact *in vivo* (Figure 2.8A). The specificity of the α-CP190 polyclonal antibody was verified using $cp190^{1}$ and $cp190^{2}$ (Butcher et al., 2004) mutant larval extracts (Figure S2.2). To determine the oocyte contribution to the amount of immunoprecipitated protein, these assays were also performed in *egl* mutant ovarian extracts. Less CP190 was pulled-down from elg^{PR29}/egl^{3e} ovaries than from egl/egl^{+} controls when UASp:dPDS5:Myc was over-expressed in both backgrounds (Figure 2.8B). These results are a strong evidence that dPDS5 co-localizes and interacts with insulator proteins in the oocyte nucleus, and consequently support the notion that dPDS5 is an insulator component.

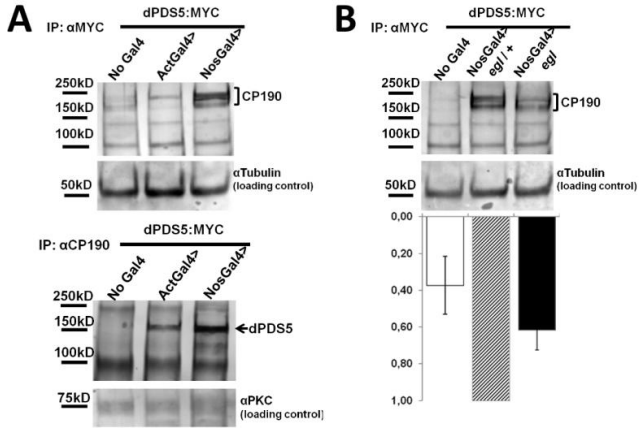

Figure 2.8 - Immunoprecipitation assays for dPDS5:Myc or CP190 in *Drosophila* ovarian extracts. (A) dPDS5 and CP190 directly interact *in vivo*. Top, pull-down of dPDS5:Myc and probing for CP190, loading control is α-tubulin. Bottom, pull-down of CP190 and probing for dPDS5:Myc using α-Myc, loading control is α-PKC. In both: showing co-immunoprecipitation in ovary extracts from control flies (No Gal4 lane) and from flies with dPDS5:Myc driven either by *act*Gal4 or *nos*Gal4. (B) The oocyte is a major contributor for the amount of CP190 that interacts with dPDS5:Myc. Top, Western blot membrane pull-down of dPDS5:Myc and probing with α-CP190, showing a decrease in the amount of detected CP190 when comparing *egl*/+; *nos*Gal4>dPDS5:Myc (middle lane) with egl^{3e}/egl^{PR29}; *nos*Gal4>dPDS5:Myc (right lane). Under the blot, graphic quantification of the amount of co-immunoprecipitated CP190 (relative band intensity) normalized to the band intensity of the loading control bands (α-tubulin). The ratio of pulled-down CP190 in egl^{3e}/egl^{PR29}; *nos*Gal4>dPDS5:Myc (right bar) and in *egl*/+; +/dPDS5:Myc (left bar) was calculated in relation to the total amount CP190 pulled-down in *egl*/+; *nos*Gal4>dPDS5:Myc (middle bar).

2.4 Discussion

It is known that dPDS5 loss results in eggshell ventralization (Barbosa et al., 2007), a phenotype associated with the activation of a DNA damage response in the germline (Abdu et al., 2002; Ghabrial and Schüpbach, 1999), and might imply a function for this protein during oogenesis. In order to understand what this function might be, we first looked at how this protein was expressed in *D. melanogaster* ovaries. Independently of the transgenic line used, dPDS5:TAG is present in nuclei from all ovarian cell types, but only in the oocyte does it form

foci (Figure 2.2 and Figure 2.3), during a specific time frame that spans from stage 4/5 to stage 10 (Figure 2.3). Additionally, we found that these foci do not appear to be related to any cohesin or cohesin accessory factor proteins (Figure 2.4 and Figure 2.5), which might indicate that whatever function dPDS5 might have during mid-oogenesis, it seems not to be related to canonical sister chromatid cohesion. On the other hand, these foci co-localize with several insulator proteins, such as the widely distributed CP190 and MOD(mdg4)2.2, favouring the hypothesis that dPDS5 is also an insulator protein (Figure 2.7).

2.4.1 dPDS5 is a component of insulator bodies in the oocyte

In mammals, CTCF was shown to co-localize with the cohesin complex and to require this co-localization to be functional as an insulator (Nativio et al., 2009; Wendt et al., 2008). The general idea in the field is that the same does not apply to the *Drosophila* insulator proteins, since no co-localization has been seen between cohesin proteins and dCTCF in several cell lines (Van Bortle and Corces, 2012; Misulovin et al., 2008). However, Bartkuhn and colleagues (2009) have shown that 80% of the cohesin protein dSCC3 sites overlap with CP190 sites (Bartkuhn et al., 2009), a result further substantiated in this work, since we show that dPDS5:TAG and CP190 foci overlap in the oocyte (Figure 2.7 and Figure 2.8). Moreover, MOD(mdg4)2.2 and BEAF32 are also present in the oocyte nucleus, form foci and co-localize with dPDS5:TAG foci (Figure 2.7), leading us to propose that dPDS5 is part of the so-called insulator bodies.

2.4.2 Peripheral chromatin loops may be present in the oocyte nucleus together with the condensed karyosome

Insulator bodies are considered to only be formed in the presence of chromatin and to arise from the clustering of distantly located insulator sites, taking the appearance of nuclear foci (Byrd and Corces, 2003). This clustering arises through a network of interactions between the different insulator proteins [Su(Hw), dCTCF, and/or BEAF32 have been shown in several occasions to co-localize in such foci] with the intervening chromatin postulated to form loops (Phillips-Cremins and Corces, 2013; Vogelmann et al., 2011). Here we show that the oocyte insulator foci comprise CP190, MOD(mdg4)2.2 and BEAF32 (Figure 2.7). The first two proteins are general/accessory insulator proteins that are thought to not directly bind DNA, and BEAF32 is a DNA-binding insulator protein. The appearance of these three proteins in co-localizing foci strongly supports the hypothesis that additional genomic material is present in the oocyte nucleus besides the karyosome. It would be interesting to determine the binding sites for these proteins in the oocyte and to design FISH probes in order to try to visualize the resulting chromatin loops.

2.4.3 The Prophase I arrest is a dynamic event

The presence of insulator bodies in the oocyte nucleus appears to be restricted to mid-oogenesis, corresponding to the Prophase I arrest animal female gametes go through (Von Stetina and Orr-Weaver, 2011). In *Drosophila* it is considered to initiate at stage 4/5 of egg chamber development and to last until stage 13, is equivalent to a diplotene-like state where the chromosomes are compacted into the karyosome (Von Stetina and Orr-Weaver, 2011). Our work provides evidence that, during mid-oogenesis, the oocyte nucleus is more dynamic than what the word “arrest” suggests: First, when looking at the

karyosome, one can observe that by stage 4, and until stage 6, it does present the morphology of a condensed hollow sphere, as it has been described to have (Ashburner et al., 2005; Spradling, 1993); however, as the egg chambers progress through meiosis, it starts to take a rosette-like shape, where you can discern separate chromatin masses, quite easily distinguishable by stage 10 (Ashburner et al., 2005). Second, the very presence of insulator bodies during this period of time is an argument in favour of chromatin dynamics. These nuclear bodies are considered to only be formed in the presence of DNA (Byrd and Corces, 2003), and their appearance, increase in number and eventual disappearance, would advocate for a considerable rearrangement of the underlying chromatin.

Author's Contributions

The initial work with the dPDS5 transgenes was performed by Vítor Barbosa, Sofia Leocádio helped map the insertion sites, Patrícia Silva and Raquel AM Santos characterized the dPDS5 transgenes dynamics and Raquel AM Santos performed the functionality tests. Patrícia Silva performed the co-immunoprecipitation assays and the immunoflourescence analysis for MOD(mgd4)2.2, Su(Hw) and CP190. Raquel AM Santos did the immunoflourescence analysis for both WAPL antibodies, BEAF32$^{GFBF.3A}$ and LamC. Both Raquel AM Santos and Patrícia Silva characterized the expression of the cohesin core proteins in the germline.

Acknowledgments

We would like to thank William Whitfield, Craig Hart and Raquel Oliveira for providing with fly lines, and Judith Kassis, David Glover for antibodies used in this work. The anti-LaminC-LC28.26, anti-Bicaudal-D 1B11 and 4C2 developed by Fisher, P.A. and Steward, R. were obtained from the Developmental Studies Hybridoma Bank developed under the auspices of the NICHD and maintained by The University of Iowa, Department of Biology, Iowa City, IA 52242.

2.5 Supplemental Material

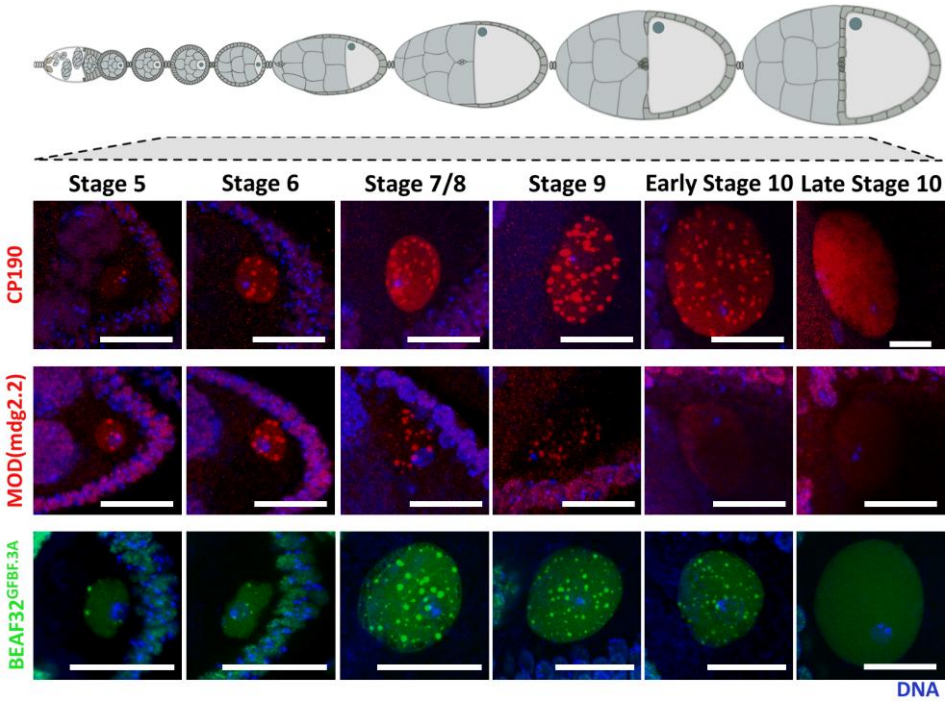

Figure S2.1 – Dynamic expression of the insulator proteins CP190 (first row), MOD(mdg2.2) (middle row) and BEAF32 (bottom row) during mid-oogenesis, from stage 5 to late stage 10, in the absence of dPDS5 overexpression. In all images: DNA is in blue; anterior to left and posterior to the right; scale bar = 20µm.

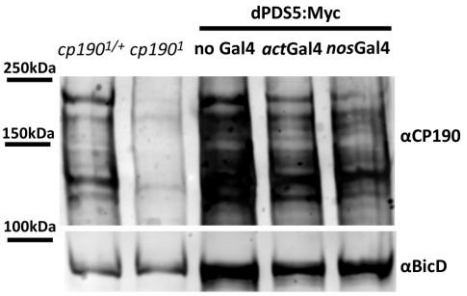

Figure S2.2 - To determine the specificity of the αCP190 (Rb188), a western blot assay was performed using protein extracts from larval brains of *cp190*$^{1/+}$ (first lane) and homozygous *cp190*^{1} (second lane) larvae. The obtained band pattern was compared to protein ovary extracts from control flies (No Gal4 lane) and from flies with dPDS5:Myc driven either by *act*Gal4 or *nos*Gal4, the loading control is αBicD.

3 dPDS5 is required for insulator body assembly in the oocyte nucleus

Summary

In order to better characterize dPDS5's function during mid-oogenesis, we analysed the effect of its absence in the formation of insulator bodies. In this chapter we describe how by removing dPDS5 the assembly of insulator bodies is disrupted. However, the functional consequences of dPDS5 abrogation appear to vary depending on the type of insulator protein. In the case of CP190, an accessory protein, the foci become less restricted and can sometimes collapse on the fragmented karyosome. As for the DNA-binding protein BEAF32, it appears to require dPDS5 to be present inside the oocyte nucleus. In addition, we show that meiotic checkpoint activation, through dCHK2, affects transcription exclusively in the oocyte.

3.1 Introduction

The cohesin complex is composed of four core proteins: dSMC1, dSMC3, dRAD21 and dSCC3 (SA). The first three core proteins are assumed to form a ring-like structure enveloping the sister chromatids, while dSCC3 interacts with dRAD21 and with cohesin accessory proteins (Nasmyth and Haering, 2005). By promoting sister chromatid cohesion, this complex has additional functions in proper chromosome segregation during mitosis and meiosis and in DSB repair (Nasmyth and Haering, 2005). Furthermore, this complex has been found to have additional roles in gene expression regulation that appear to be cohesion independent, since a small decrease in cohesin levels affects gene expression but not sister chromatid cohesion (Dorsett, 2011; Pauli et al., 2008; Rollins et al., 1999). Aside from mutations in the cohesin core complex, this phenotype was first described for the cohesin accessory factor *Nipped-B*, that is part of the kollerin complex required for the uploading of cohesin onto chromatin (Dorsett and Merkenschlager, 2013; Rollins et al., 1999). In *Drosophila*, mutations in *dPds5*, that is both required for the unloading of cohesin from chromatin and for the maintenance of sister chromatid cohesion, have also been shown to affect transcription (Dorsett and Merkenschlager, 2013; Dorsett et al., 2005). The mode through which cohesion influences gene expression is still not clear. It is, however, known that cohesin binds preferentially to genes associated with high levels of RNA Polymerase II (RNA PolII), and evidence suggests that it might facilitate the transition from promoter-proximal paused to elongating RNA PolII (Schaaf et al., 2013). Additionally, cohesin has also been shown to interact with the Mediator complex (Kagey et al., 2010), as well as, with other transcription related proteins (Dorsett and Merkenschlager, 2013). The Mediator complex is a transcriptional co-activator, that has been shown to bind RNA polymerase,

regulating several aspects of transcriptional activation and repression, such as enhancer-promoter looping and RNA PolII phosphorylation and elongation (Dorsett and Ström, 2012; Kagey et al., 2010).

The first *Nipped-B* mutations were isolated in a screen designed to identify proteins involved in enhancer-promoter communication, by looking at the *cut* gene expression. The expression of this gene is influenced by the presence of a *gypsy* transposon which is recognized by the insulator protein Su(Hw), that blocks interactions between enhancers and promoters. *Nipped-B* mutations increase the inhibitor effect of Su(Hw) (Rollins et al., 1999), suggesting a role for this protein in enhancer-promoter communication and a possible cross-talk between cohesin proteins and insulator proteins. Despite this evidence and the fact that 80% of the DNA-binding sites of the insulator accessory factor CP190 overlap with cohesin, specifically dSCC3 (Bartkuhn et al., 2009), in *Drosophila* these two protein types are not thought to interact. On the contrary, in mammals CTCF has been shown to interact with cohesin and to depend on this interaction to fulfil its function as an insulator (Nativio et al., 2009; Wendt et al., 2008). In *Drosophila*, this role appears to be performed by two insulator accessory proteins, namely CP190 and MOD(mdg4) (Gerasimova et al., 2007; Ghosh et al., 2001). Furthermore, CP190 has been shown to be essential for the clustering of several insulators, forming the so called insulator bodies (Gerasimova et al., 2007; Pai et al., 2004).

Insulators are considered to influence gene expression through the mediation of enhancer-promoter interactions and the establishment of boundaries between heterochromatin and euchromatin (Phillips-Cremins and Corces, 2013; Vogelmann et al., 2011). Recent work has called for a reappraisal of the function traditionally attributed to these DNA-protein complexes. Work from the Corces lab has shown that more than acting as boundary elements

that stop the spread of repressive transcription marks, insulators seem to promote their accumulation within a given domain and therefore assist in the maintenance of a certain level of silencing (Bortle et al., 2012). In addition, it has been suggested that insulators might differently regulate gene expression through the formation of long-range inter- and intra-chromosome interactions. The nature of these interactions depends on the genomic and chromatin context where they occur, which in turn influences the network of interacting proteins and posttranslational modifications (Phillips-Cremins and Corces, 2013).

It is known that in *dPds5* mutants a DNA Damage Response (DDR) is activated (Barbosa et al., 2007). In mitotic cells, checkpoint activation has been shown to, aside from recruiting repair proteins to DSB sites, result in chromatin modifications in the surrounding areas, mainly through ATM. These range from post-translational modifications of the circumjacent histones to chromatin remodelling, such as decondensation (Polo and Jackson, 2011; Shiloh and Ziv, 2013). One obvious consequence of such events would be alterations in the transcriptional state of the affected genomic region. Indeed, two independent studies have shown that upon ATM activation, transcription is inhibited (Kruhlak et al., 2007; Shanbhag et al., 2010).

In order to continue to understand dPDS5 function during mid-oogenesis, we addressed the functional consequences of its depletion in term of insulator body assembly and gene expression regulation, by analysing two different *dPds5* alleles.

3.2 Material and Methods

3.2.1 Fly stock maintenance

All *Drosophila* stocks were raised under standard conditions at 23°C. The *dPds5*^{2} and *dPds5*^{6} alleles were obtained in a screen to unveil mutations that present DDR-induced eggshell ventralization (Barbosa et al., 2007); the BEAF32$^{GFBF.XA}$ and BEAF32$^{GFBF.3A}$ transgenic line were given by Craig Hart (Roy et al., 2007); *dChk2*^{p6}, *dRad54*^{AA}, *dRad54*^{RU}, OregonR were part of the lab stock collection; the *ovo*^{D} line (#4434) was obtained from Bloomington Stock Center; PABP2:GFP (flytrap line Pabp2ZCL3178) (Morin et al., 2001) was obtained from the Kyoto Stock Center.

3.2.2 Induction of germline clones

Germline clones where induced using the FLP/FRT system (Xu & Rubin, 1993). *dPds5* single mutant germline clones were obtained either in a *FRT42B nls-GFP* background, where *y w P{ry*^{1} *hs-FLP*$_{22}$*}; P{w*^{1} *FRT42B} P{w*^{1} *FRT nls-GFP}/CyO, hs-hid* females were crossed with *w P{w*^{1}*faf-LacZ}/Y; P{w*^{1} *FRT 42B} dPds5*$^{2\ or\ 6}$*/CyO, hs hid,* or in *FRT42B ovo*^{D} background, by crossing *w P{w*^{1}*faf-LacZ}; P{w*^{1} *FRT 42B} dPds5*$^{2\ or\ 6}$*/CyO, hs hid* females with *y w P{ry*^{1} *hs-FLP*$_{22}$*}/Y; P{w*$^{+mW.hs}$*=FRT(w*^{hs}*)}G13 P{w*$^{+mC}$*=ovo*^{D1}*-18}2R /CyO, hs-hid* males. To obtain *dChk2*^{p6} *dPds5* double mutant germline clones, y *w P{ry*^{1} *hs-FLP*$_{22}$*}; dChk2*^{p6} *P{w*^{1} *FRT42B} P{w*^{1} *FRT nls-GFP}/CyO, hs-hid* females were crossed with *y w P{ry*^{1} *hs-FLP*$_{22}$*}/Y; dChk2*^{p6} *P{w*^{1} *FRT 42B} dPds5*$^{2\ or\ 6}$*/CyO, hs hid* males. Three days after establishing the crosses the adults were transferred to a new vial and after another three days the third instar larvae were heat-shocked for 1h at 37°C for two consecutive days. The female flies were fed a fresh yeast supplement four days after eclosion and dissected, as described, on the fifth

day. Germline clones were identified either by the lack of auto-fluorescent nuclear GFP when obtained in a *FRT42B nls-GFP* background or by survival beyond stage 7/8, if obtained in a *FRT42B ovo^{D}* background.

3.2.3 Dissection of Drosophila *ovaries*

Ovaries were processed for immunofluorescence as described by Navarro and colleagues (Navarro et al., 2004). For each genotype five to six pairs of ovaries were dissected in 1xPBS. Fixation was performed at room temperature (RT) for 20 minutes in 1xPBS containing 3% to 6% of EM grade formaldehyde and 0.5% of NP-40, in a 1:3 ratio with heptane. The samples were rinsed three times and washed three times for 5 minutes with 1xPBST (1xPBS with 0.2% Tween-20). Afterwars, the ovarioles were separated using a tungsten needle, and subsequently permeabilized and blocked for one hour in 1xPBST with 1% Triton X-100 and 1% BSA at RT. After washing the samples three times for 20 minutes with 1xPBST they were ready to be processed for immunofluorescence or DNA staining.

3.2.4 Immunofluorescence of Drosophila *ovaries*

Primary antibodies were used at the following dilutions: 1:1000 for α-CP190 antibody Rb188 (Whitfield et al., 1988) 1:500 for α-PABP2 (Benoit et al., 1999); and 1:500 for α-Myc c-Myc antibody (9E10) (Santa Cruz Biotechnology, Inc.). Alexa 546-conjugated and Alexa 488-conjugated secondary antibodies (Molecular Probes, Eugene, OR) were used at a dilution of 1:500. DNA was stained either with TOTO-3® or DAPI (Molecular Probes, Eugene, OR) diluted 1:1000 or 0.3µM, respectively *as per* company instructions. Ovaries were

mounted in Vectashield (Vector Labs, Burlingame, CA) and visualized in Leica SP5 Live (Leica, Bannockburn, IL) or Zeiss Meta 501 (Carl Zeiss Microscopy, Germany) confocal microscopes.

3.2.5 Imaris analysis

A Leica SP5 confocal microscope (Leica, Bannockburn, IL) was used to obtain complete z-stacks of the oocyte nucleus using a HyD detector and photon counting. The following settings were maintained identical in all acquisitions: gain, zoom and 0.29µm of spacing between stacks. Taking advantage of the volume rendering tool in the Imaris software (Bitplane Inc., Scientific Software) a 3D multichannel image for each oocyte nucleus was obtained and analysed. A volume selection of the oocyte nucleus was created and the surface contours of the CP190 foci where defined in each oocyte nucleus using the intensity threshold (with surface roughness set to 0.145µm). To control background interference, a volume selection identical to the one drawn for the oocyte nucleus was drawn in the background staining of the egg chamber and the same procedure was applied. Objects defined in the oocyte nucleus were considered to be CP190 foci only if their volume was over the maximum volume measured in the background staining. After these background exclusions, the average foci volume was calculated for each oocyte nucleus using the number of foci and their size. Using the excel output file with objects statistics created by the MeasuremntPro features of the Imaris software, the graphic and statistical data obtained were processed with the R software, the median of the average foci volume for each genotype were compared using the Mann-Whitney test.

3.2.6 Click-IT® RNA Imaging Kit

The Click-IT RNA Imaging Kit (Molecular Probes, Eugene, OR) was used to visualize nascent RNA in *Drosophila* ovaries. The following alterations were introduced to the manufacturer's instructions: ovaries were dissected in Grace's Insect Medium (Sigma-Aldrich LLC, Co) pre-warmed to RT, and then transferred and incubated in Grace's Insect Medium supplemented with 1mM of EU-N_3 for 1h at RT; subsequently fixed for 20min at RT in 6% formaldehyde in 1xPBS; washed once in 1xPBS; and permeabilized for 20min at RT in 0,5% Triton X-100 in 1xPBS; after which we proceeded as described in the manufacturer's instructions.

In the case of germline clones induced in a *FRT42B nls-GFP* background, additional steps had to be performed in-between the permeabilization and the Click-IT reaction in order to preserve the GFP fluorescence. After permeabilizing the ovaries, as previously described, these were washed two times in 1xPBT, blocked for 1h at RT in 2% BSA in 1xPBT, and finally incubated for 1h in a 1:200 GFP-Booster _Atto488 (Chromotek, Germany) solution in 1xPBT with 2% BSA. After the GFP-Booster _Atto488 (Chromotek, Germany) incubation, the ovaries were washed two times in 1xPBT with 2% BSA and once in 1xPBS, and then we followed the Click-IT® RNA Imaging kit instructions. The processed ovaries were mounted in Vectashield (Vector Labs, Burlingame, CA) and visualized in a Leica SP5 Live confocal microscope (Leica, Bannockburn, IL). The frequency of ovaries incorporating EU-N_3 was calculated using the Microsoft Excel software (Microsoft Corporation) and R software was used to run Fisher's Exact Statistical test and the "Bonferroni" correction, to adjust the p-values for multiple comparisons.

3.3 Results

3.3.1 Eight novel point mutations map to the cohesin accessory factor dPDS5

In a screen designed to identify mutations that elicit eggshell ventralization through the activation of a DDR, the *cohiba* locus was identified as the *Drosophila* homologue of the conserved cohesin accessory factor *PDS5* (Barbosa et al., 2007). A total of eight new EMS-generated *dPds5* mutations were obtained, all of them lethal when *in trans* with the hypomorphic P-element P{LacW}l(1)k13312^{k13312} insertion (*dPds5^{k}*) (Fly Base ID: FBgn0021887). This *dPds5^{k}* allele was used to find the *dPds5* locus (Barbosa et al., 2007). We defined an allelic series based on the viability of our *dPds5* alleles over *dPds5^{k}*. Of the eight alleles, three had lower viability than *dPds5^{k}*/DF(2R)BSC39 (Figure 3.1 and Table S3.1). Two alleles were used in this work, *dPds5^{6}* and *dPds5^{2}*.

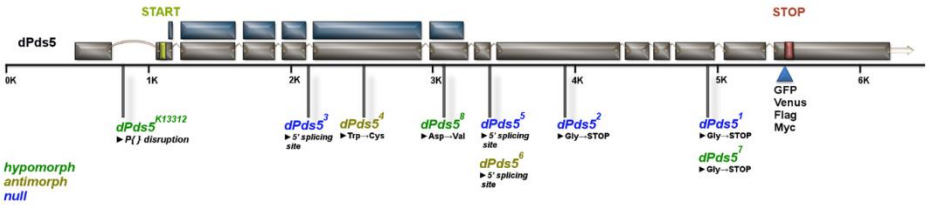

Figure 3.1 – Schematic representation of *dPds5* gene locus (CG17509) adapted from Flybase (FBgn0021887), where exons are depicted by grey boxes, introns by lines and the region of homology with the human *Pds5* by blue boxes. The location of the mutated sites in each of the eight *dPds5* mutant alleles (Barbosa et al., 2007), as well as, the insertion sites of both the P-element P{LacW}l(1)k13312^{k13312} (*dPds5^{k13312}*) and of the tags used to determine dPDS5 expression pattern are indicated.

3.3.2 dPDS5 is required to restrain CP190 to foci in the oocyte nucleus

To determine if dPDS5 is required for insulator foci assembly in the oocyte nucleus, we induced *dPds5* mutant germline clones and looked at the

localization of two insulator proteins. We started by looking at the accessory protein CP190, known to be required for insulator body assembly (Pai et al., 2004). In both alleles, CP190 appears as large nuclear aggregates that sometimes accumulate on the fragmented karyosome of stage 6 oocytes (Figure 3.2B). However, *dPds5* mutants elicit a persistent DDR leading to the appearance of certain phenotypes, such as egg ventralization and karyosome fragmentation (Barbosa et al., 2007). To determine if the observed phenotype was a consequence of checkpoint activation upon dPDS5 loss, we induced germline clones in a *dChk2*^{p6} mutant background. By removing the checkpoint effector protein dCHK2 we are ensuring that any phenotype present is a direct consequence of our mutant; for example, in repair mutants egg ventralization is abolished when dCHK2 is lost, since it is a consequence of checkpoint activation and not directly due to the loss of the repair protein (Ghabrial et al., 1998; Staeva-Vieira et al., 2003). In this background, CP190 mislocalization was maintained, appearing in large foci when compared with the respective controls (Figure 3.2C).

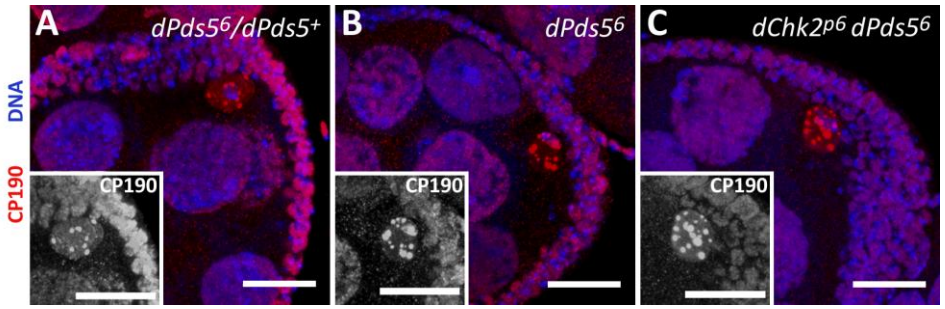

Figure 3.2 - dPDS5 is required to restrict CP190 to foci in the oocyte nucleus. (A) In a control oocyte (*dPds5*^{6}/*dPds5*$^{+}$) normal sized foci are observed, some located in close proximity to the karyosome. (B) In a *dPds5*^{6} single mutant the CP190 foci appear bigger and some seem to be spread on top of the fragmented karyosome. (C) In a *dChk2*^{p6} *dPds5*^{6} double mutant the CP190 foci are similar to the ones observed in B. In all images: CP190 is in red; DNA is in blue; insets, detail of CP190 in the oocyte nucleus; anterior to left, posterior to the right; scale bar = 20µm.

To get a more accurate understanding of the observed phenotype, the Imaris software (Bitplane) was used to define the surface of the CP190 bodies and quantify their volume in oocytes of the desired genotypes (Figure 3.3A-C). The average foci volume per oocyte nucleus was determined (Table S3.2 and Table S3.3) and the median of the averages compared between genotypes (Figure 3.3D). The majority of the analysed *dPds5*^{2} (n=10) and *dPds5*^{6} (n=9) stage 6 oocytes presented the described CP190 mislocalization, that was never observed in the respective controls, *dPds5*^{2}*/dPds5*$^{+}$ (n=12) and *dPds5*^{6}*/dPds5*$^{+}$ (n=14). Furthermore, the median foci volume was found to be significantly bigger in the *dPds5*^{2} (7.10µm^{3}) and *dPds5*^{6} (7.86µm^{3}) germline clones, when compared to their respective controls *dPds5*^{2}*/dPds5*$^{+}$ (3.92µm^{3}) and *dPds5*^{6}*/dPds5*$^{+}$ (3.01µm^{3}) ($p<0.01$ and $p<0.0001$, respectively; Mann-Whitney test) (Figure 3.3D). The same analysis was performed for stage 6 *dChk2*^{p6} *dPds5* germline clones (Table S3.2 and Table S3.3), and in accordance to the previously described phenotype (Figure 3.2), the median of the average volume of CP190 foci in *dChk2*^{p6} *dPds5*^{2} (6.24µm^{3}; n=11) and *dChk2*^{p6} *dPds5*^{6} (6.63µm^{3}; n=14) is significantly bigger than their respective controls, *dChk2*^{p6} *dPds5*^{2}*/dChk2*^{p6} *dPds5*$^{+}$ (3.10µm^{3}; n=10) and *dChk2*^{p6} *dPds5*^{6}*/dChk2*^{p6} *dPds5*$^{+}$ (3.,98µm^{3}; n=14) ($p<0.02$ and $p<0.01$, respectively; Mann-Whitney test) (Figure 3.3D); however, no significant difference in size was observed between the single and the respective double mutant germline clones ($p>0.05$, Mann-Whitney test; Figure 3.3D). Furthermore, no significant difference in foci number was observed between the single *dPds5* mutants and *dChk2 dPds5* double mutants (data not shown). These results lead us to conclude that the CP190 mislocalization phenotype is not a consequence of checkpoint activation upon dPDS5 loss. This conclusion is further supported by the fact that the CP190 foci do not appear to be bigger in both *dRad51*$^{003/057}$ and *dRad54*$^{AA/RU}$ repair mutants (Figure 3.4), where the dATR-mediated checkpoint is

permanently active (Ghabrial et al., 1998; Staeva-Vieira et al., 2003). Hence, dPDS5 is specifically required in the oocyte nucleus to constrain the volume of the CP190 foci.

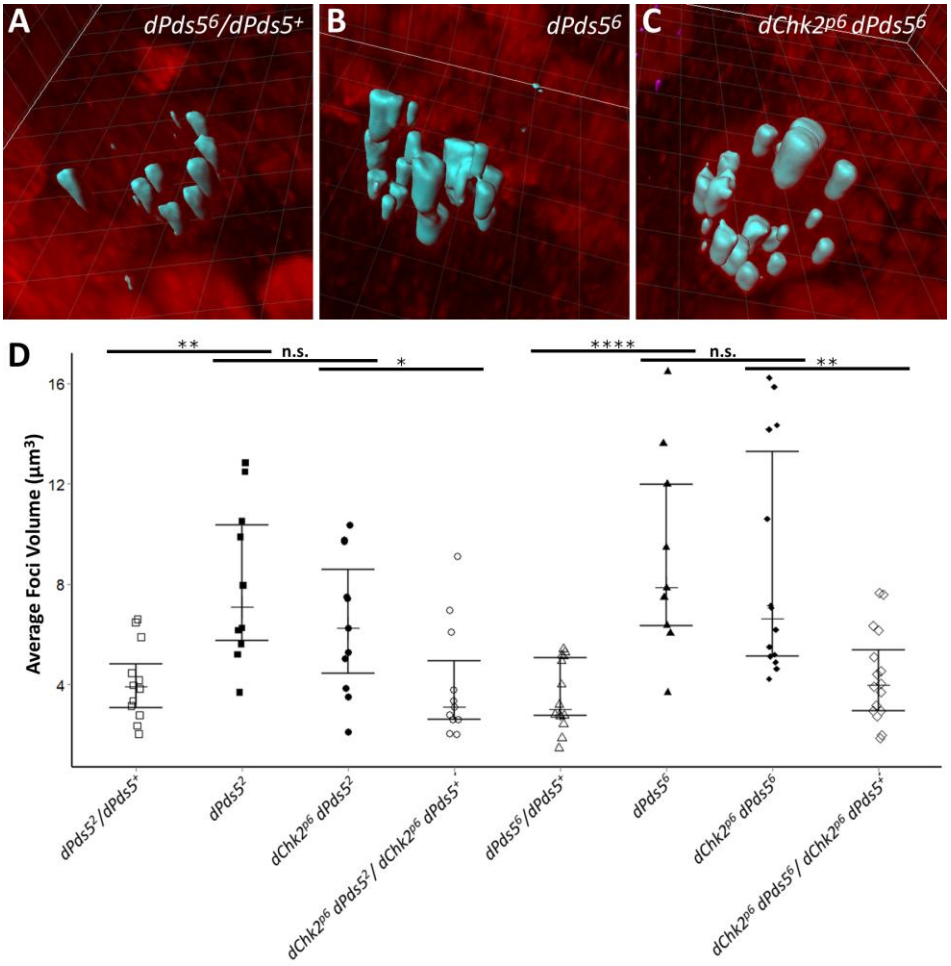

Figure 3.3 - Quantification of CP190 foci in stage 6 *dPds5* single mutant and *dChk2^{p6} dPds5* double mutant germline clones. (A-C) Exemplification of how the CP190 foci surfaces were determined based on the oocytes shown on figure 3.1 using the Imaris software, in turquoise. (D) Graphic representation of the average foci volume per oocyte for the different genotypes analysed Significance values were obtained using the Mann-Withney test (n.s., p-value>0.05; *, p-value<0.05; **, p-value<0.01; ****, p-value<0.0001).

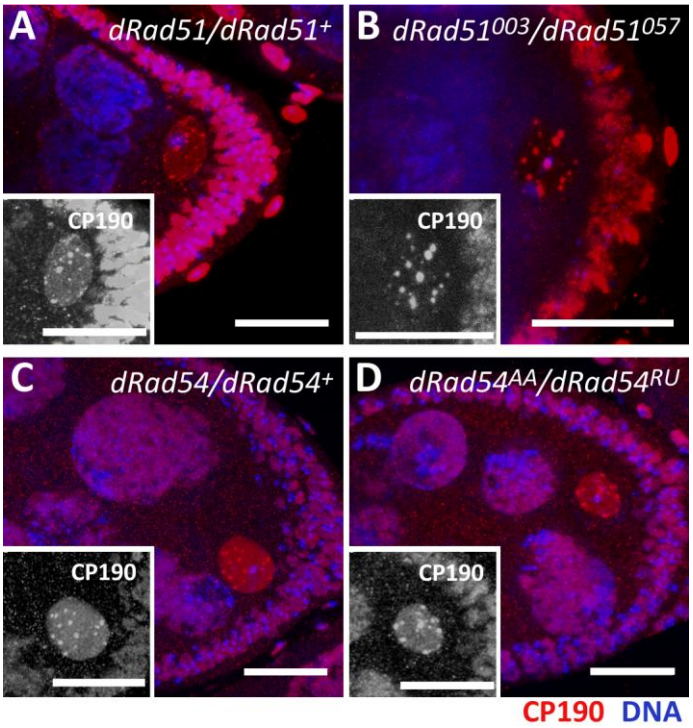

Figure 3.4 - CP190 localization is not affected in stage 6 egg chamber of DSB repair mutants. (A) *dRad51/dRad51*$^{+}$ (B) *dRad51*^{003}*/dRad51*^{057} (C) *dRad54/dRad54*$^{+}$ (D) *dRad54*^{AA}*/dRad54*^{RU} In all images: CP190 is in red; DNA is in blue; insets, detail of the oocyte in CP190 channel; anterior to left, posterior to the right; scale bar = 20µm.

3.3.3 dPDS5 is required for the presence of BEAF32 in the oocyte nucleus

We next looked at BEAF32:GFP (BEAF32$^{GFBF.3A}$) localization in *dPds5* germline clones. Only stage 7/8 or later egg chambers were considered, because *dPds5/ovo*^{D} heterozygous egg chambers can persist until stage 6. Contrary to what is seen for CP190, where only stage 6 egg chambers present an increase in average volume of this protein foci, BEAF32 localization was affected in all analysed stages for both *dPds5*^{2} and *dPds5*^{6} germline clones (Figure 3.5).

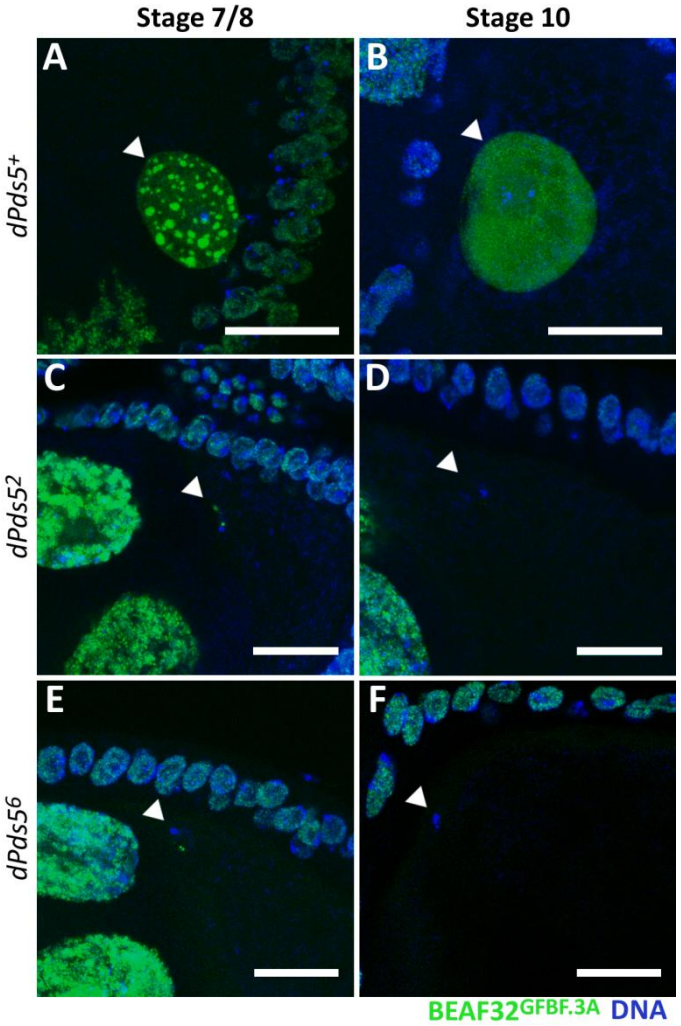

Figure 3.5 – BEAF32$^{GFBF.3A}$ is excluded from the oocyte nucleus in *dPds5*^{2} and *dPds5*^{6} germline clones. (A-B) *dPds5*$^{+}$ control; (C-D) *dPds5*^{2}; (E-F) *dPds5*^{6}. In all images: BEAF32$^{GFBF.3A}$ is in green; DNA is in blue; arrowhead indicates the oocyte nucleus; anterior to left, posterior to the right; scale bar = 20µm.

While 98% (n=66) of *dPds5*$^{+}$ control egg chambers presented a nuclear BEAF32$^{GFBF.3A}$ signal (either in foci or evenly distributed in the nucleoplasm) (Figure 3.5AB, Figure 3.7A and Table S3.4), only 38% and 29% of *dPds5*^{2} and *dPds5*^{6} germline controls, respectively, had BEAF32$^{GFBF.3A}$ in their oocyte

nucleus (Figure 3.5C-F, Figure 3.7A and Table S3.4). However, the presence of BEAF32$^{GFBF.3A}$ appears to be unaffected in the equally mutant nurse cells, of the same germline clones of both alleles (Figure 3.5). A preliminary analysis using a second insertion line on the X chromosome, presented a similar phenotype (Table S3.4).

The fly lines that would allow us to determine if the observed phenotype was consequence of checkpoint activation upon dPDS5 loss [*BEAF32*$^{GFBF.XA}$*;dPds5*$^{2\ or\ 6}$*/CyO, hshid; dChk2 RNAi/TM6* and *BEAF32*$^{GFBF.XA}$*; FRT42B ovo*^{D}*/CyO, hshid; dChk2 RNAi/TM6* (the *dChk2* RNAi line and *MTD*Gal4 line are described in chapter 4)] were not finished due to their decrease viability, and also due to time constraints. Nonetheless, preliminary data obtained using the *dRad54* repair mutant, which activates both dATR and dCHK2, suggest that the latter might be true. In 100% of *dRad54*$^{AA/RU}$ (n=75) mutant egg chambers BEAF32$^{GFBF.3A}$ was present in the oocyte nucleus, a clear contrast to what happens in *dPds5* germline clones (Figure 3.6, Figure 3.7 and Table S3.4). This leads us to propose that dPDS5 is necessary for the recruitment of BEAF32 to the oocyte nucleus.

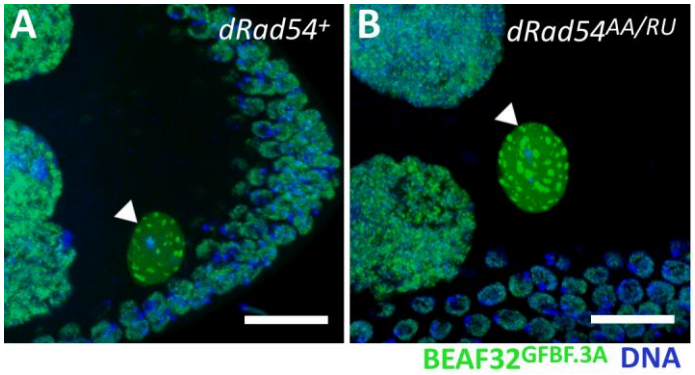

Figure 3.6 - BEAF32$^{GFBF.3A}$ localization is not affected in the repair mutant *dRad54*. Stage 7/8 egg chamber of (A) *dRad54*$^{+}$ control and (B) *dRad54*$^{AA/RU}$. In all images: BEAF32$^{GFBF.3A}$ is in green; DNA is in blue; arrowhead indicates the oocyte nucleus; anterior to left, posterior to the right; scale bar = 20µm.

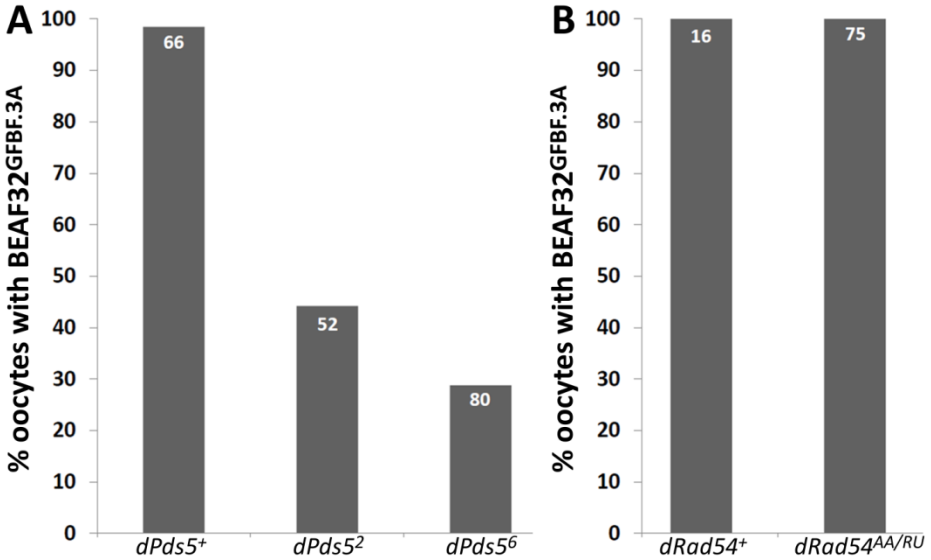

Figure 3.7 - Quantification of the frequency of oocytes presenting BEAF32$^{GFBF.3A}$ in their nucleus: (A) stage 7/8 to 10 in *dPds5*$^{+}$, *dPds5*^{2} and *dPds5*^{6} germline clones; (B) stage 4 to 10 in *dRad54*$^{+}$ controls and respective *dRad54*$^{AA/RU}$ mutant oocytes. On top of each bar is given the total number of scored oocytes.

3.3.4 The oocyte nucleus presents two phases of active transcription during the Prophase I arrest

The requirement of dPDS5 to either restrain or recruit insulator proteins to nuclear foci in the oocyte raises the possibility of this protein also being involved in gene expression regulation in the oocyte. We addressed this possibility by first looking at the localization of an indirect transcription marker, the Poly-A Binding Protein II (PABP2) that is required for mRNA polyadenylation (Benoit et al., 1999). Using both a PABP2:GFP trap line (Morin et al., 2001) and an antibody against PABP2 (Benoit et al., 1999), we found that PABP2 appears as nuclear foci in the oocyte nucleus at stage 4. These foci increase in number until stage 6 or 7/8 and are maintained thereafter. The foci

can either be located in close proximity to the karyosome or away from it in the nucleoplasm (Figure 3.8A-F).

The Click-IT® detection assay was then subsequently used to allow for a more direct assessment of RNA synthesis and a better understanding of its temporal dynamics. Ovaries were incubated *in vivo* for an hour in the presence of an Uracil analogue (EU-N_3), after which they were fixed and EU-N_3 fluorescently labelled using the RNA Click-IT® imaging kit. RNAseA treatment of the ovaries, after EU-N_3 incorporation and detection, reduced the EU-N_3 to background levels confirming that the obtained signal results from the incorporation of this Uracil analogue (Figure S3.1). For all analysed genotypes (OregonR control line, *dPds5*$^{2\ or\ 6}$ single mutants, *dChk2*^{p6} *dPds5*$^{2\ or\ 6}$ double mutants, *dRad51*$^{003/057}$ and *dRad54*$^{AA/RU}$ mutants, and for their respective controls) EU-N_3 incorporation was detected both in follicle and nurse cell nuclei of all stages, as expected (Figure 3.8E-L). Furthermore, two transcriptional phases were detected in the oocyte nucleus, the first one until stage 4 and the second one starting at stage 6 (Figure 3.8E-L and Table S3.5). Until stage 4, transcription appears as a well-defined round domain juxtaposed to the karyosome (Figure 3.8E). With the incubation time used, we failed to detect any EU-N_3 incorporation during stage 5 (Figure 3.8F and Table S3.5). In a small percentage of stage 6 oocytes, the EU-N_3 signal could be discerned as a fiber-like pattern on the karyosome surface. However, by stage 7/8 this signal becomes quite preponderant and surrounds most of the karyosome surface (Figure 3.8J and Table S3.5), becoming increasingly stronger as oogenesis progresses (Figure 3.8KL). In conclusion, the oocyte nucleus is transcriptionally active, presenting two morphologically distinct phases and a quiescence window, the latter overlapping with the initial insulator body appearance.

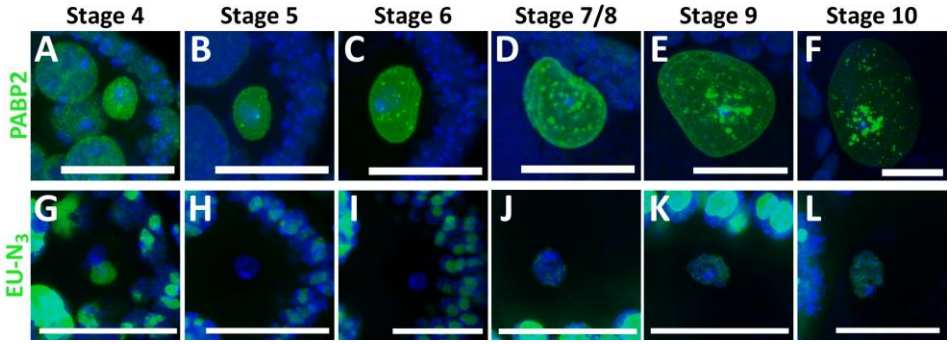

Figure 3.8 - The oocyte nucleus is transcriptionally active, presenting two distinct phases of EU-N_3 incorporation. (A-F) Expression of PABP2 from stage 4 to 10 of oogenesis, using PABP2:GFP trap line (Morin et al., 2001). (E-L) Dynamics of EU-N_3 incorporation from stage 4 to 10 in an *OregonR* wildtype background. In all images: DNA is in blue; anterior to left, posterior to the right; scale bar = 20µm.

3.3.5 Checkpoint activation in dPds5 mutants delays the start of the second transcriptional phase of the oocyte

Having clearly defined the transcription dynamics of the oocyte, we then enquired if dPDS5 played a role in the regulation of this cellular process. This question was addressed by incubating ovaries of the genotypes of interest in EU-N_3 and processing them as described in the previous section. Overall, the initial transcriptional phase does not appear to be majorly affected (Figure 3.9D, Figure 3.10 and Table S3.5). By looking at germline clones obtained in a *FRT42B nls-GFP*, we saw that even though a decrease in the frequency of transcribing stage 4 oocyte is seen for $dPds5^{2}$ (44%; n=18) when compared with the respective $dPds5^{2}/dPds5^{+}$ control (88%; n=11), the same is not observed for $dPds5^{6}$ (71%; n=24) and $dPds5^{6}/dPds5^{+}$ (71%; n=17); for neither allele were the comparisons found to be significantly different (p-value>0.05, Fisher's exact test).

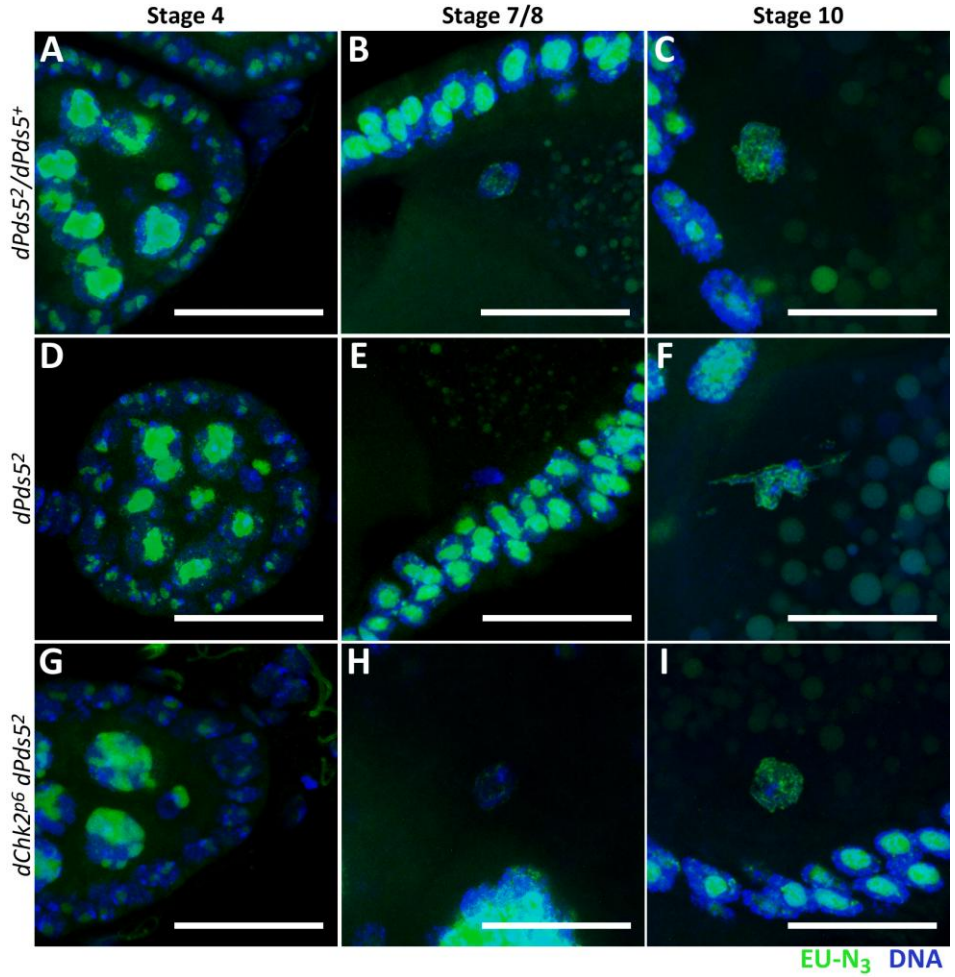

Figure 3.9 - Checkpoint activation in *dPds5* germline clones affects the start of the second transcriptional phase of the oocyte. (A-C) $dPds5^{2}/dPds5^{+}$ control egg chambers. (D-F) $dPds5^{2}$ germline clones. (G-I) $dChk2^{p6}$ $dPds5^{2}$ germline clones. For all genotypes an example of a stage 4 (left), a stage 7/8 (middle) and a stage 10 (right) is shown. In all images: EU-N_3 is green; DNA is in blue; anterior to left, posterior to the right; scale bar = 20µm.

When looking at stage 6 germline clones, generated in a *FRT42B nls-GFP* background, a decrease in the frequency of oocytes incorporating EU-N_3 can be seen for both alleles, $dPds5^{2}$: 5% (n=20) and $dPds5^{6}$: 6% (n=17) when comparing with their respective controls $dPds5^{2}/dPds5^{+}$: 27% (n=15) and $dPds5^{6}/dPds5^{+}$: 19% (n=21). However, these differences in frequency are not

significant (p-value>0.05, Fisher's exact test), although they already show a tendency for a delay in the start of the second transcriptional phase. A tendency that is confirmed when looking at stage 7/8 germline clones, both in *FRT42B nls-GFP* and *FRT42B ovo^{D}* backgrounds, where a significant decrease in the number of transcribing oocytes is observed, *dPds5^{2}*: 23% (n=13) vs. *dPds5^{2}/dPds5^{+}*: 94% (n=16) and *dPds5^{6}*: 14% (n=22) vs. *dPds5^{6}/dPds5^{+}*: 90% (n=19) (for both alleles p-value<0.01, Fisher's exact test) These results suggest that dPDS5 is in fact involved in gene expression. However, by stage 10 the frequency of transcribing oocytes (*dPds5^{2}*: 80%, n=10; *dPds5^{6}*: 100%, n=6) is close to the one observed for the controls (*dPds5^{2}/dPds5^{+}*: 94%, n=18; *dPds5^{6}/dPds5^{+}*: 100%, n=13) (p-value>0.05, Fisher's exact test; Figure 3.9; Figure 3.10 and Table S3.5).

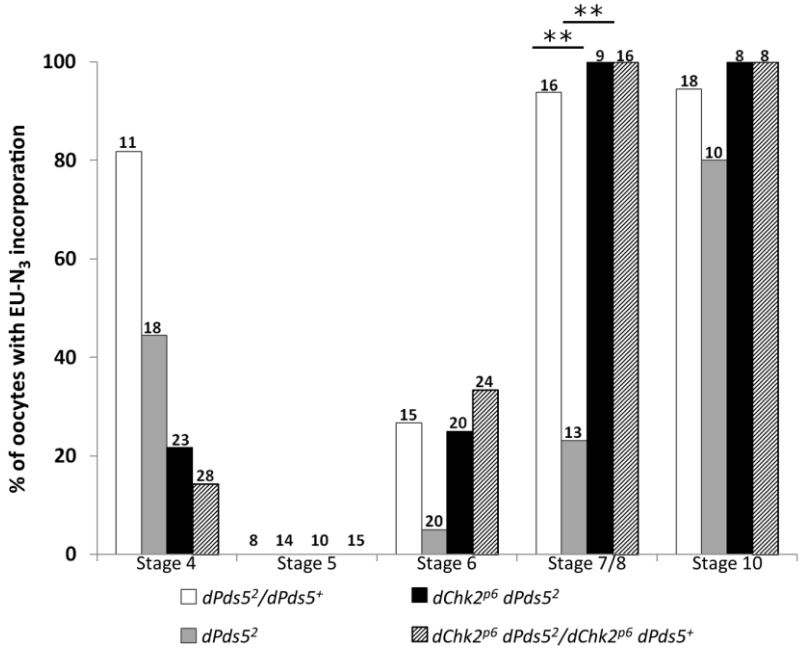

Figure 3.10 - Quantification of the frequency of oocytes showing signs of EU-N_3 incorporation in *dPds5^{2}/dPds5^{+}* controls, *dPds5^{2}* germline clones, *dChk2^{p6} dPds5^{2}* double mutant germline clones and *dChk2^{p6} dPds5^{2}/dChk2^{p6} dPds5^{+}* controls. On top of each bar the total number of scored oocytes is given. Significance values were obtained using Fisher's exact test (**, p-value<0.01).

The following step was to verify if the observed phenotype was a consequence checkpoint activation due to lack of dPDS5. We crossed *dChk2^{p6} FRT42B nls-GFP* females with *dChk2^{p6} FRT42B dPds5$^{2\ or\ 6}$* males, and induced recombination, allowing us to obtain *dChk2^{p6} FRT42B dPds5$^{2\ or\ 6}$* double mutants, where checkpoint activation is abolished. In these double mutants, the frequency of EU-N_3 incorporation in stages 6 and 7/8 oocytes was restored to control levels: for stage 6, 25% (n=20) of *dChk2^{p6} dPds5^{2}* compared to 33% (n=24) *dChk2^{p6} dPds5^{2}/dChk2^{p6} dPds5^{+}* (p-value>0.05, Fisher's exact test; for stage 7/8, 100% (n=9) of *dChk2^{p6} dPds5^{2}* compared to 100% (n=16) *dChk2^{p6} dPds5^{2}/dChk2^{p6} dPds5^{+}* (p-value=1, Fisher's exact test). For *dPds5^{6}*, our data is still preliminary, particularly for stage 7/8. Nonetheless, a certain level of recovery is seen for stage 6 with 13% (n=18) of *dChk2^{p6} dPds5^{6}* of the oocytes incorporating the Uracyl analogue in contrast with the 6% (n=17) seen on the single mutant and this difference was revealed to be not significant (p-value>0.05, Fisher's exact test). In conclusion, dPDS5 influences gene expression in the oocyte by delaying the start of the second transcriptional phase through the activation of a DNA damage response. This conclusion is further supported by the fact that a similar delay is observed in *dRad54$^{AA/RU}$* mutants (Figure S3.2). In addition, an analogous analysis performed for PABP2 revealed that the localization of this protein in the oocyte nucleus was also affected in *dPds5* mutant germline clones due to checkpoint activation. Furthermore, both *dRad51* and *dRad54* mutants presented a defective PABP2 expression exclusively in the oocyte (Figure S3.3).

3.4 Discussion

3.4.1 dPDS is required for insulator body assembly in the oocyte nucleus

In the previous chapter we determined that dPDS5:TAG co-localizes with insulator protein foci, also known as insulator bodies, containing CP190, MOD(mdg4)2.2 and BEAF32 in the oocyte nucleus. In the present chapter, we set out to verify if dPDS5 has any role in the assembly of these nuclear structures, by looking at what happens to them in our mutant alleles. Our analysis revealed that dPDS5 is differently required for the localization of CP190 and BEAF32. In the *dPds5* mutant background, while CP190 is still present in the oocyte nucleus but improperly arranged (Figure 3.2), BEAF32 appears to be mostly absent (Figure 3.5). This difference might be a consequence of the functions of these proteins, since CP190 is an accessory insulator protein, known to interact with several other insulator proteins and to be required for insulator body assembly (Pai et al., 2004; Phillips-Cremins and Corces, 2013), while BEAF32 is a DNA-binding insulator protein. In *Drosophila*, the general consensus is that cohesin is not involved in insulator function, since little to no overlap was observed in several cell lines between NIPPED-B binding sites and dCTCF (Dorsett, 2009; Misulovin et al., 2008; Phillips-Cremins and Corces, 2013). On the other hand, evidence showing that there is an 80% overlap between CP190 and dSCC3 binding sites in S2 cells (Bartkuhn et al., 2009). However, it is known that in mammalian cells, cohesin proteins allow CTCF to function as an insulator and are also required for CTCF to control the transcription of the *H19/EFG2* locus. In addition, in the mammalian system, cohesin proteins have been shown to be critical in the maintenance of the CTCF-mediated chromatin conformation of this locus (Nativio et al., 2009; Wendt et al., 2008). Evidence also shows that upon

depletion of cohesins there is a 50% reduction in CTCF binding (Wendt et al., 2008). In this work, we present evidence that a cohesin-related protein, dPDS5, is required for proper localization or even recruitment of two insulator proteins, CP190 and BEAF32, in *Drosophila* oocytes. This suggests that the role of cohesions in ensuring proper insulator protein localization and function is a more conserved role than initially thought. Nonetheless, further work is required to assure that the BEAF32 absence phenotype is not a consequence of checkpoint activation upon dPDS5 loss, by looking at *dChk2^{p6} dPds5* double mutants. In addition, we should extend this analysis to other oocyte insulator proteins, such as MOD(mdg4)2.2, and verify if the observed differences are maintained between insulator accessory proteins and DNA-binding proteins. It would also be interesting to look at diploid somatic cells known to also present insulator bodies and see what happens to these nuclear structures in a *dPds5* mutant background. This would allow us to determine if dPDS5 role in insulator body assembly is a general or an oocyte-specific role.

3.4.2 Checkpoint activation specifically affects oocyte transcription

The co-localization between dPDS5 and insulator proteins and the requirement of this protein in the oocyte for the proper assembly of insulator bodies, suggests that dPDS5 is involved in oocyte gene expression regulation. Furthermore, cohesins themselves and dPDS5, in particular, have been shown to regulate transcription (Dorsett et al., 2005). Consequently, incorporation and subsequent detection of an Uracil analogue (EU-N_3) was used to obtain a more accurate description of gene expression in the oocyte nucleus. This analysis revealed two morphologically distinct transcriptional phases during Prophase I, with stage 5 of oogenesis corresponding to an intervening quiescent phase (Figure 3.8). These results are in agreement with early findings

by Mahowald and Tiefert (1970) and Dävring and Sunner (1982), where they injected *Drosophila* females with uridine [5-H^3] in their abdomen, and subsequently the ovaries were dissected and autoradiographed, and found incorporation of this modified uridine in stages 10 and stages 7/8 of oogenesis, respectively (Dävring and Sunner, 1982; Mahowald and Tiefert, 1970). Due to the increased power of today's microscopes, we were able to look at earlier oogenesis stages, giving us a finer temporal of how transcription proceeds during egg development.

In both mutant alleles used in this work, a delay in the start of the second transcriptional phase is seen, as a significant decrease in the number of stage 7/8 oocytes incorporating EU-N_3 is observed (Figure 3.9 and Figure 3.10). Nonetheless, by stage 10 the frequency of transcribing oocytes is close to wildtype levels (Figure 3.9 and Figure 3.10). Despite the observed delay phenotype, analysis of *dChk2^{p6} dPds5* double mutants revealed that this phenotype was a consequence of checkpoint activation due to dPDS5 loss (Figure 3.9 and Figure 3.10). Furthermore, this phenotype is also present in repair mutants, such as *dRad54*, that are known to activate the meiotic checkpoint through dATR and dCHK2 (Figure S3.2). This is the first time that transcription is described to be affected during *Drosophila* oogenesis upon meiotic checkpoint activation. However, recent work from both Kruhlak and colleagues (2009) and Shanbhag and colleagues (2010) has shown that upon ATM activation during DDRs, transcription can be inhibited (Kruhlak et al., 2007; Shanbhag et al., 2010), which is in accordance with the results here presented. As future work, it would be extremely interesting to determine if the oocyte transcripts vary between our mutant *dPds5* alleles and their controls, specially taking into consideration the phenotypes here described for the insulator proteins.

In conclusion, dPDS5 appears to be necessary for proper organization of the nuclear structure of the oocyte nucleus through interaction and subsequent localization of insulator proteins.

Author's Contributions

Identification and mapping of *dPds5* mutant alleles was performed by Vítor Barbosa, gene scheme was drawn by Patrícia Silva. Both CP190 immunofluorescence and statistical analysis were performed by Patrícia Silva. BEAF32:GFP confocal imaging was mainly performed by Raquel AM Santos, with help from Patrícia Silva; data analysis performed by Raquel AM Santos. PABP2 imaging and data analysis performed by Patrícia Silva. Click-IT® RNA imaging assay, confocal imaging and data analysis performed by Raquel AM Santos.

Acknowledgements

We would like to thank Craig Hart for providing with fly lines, and Béatrice Benoit and David Glover for antibodies used in this work.

3.5 Supplemental Material

Table S3.1 - Table with the viability of each of the allele *dPDs5* alleles in transheterozygosity over $dPds5^{13312}$, as well as of the deficiency DF(2R) BSC39 over $dPds5^{k13312}$ and $dPds5^{k13312}/dPds5^{k13312}$ used to determine the allelic series of our point mutations. Total number (N) of scored flies given between brackets.

Allele	$dPds5^{6}$	$dPds5^{4}$	$dPds5^{1}$	$dPds5^{2}$	$dPds5^{5}$
Viability (N)	0% (359)	2% (365)	4.4% (493)	5.0% (331)	5.4% (369)
Allele	$dPds5^{3}$	**DF(2R)BSC39**	$dPds5^{k}$	$dPds5^{7}$	$dPds5^{8}$
Viability (N)	5.8% (400)	25% (389)	32.3% (389)	41.8% (519)	45.6% (601)

Table S3.2 – Total foci number and average foci volume (μm^3) *per* analysed oocyte for $dPds5^{2}$ and $dChk^{p6}$ $dPds5^{2}$ double mutant germline clones and respective control.

$dPds5^{2}/dPds5^{+}$		$dPds5^{2}$		$dChk2^{p6}$ $dPds5^{2}$ / $dChk2^{p6}$ $dPds5^{+}$		$dChk2^{p6}$ $dPds5$	
Foci Nr.	Avr. Vol. (μm^3)	Foci Nr.	Avr. Vol. (μm^3)	Foci Nr.	Avr. Vol. (μm^3)	Foci Nr.	Avr. Vol. (μm^3)
4	2,79	20	3,68	2	9,13	7	9,77
5	3,16	7	6,25	2	2,80	7	5,05
6	3,85	7	9,88	18	2,02	5	7,49
6	2,04	6	5,62	15	3,10	19	3,86
7	4,46	6	12,83	12	2,62	10	6,24
9	5,89	14	5,20	14	2,05	14	2,11
5	3,98	8	12,47	8	2,61	9	9,70
7	3,36	7	6,16	2	3,78	12	3,53
4	2,37	8	7,95	6	3,35	15	10,35
5	6,48	12	10,51	6	6,96	12	5,29
12	6,61			8	6,09	6	7,44
7	4,18						

Table S3.3 - Total foci number and average foci volume (µm^3) *per* analysed oocyte for *dPds5^6* and *dChk^{p6} dPds5^6* double mutant germline clones and respective control.

dPds5^6/dPds5$^+$		***dPds5^6***		***dChk2^{p6} dPds5^6/ dChk2^{p6} dPds5$^+$***		***dChk2^{p6} dPds5^6***	
Foci Nr.	Avr. Vol. (µm^3)	Foci Nr.	Avr. Vol. (µm^3)	Foci Nr.	Avr. Vol. (µm^3)	Foci Nr.	Avr. Vol. (µm^3)
10	4,94	20	3,68	7	7,65	18	14,34
9	2,81	11	9,48	6	3,18	7	15,86
9	2,79	8	11,98	1	6,17	19	14,17
13	2,76	9	13,60	4	5,10	10	4,24
5	4,01	13	7,86	8	1,88	5	5,20
12	2,44	5	6,36	10	3,91	8	6,19
5	5,19	4	6,04	6	7,59	8	5,12
7	1,89	6,	7,47	5	6,34	5	4,89
3	1,47	6	16,46	10	3,71	5	4,63
9	3,21			4	4,05	8	7,16
5	2,80			11	4,41	5	10,61
6	5,13			17	4,55	3	5,51
15	5,30			21	2,97	3	16,23
12	5,41			10	2,00	6	7,06

Table S3.4 - Number of oocytes with BEAF32, total number of scored oocytes given between brackets. Either using a BEAF32:GFP transgene inserted on the X chromosome, BEAF32$^{GFBF.XA}$, or on the third chromosome, BEAF32$^{GFBF.3A}$, in *dPds5* germline clones induced in an *ovo^{D}* background, stage 7/8 to 10, or in a *dRad54* mutant background, stage 4 to 10, and respective controls.

Genotype		Oogenesis Stage					
		<4	**5**	**6**	**7/8**	**9**	**>10**
BEAF32$^{GFBF.3A}$	*dPds5^{+}*	--	--	--	27 (28)	8 (8)	30 (30)
	dPds5^{2}	--	--	--	5 (19)	0 (5)	15 (28)
	dPds5^{6}	--	--	--	11 (30)	0 (3)	12 (24)
	dRad54/dRad54^{+}	3 (3)	3 (3)	5 (5)	3 (3)	0	2 (2)
	dRad54^{AA}/dRad54^{RU}	10 (10)	15 (15)	28 (28)	9 (9)	6 (6)	7 (7)
BEAF32$^{GFBF.XA}$	*dPds5^{+}*	--	--	--	2 (2)	3 (3)	6 (6)
	dPds5^{2}	--	--	--	0 (2)	0 (1)	0 (3)
	dPds5^{6}	--	--	--	0	0	0

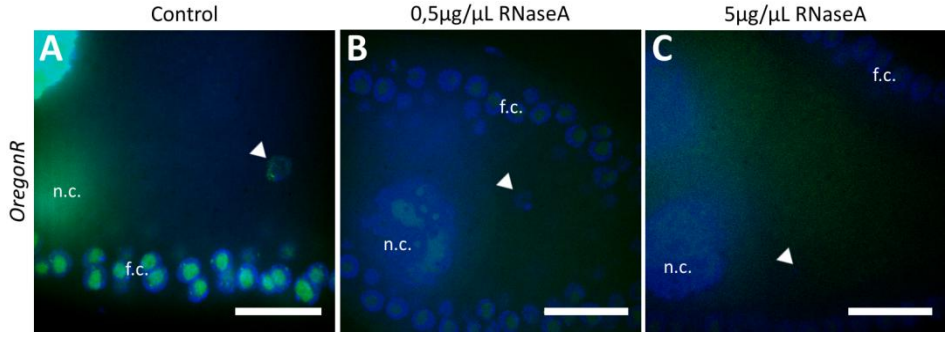

Figure S3.1 – RNaseA treatment for 30 minutes of *OregonR* ovaries, previously incubated for one hour in the presence of 1mM of the Uracil analogue EU-N_3, decreases the signal almost to background levels. (A) No treatment. (B) 0,5µg/µL of RNaseA. (C) 5µg/µL of RNaseA. In all images: EU-N_3 is green; DNA is in blue; anterior to left, posterior to the right; scale bar = 20µm.

Table S3.5 - Frequency of oocytes that showed EU-N_3 incorporation for all analysed genotypes, between brackets is indicated the total number of scored egg chambers. [a, b and c], for *dChk2^{p6} dPds5^{6}* we are showing the number of oocytes with transcription out of all the oocytes scored for these stages.

Genotype	Stage 4	Stage 5[a]	Stage 6	Stage 7/8[b]	Stage 10[c]
OregonR	79% (14)	0% (8)	0% (14)	60% (15)	100% (9)
dPds5^{2}/dPds5^{+}	82% (11)	0% (8)	27% (15)	94% (16)	94% (18)
dPds5^{2}	44% (18)	0% (14)	5% (20)	23% (13)	80% (10)
dPds5^{6}/dPds5^{+}	71% (17)	0% (13)	19% (21)	90% (19)	100% (13)
dPds5^{6}	71% (24)	0% (7)	6% (17)	14% (22)	100% (6)
dChk2^{p6} dPds5^{2}/dChk2^{p6} dPds5^{+}	14% (28)	0% (15)	33% (24)	100% (16)	100% (8)
dChk2^{p6} dPds5^{2}	22% (23)	0% (10)	25% (20)	100% (9)	100% (8)
dChk2^{p6} dPds5^{6}/dChk2^{p6} dPds5^{+}	37% (19)	0% (11)	30% (20)	100% (4)	100% (4)
dChk2^{p6} dPds5^{6}	46% (11)	0/4	13% (18)	1/1	1/1
dRad54^{+}	20% (30)	0% (14)	16% (32)	86% (14)	91% (11)
dRad54$^{AA/RU}$	13% (24)	0% (30)	0% (55)	19% (36)	83% (6)

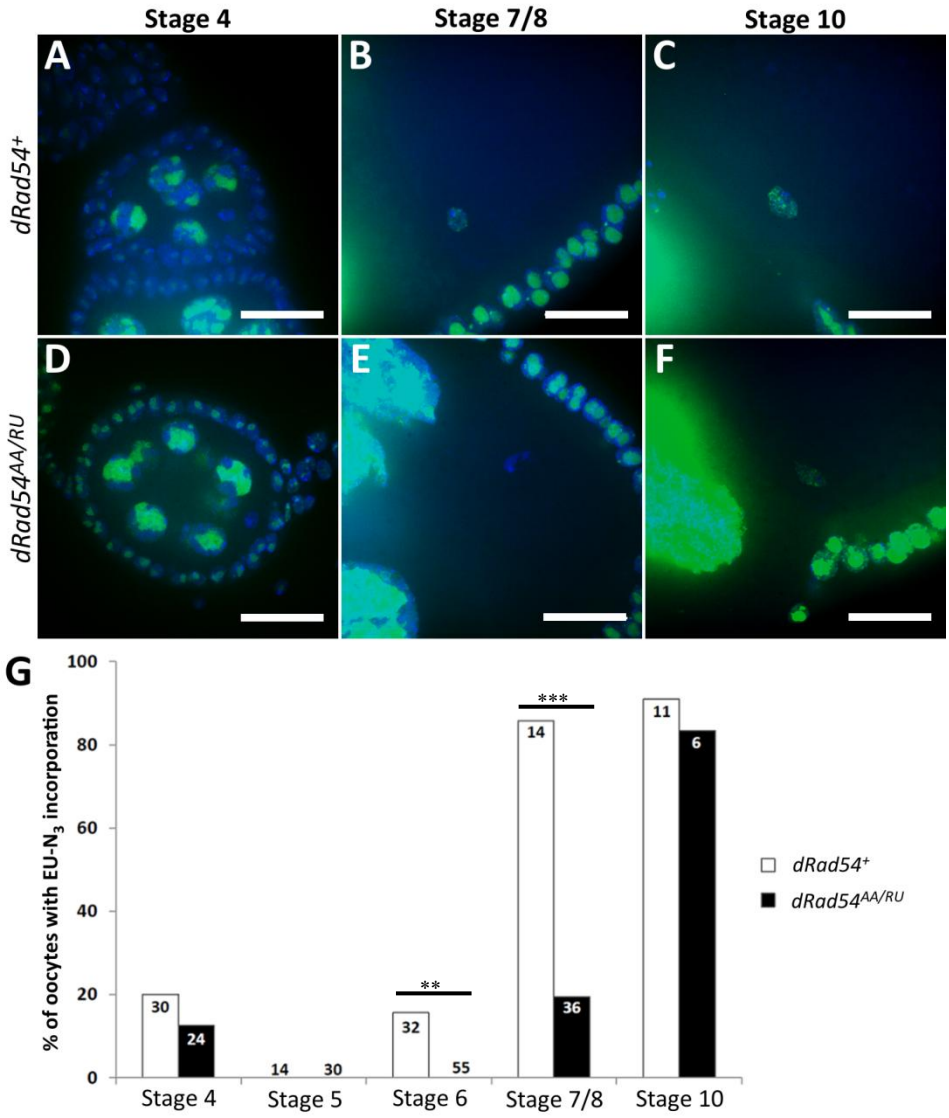

Figure S3.2 – *dRad54* repair mutants also show a delay in the start of the second transcriptional phase. (A-C) *dRad54*$^{+}$ control egg chambers. (D-F) *dRad54*$^{AA/RU}$ mutant egg chambers. (G) Graphic representation of the frequency of oocytes that show EU-N_3 incorporation. For both genotypes an example of a stage 7/8 (left) and a stage 10 (right) is shown. On top of each bar is given the total number of scored oocytes. In all images: EU-N_3 is green; DNA is in blue; anterior to left, posterior to the right; scale bar = 20µm.

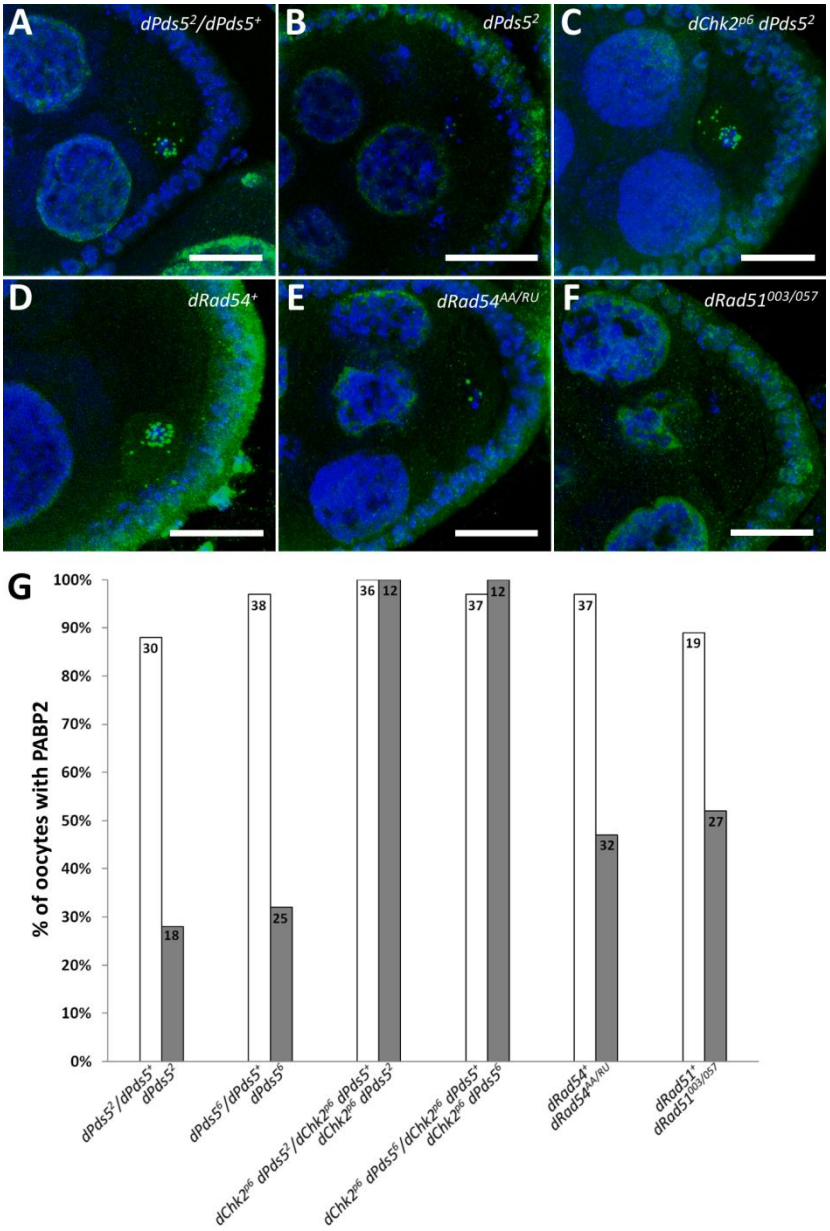

Figure S3.3 – Checkpoint activation in *dPds5* mutants and in the repair mutants *dRad51* and *dRad54* also affects PABP2 localization exclusively in the oocyte nucleus. (A-F) PABP2 localization, using a antibody anti-PABP2, in the genotypes of interest: (A) *dPds5²/dPds5⁺*; (B) *dPds5²*; (C) *dChk2^p6 dPds5²*; (D) repair mutant control *dRad54⁺*; *dRad54^AA/RU* and *dRad51^003/057*. In all images PABP2 is in green; DNA is blue; anterior to the left; posterior to the right; scale bar = 20µm.

4 A new dATM-dependent checkpoint monitors dPDS5 during oogenesis

Summary

Mutations in the cohesin accessory gene *dPds5* have been shown to trigger a DNA damage response in the *Drosophila* female germline that does not depend on dATR activation (Barbosa et al., 2007). To characterize this DDR, we performed genetic interaction assays with known checkpoint kinases, such as dATM and dCHK2, and also tried to identify other potential proteins under its surveillance. We have determined that both dATM and dCHK2 are part of this checkpoint pathway. Furthermore, our preliminary results suggest that another cohesin accessory protein, NIPPED-B, might be under DDR surveillance in the germline.

4.1 Introduction

Genetic recombination during gametogenesis allows the increase of variability. This cellular process requires the induction of endogenous Double Strand Breaks (DSBs) that trigger the activation of a meiotic checkpoint. This meiotic checkpoint is part of a network of pathways, generally known as DNA Damage Responses (DDRs), that both recruit repair proteins and stall the cell cycle until repair is complete (Harper and Elledge, 2007). Two main transducer kinases have been described to participate in these DDRs: Ataxia Telangiectasia–Mutated (ATM) and Ataxia Telangiectasia–Related (ATR). Both transducer kinases are frequently found in the same repair pathway. Upon DSB induction, these are recognized by the MRN (MRE11-RAD50-NBS1) complex, which recruits ATM (Burgoyne et al., 2007; Joyce et al., 2011). Furthermore, the MRN complex is required for resection at DSB sites, originating single strand DNA (ssDNA) overhangs that are coated with the Replication Protein A (RPA) allowing for ATR displacement to the lesion site (Burgoyne et al., 2007; Joyce et al., 2011). Furthermore, ATM and ATR are known to share substrates upon activation, such as CHK2 and the histone H2Av. Once activated CHK2 is required, among other things, for the arrest of cell cycle progression. On the other hand, H2Av phosphorylation (γH2Av) in the chromatin surrounding the lesion site is believed to facilitate the access of repair proteins (Gospodinov and Herceg, 2013). In recent years, evidence has accumulated that this and other chromatin modifications are of major importance for the assembly and stabilization of the repair machinery (Gospodinov and Herceg, 2013). Moreover, ATM appears to respond to alterations in chromatin structure without requiring direct binding to DSB sites (Bakkenist and Kastan, 2003), and to be able to be activated in a MRN-independent manner (Bencokova et al.,

2009; Kaidi and Jackson, 2013), suggesting that not only DNA damage but also chromatin structure might be under ATM surveillance.

During *Drosophila* oogenesis, persistent activation of dATR and dCHK2 due to unrepaired meiotic DSBs, e.g. in *dRad54* and *dRad51* repair mutants, causes defects both in karyosome condensation and in the translation of the TGFα-like ligand GURKEN (GRK) (Ghabrial and Schüpbach, 1999; Ghabrial et al., 1998; Staeva-Vieira et al., 2003). Abnormal GRK expression affects the establishment of the dorsal-ventral polarity of the eggshell and the eggs are said to become ventralized (known as the "spindle" phenotype). These phenotypes were used by Barbosa and colleagues (2007) in a screen designed to identify genes required for meiotic progression. This screen revealed that mutations in the cohesin accessory factor *dPds5* results in the "spindle" phenotype (Barbosa et al., 2007). Based on γH2Av analysis, dPDS5 was shown to be required upon DSB induction, as would be expected from a protein required for the maintenance of sister chromatid cohesion (Vítor Barbosa, personal communication). Strikingly, through a series of epistatic analyses, it was shown that dATR was not the transducer kinase that was eliciting the DDR in these *dPds5* mutant alleles. These results led Barbosa and colleagues to propose that *dPds5* mutants activate a DDR independently of dATR (Barbosa et al., 2007).

In this chapter, we start to characterize this new meiotic checkpoint by looking for an alternative transducer kinase and for other possible proteins that might be under its surveillance.

4.2 Material and Methods

4.2.1 Fly Stock Maintenance

All *Drosophila* stocks were raised under standard conditions at 23°C, unless otherwise stated. The *dPds5*^{2} and *dPds5*^{6} alleles were obtained in a screen to unveil mutations that result in meiotic progression delay (Barbosa et al., 2007) and are described in Chapter 3; *beaf*$^{AB\text{-}KO}$ line was given by Craig Hart (Roy et al., 2007); *wapl*^{2} line (Cunningham et al., 2012) was provided by Judith Kassis; *dAtm*^{8} and the *dAtm* deficiency (*Df(3R)PG4, Ki/TM6b*, *Sb*^{1}) lines (Silva et al., 2004), *dChk2*^{p6}, *dRad51*^{003}, *dRad51*^{057} *act*Gal4 and *nos*Gal4 were already present in the lab; the *FRT101 ovo*^{D} (#1813), *MTD*Gal4 (#31777) and all TRiP RNAi lines (Table 4.1) were obtained from the Bloomington Stock Center.

Table 4.1 – TRiP line reference number and Bloomington Stock number for each of RNAi lines used.

Target Gene	TRiP Line Nr.	Vector	Bloomington Stock Nr.
BEAF32	GLV21006	VALIUM21	35642
dCHK2	GL00020	VALIUM22	35152
dCTCF (#1)	HMS02017	VALIUM20	40850
dCTCF (#2)	GL00266	VALIUM22	35354
CP190 (#1)	HMS00895	VALIUM20	33944
CP190 (#2)	HMS00845	VALIUM20	33903
SMC1	GL00558	VALIUM22	36598
SMC3	HMS00318	VALIUM20	33431
NIPPED-B	HMS00401	VALIUM20	32406
WAPL	GL00576	VALIUM22	36616
ZW5	GLV21031	VALIUM21	35666

4.2.2 Induction of germline clones and egg lays

Germline clones were induced using the FLP/FRT system (Xu & Rubin, 1993). To obtain *;dChk2^{p6} dPds5;* double mutant germline clones, y *w P{ry^{1} hs-FLP$_{22}$}; dChk2^{p6} P{w^{1} FRT42B} P{w^{1} FRT nls-GFP}/CyO, hs-hid* females were crossed with *y w P{ry^{1} hs-FLP$_{22}$}/Y; dChk2^{p6} P{w^{1} FRT 42B} dPds5$^{2\ or\ 6}$/CyO, hs hid* males. *;dPds5; dAtm^{8}* double mutant germline clones were obtained by crossing *w P{ry^{+} FLP22}; FRT42B dPds5$^{2\ or\ 6}$/CyO; FRT82B e^{1} dAtm^{8}/TM6b* females with *Y; FRT42B ovo^{D}; Df(3R)PG4,Ki/TM6b* males, these crosses were maintained at 18°C until heat-shock. *wapl^{2}* mutant germline clones were obtained by crossing *wapl^{2} FRT w^{hs} 101/FM7c;;* females with *w* ovo^{D1} v^{24} P{w$^{+mW.hs}$=FRT(w^{hs})}101/Y; P{ry$^{+t7.2}$=hsFLP}38;; males.* Three days after establishing the crosses, the adults were transferred to a new vial and after another three days the third instar larvae were heat-shocked for 1h at 37°C for two consecutive days. In the case of the *dPds5$^{2\ or\ 6}$; dAtm^{8}* double mutants, after heat-shock the crosses either were kept at 18°C or transferred to 23°C. The female flies were fattened on fresh yeast four days after eclosion and put to lay eggs on the fifth day.

4.2.3 Expression of TRiP RNAis in the female germline

To induce expression of the TRiP RNAi hairpins, females from each of the RNAi lines were crossed, at 23°C, with males from one of three drivers: the ubiquitous driver, *;;P{w^{+mC}=Act5C-GAL4}17bFO1/TM6B, Tb^{1}* (*act*GAL4), and two germline specific drivers, *w^{1118}; P{w^{+mC}=GAL4::VP16-nos.UTR}CG6325^{MVD1}* (*nos*GAL4) and *P{otu-GAL4::VP16.R}1, w*; P{GAL4-nos.NGT}40; P{GAL4::VP16-nos.UTR}CG6325^{MVD1}* (*MTD*Gal4). After five days the adults were removed and five days after eclosion the females were fattened overnight with fresh yeast

and put to lay eggs for twenty-four hours, with the plates changed after twelve hours.

4.3 Results

4.3.1 dPds5 *mutations activate a dATM-dependent DDR during oogenesis*

The first step towards unravelling the DDR elicited upon dPDS5 loss was to compare GRK expression in *dPds5* single mutant and *dChk2^{p6} dPds5* double mutant germline clones. In 70% of *dPds5^{2}* (N=60) and 80% of *dPds5^{6}* (N=45) mutant clones GRK was not detectable; however, the frequency of *dChk2^{p6} dPds5* double mutants with detectable GRK was close to control levels (*dChk2^{p6} dPds5^{2}*, N=36 and *dChk2^{p6} dPds5^{6}*, N=27) (Figure 4.1A). This rescue is similar to what can be seen for the repair mutant *dRad51$^{003/057}$* (Figure 4.1), known to activate dCHK2 through dATR (Staeva-Vieira et al., 2003). Another persistent checkpoint activation phenotype is karyosome fragmentation, that in average is present in more than 75% of the mutant clones homozygous for either *dPds5^{2}* or *dPds5^{6}*, but in less than 7.5% of their respective double mutant clones (Figure 3.9D-I). Together with the previously published results for the epistatic analysis between *dPds5* and *dAtr* (Barbosa et al., 2007), our data supports the dATR-independent and dCHK2-mediated activation of a DDR upon dPDS5 loss.

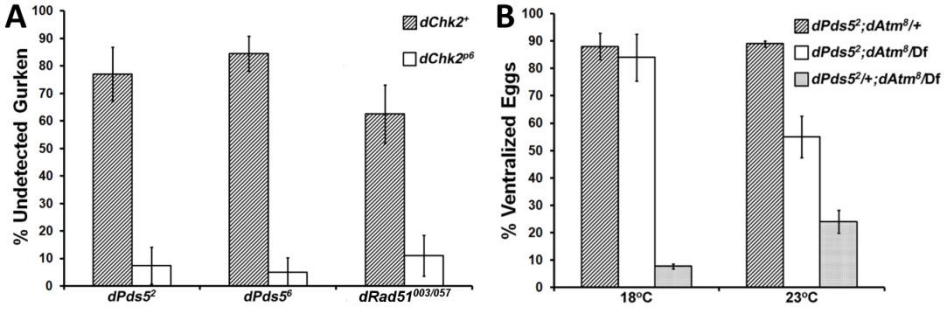

Figure 4.1 - *dPds5* mutant germline clones activate a dATM-dependent DDR. (A) Frequency of oocytes without GURKEN expression in $dPds5^{2}$ and $dPds5^{6}$ mutants, with and without the presence of an additional mutation for *dChk2* ($dChk2^{p6}$). The repair mutant $dRad51^{057/003}$ (that activates the dATR-dependent meiotic checkpoint) is also depicted under similar settings. (B) Frequency of ventralized eggs laid by females at both the permissive (18°C) and restrictive (23°C) temperature for the temperature sensitive $dAtm^{8}$ mutant allele.

The second step was to uncover the transducer kinase that monitors dPDS5 function. dATM was considered to be the most probable candidate, since dCHK2 is also a known target of this checkpoint kinase (Wood and Chen, 2008). Consequently, we produced double mutant germline clones between the *dPds5* alleles and the temperature sensitive $dAtm^{8}$ mutant allele. At 18°C (permissive temperature) $dAtm^{8}$ presents close to normal activity, while at 23°C (restrictive temperature) its activity is decreased (Silva et al., 2004). A high frequency of eggshell ventralization was seen for *dPds5;* $dAtm^{8}$ mutants raised at permissive temperature after clone induction. On the other hand, for the flies that were transferred to restrictive temperature after clone induction, a sharp decrease in the frequency of ventralized eggs is observed (Figure 4.1B). The eggshell phenotype suppression is not as evident in the *dPds5;* $dAtm^{8}$ double mutants as it is for the $dChk2^{p6}$ *dPds5* double mutants, which can be explained by the low, yet reproducible, level of eggshell ventralization that can already be seen for the $dAtm^{8}$ single mutants (Figure 4.1B). The presence of eggshell ventralization upon loss of *dAtm* was previously reported both for the

dAtm^{8} temperature sensitive allele (Joyce et al., 2011), as well as for another functional allele (*dAtm*^{6}) (Silva et al., 2004), in accordance with the results here presented.

In light of these results, we can conclude that during oogenesis, dPDS5 is under the surveillance of dATM but not of dATR.

4.3.2 The cohesin accessory protein NIPPED-B appears to be under meiotic checkpoint surveillance

In order to determine the cellular process(es) under dATM surveillance, we knocked out, by *in vivo* germline-specific RNAi (driver: *MTD*Gal4), the expression of genes related to *dPds5*. Since dPDS5 is a cohesin accessory factor and a component of insulator bodies in the oocyte, we chose as initial candidates four cohesin-related genes (*dSmc1*, *dSmc3*, *nipped-B* and *wapl*) and four insulator genes (*beaf32*, *dCtcf*, *cp190* and *zw5*). Null mutations of these genes are mostly described as being lethal, so as an initial trial for hairpin functionality we used an ubiquitous driver (*act*Gal4). To control for possible side effects of activating the RNAi pathway in the ovary, we also expressed a *mCherry* RNAi hairpin using both drivers, which leads to negligible effects on eggshell morphology, our chosen readout for persistent checkpoint activation (Figure 4.2 and Table S4.1).

Of the four cohesin-related RNAis, only *SMC3* and *NIPPED-B* hairpins were lethal when expressed under *act*Gal4, as no adults were obtained upon expression of these two hairpins (Table S4.1). Of these two, only for *NIPPED-B* RNAi did we observe an increase in the frequency of abnormal eggshells, suggestive of meiotic checkpoint activation [*Nipped-B* RNAi=53% (N=313),

mCherry RNAi=5% (N=1316); Figure 4.2 and Table S4.2]. Although the *WAPL* hairpin failed to cause either lethality or eggshell ventralization, we had available the lethal *wapl*^{2} allele for which we could induce germline clones using *ovo*^{D} *FRT101* males (Perrimon et al., 1985). After clone induction in both *wapl*^{2} and in control females (*wapl*$^{+}$), both laid a similar frequency of ventralized eggs, (*wapl*^{2}=8%, N=76 vs. *wapl*$^{+}$=5%, N=66) (Table S4.2); ruling out the possibility of checkpoint activation due to *wapl* loss.

Regarding the insulator genes, a total of six hairpins were tested (two different RNAis for *cp190* and *dCtcf*). Only the two *CP190* RNAis and one of *dCTCF* (#1) were lethal under *act*Gal4 (Table S4.1). However, for neither of these hairpins did we observe a significant increase in eggshell ventralization (Figure 4.2 and Table S4.1).

Despite the lack of an RNAi-derived phenotype for *beaf32*, we also analysed the *beaf*$^{AB\text{-}KO}$ allele. This allele is a female sterile homozygous mutant that has been shown to affect chromosome condensation in both the nurse cells and the oocyte, with egg chamber degeneration occurring around stage 7/8 (Roy et al., 2007). To determine if the meiotic checkpoint was somehow involved in this condensation phenotype, we expressed the *dCHK2* RNAi in this mutant background. However, our preliminary results suggest that abolishing the checkpoint does not rescue egg lay ability (Table S4.2). The next step would be to dissect the ovaries of these females and analyse germ cell chromatin. Yet, due to time constraints, it was not possible to perform this experiment. As a control for *dCHK2* RNAi activity, this hairpin was expressed using *Nos*Gal4 in a genetic background with persistent activation of the meiotic checkpoint (*dRad54*$^{AA/RU}$) (Abdu et al., 2002; Ghabrial et al., 1998). As expected, we observed a decrease in the frequency of ventralized eggs, indicative downregulation of dCHK2 (Table S4.2).

Globally, our preliminary results suggest that the cohesin accessory factor NIPPED-B might be under checkpoint activation.

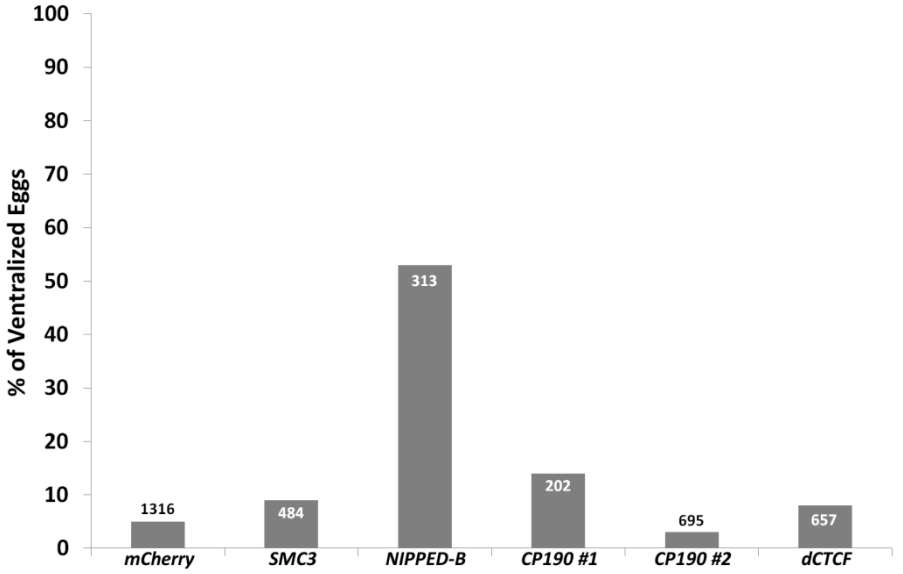

Figure 4.2 - Frequency of ventralized eggs laid by females expressing hairpins against two cohesion-related mRNAs (*smc3* and *nipped-B*) and two insulator mRNAs (c*p190* and *dCtcf*). Total number of scored eggs is listed on the top of each bar.

4.4 Discussion

In a screen designed to identify mutations that delay meiotic progression, *dPds5* mutations were found to present the typical phenotypes of persistent meiotic checkpoint activation. However, through genetic interaction assays, Barbosa and colleagues (2007) have demonstrated that while this protein is required following DSBs, it is not under dATR surveillance (Barbosa et al., 2007). In this chapter, we set out to determine the components of the DNA damage response activated in these mutants and other possible proteins under its surveillance. We show that dPDS5 is monitored by dATM in the *Drosophila* female germline and that dCHK2 is also an effector kinase for this

pathway (Figure 4.1). Our very preliminary analysis suggests that another cohesin accessory protein, NIPPED-B, might also be under meiotic checkpoint supervision (Figure 4.2).

4.4.1 dATM and dATR are transducer kinases for two parallel checkpoints in the Drosophila *ovary*

For recombination to occur during oogenesis, dSPO11 induces endogenous DSBs. The presence of these DSBs leads to the activation of a dATR-dependent DDR that, through the phosphorylation of dCHK2, results in the arrest of meiosis until repair is complete (Abdu et al., 2002; Ghabrial and Schüpbach, 1999). Work by Joyce and colleagues (2011) has recently shown that dATM is also functional during *Drosophila* oogenesis, being required in parallel with dATR for the phosphorylation of H2Av following DSB induction (Joyce et al., 2011). More specifically, they propose that while dATM is required for the restriction of the number of occurring DSBs, this kinase may not be necessary for DSB checkpoint activation. Due to the spreading of the γH2AV signal in $dAtm^{8}$ mutants coupled to the typical persistent checkpoint activation phenotypes of karyosome fragmentation and GRK misexpression, at restrictive temperature; and the fact that at permissive temperature $dAtr^{D3}$;; $dAtm^{8}$ double mutants presented a similar number of γH2Av foci to $dAtr^{D3}$ single mutants, while at restrictive temperature no γH2Av foci were observed in these double mutants (Joyce et al., 2011). In this work, we confirmed that the $dAtm^{8}$ allele does maintain a certain level of eggshell ventralization at the restrictive temperature. However, taking into account that by removing dATM we are capable of rescuing the "spindle" and karyosome fragmentation phenotypes observed in *dPds5* alleles (both still maintained in $dAtr^{D1}$; *dPds5*

double mutants), we propose that dATM acts in parallel to dATR in the *Drosophila* ovary.

The fact that dPDS5 is under the surveillance of a transducer kinase other than dATR raises the possibility that the function being monitored by dATM during oogenesis is not DSB repair and/or sister chromatid cohesion-related (further discussed in Chapter 5). As so, it would be of interest to determine if DSBs are in fact repaired in our mutant background. Even though the γH2Av signal is commonly used as a readout for DSB presence, H2Av is a target of both kinases. Therefore, in order to clarify the possible existence of functional differences between both, an alternative readout must be used. One such alternative could be the TUNEL assay. This assay is generally used to detect apoptotic cell death, and at its basis consists on the labelling of DNA strand breaks through the use of the Terminal Deoxynucleotidyl Tranferase enzyme (Gavrieli et al., 1992). Yet, the use of this assay in the *Drosophila* female germline requires significant optimization so that the penetrance of the labelling enzyme and/or of the detection reagent in the germarium is satisfactory. Another possible method would be to determine if the MRN complex is a component of the pathway triggered by dPDS5 loss. This could be performed by genetic interaction experiments between *dPds5* and components of this complex, such as *nbs1*. The MRN complex is known to detect and localize to DSBs, before recruiting ATM (Soutoglou and Misteli, 2008). However, recent work has shown that dATM can be activated independently of DSB presence and without requiring the MRN complex (Kaidi and Jackson, 2013). Hence, if dATM is found to be active during oogenesis independently of the MRN complex, this would greatly favour our hypothesis that dATM is not directly required to ensure DSB repair and that is monitoring another cellular process.

4.4.2 Both dATM and dATR DDRs converge in the activation of dCHK2

As demonstrated by the suppression of the persistent checkpoint activation phenotypes in double mutants between *dChk2* and genes that activate dATR (*dRad51* or *dRad54*) (Ghabrial and Schüpbach, 1999; Staeva-Vieira et al., 2003) and dATM (*dPds5*), activation of these two transducer kinases during oogenesis results in the phosphorylation of dCHK2.

How is it that, even though both dATM and dATR ultimately result in dCHK2 activation and both redundantly phosphorylate H2Av, only *dAtm* presents the "spindle" phenotype and karyosome defects? One possible explanation is that while dATR appears to only have functions as a checkpoint transducer in the germline, dATM might also be required to restrict the number of occurring DSBs (Joyce et al., 2011). Consequently, in the absence of dATM, germ cells might not be able to repair all DSBs, resulting in the maintenance of the checkpoint signal.

4.4.3 Two cohesin accessory proteins appear to be under meiotic checkpoint surveillance

Of the eight tested TRiP lines, only for *NIPPED*-B did we observe a phenotype. NIPPED-B is a cohesin accessory protein, required for the loading of cohesin onto chromatin, and has been shown to be involved in gene expression regulation (Misulovin et al., 2008; Rollins et al., 1999). Both characteristics make NIPPED-B a good candidate to be under dATM surveillance during oogenesis. However, since this protein is required for the loading of cohesin onto chromatin it can also be necessary for DSB repair and, hence, be under dATR surveillance. Additional work would help to elucidate this question. Namely, this phenotype should be confirmed in *nipped-B* alleles

and by performing epistatic analysis with dATR, dATM and dCHK2 to determine that it is indeed the outcome of checkpoint activation due to NIPPED-B loss. The latter experiments would also elucidate which transducer kinase is monitoring NIPPED-B function.

Both NIPPED-B and dPDS5 have been shown to regulate the expression of the *cut* gene (Dorsett et al., 2005; Rollins et al., 1999). The activation of this gene depends on a transcriptional enhancer that is located approximately 80kbp upstream of its transcription starting site. NIPPED-B has been shown to facilitate *cut* activation by regulating the binding of cohesin to the Su(Hw) insulator that localizes between the two genomic loci (Rollins et al., 1999). This suggests a cross-talk between NIPPED-B and insulators. Since both NIPPED-B and dPDS5 appear to interact with insulator proteins, and that dPDS5 is required for the proper localization of insulator proteins during oogenesis, one might expect the presence of the "spindle" phenotype when knocking-out insulator genes. This was not seen for the insulator TRiP lines here used. However, we cannot completely rule out that mutations in these genes do not lead to meiotic checkpoint activation, since the used hairpins might not be functional (*BEAF32*, *dCTCF #2* and *ZW5*) or completely abolish their expression, as we did not measure in any manner protein production after RNAi expression. Consequently, we could either try other RNAi lines, if available, obtain null mutants in a *FRT* background to generate germline clones or viable transheterozygotes and analyse eggshell morphology.

In conclusion, in this chapter we show that dATM has checkpoint functions during *Drosophila* oogenesis, via the monitoring of yet-undefined dPDS5 function(s).

Author's Contributions

Genetic interaction experiments between the *dPds5* alleles and *dChk2*^{p6} and *dAtm*^{8}, were performed by Vítor Barbosa. Eggshell phenotype analysis of the TRiP RNAi lines, *beaf*$^{AB\text{-}KO}$ and *wapl*^{2} were performed by Raquel AM Santos.

Acknowledgements

We would like to thank Craig Hart and Judith Kassis for providing mutant fly lines used in this work, as well as the TRiP at Harvard Medical School (NIH/NIGMS R01-GM084947) for providing transgenic RNAi fly stocks.

4.5 Supplemental Material

Table S4.1 – Frequency of eggs laid by females expressing either a control RNAi hairpin (mCherry), a cohesin related RNAi hairpin or an insulator RNAi hairpin. Where: WT, represents eggs with two dorsal appendages; No DA, represents egg with less than two dorsal appendages and/or collapsed; Total N, is the total number of scored eggs.

RNAi	*Act*Gal4>			MTD>		
	WT	No DA	Total N	WT	No DA	Total N
mCherry	96%	4%	489	95%	5%	1316
SMC1	83%	17%	87	95%	5%	91
SMC3	--	--	Lethal	90%	9%	484
NIPPED-B	--	--	Lethal	47%	53%	313
WAPL	89%	11%	671	93%	7%	658
BEAF32	76%	24%	420	81%	19%	427
CP190 #1	--	--	Lethal	86%	14%	202
CP190 #2	--	--	Lethal	97%	3%	695
dCTCF #1	--	--	Lethal	92%	8%	657
dCTCF #2	82%	18%	48	100%	0%	218
Zw5	89%	11%	340	78%	22%	1149

Table S4.2 - Frequency of eggs laid by *wapl*^{2} mutant females and respective controls, and *beaf*$^{AB\text{-}KO}$ and *dRad54*$^{AA/RU}$ mutants expressing either a control RNAi hairpin (mCherry) or a CHK2 RNAi hairpin under the control of the MTD driver. Where: WT, represents eggs with two dorsal appendages; No DA, represents egg with less than two dorsal appendages and/or collapsed; Total N, is the total number of scored eggs.

Genotype	WT	0 DA	Total N
wapl^{+}	97%	5%	66
wapl^{2}	92%	8%	76
beaf$^{AB\text{-}KO}$	--	--	0
beaf$^{AB\text{-}KO/CyO}$	94%	6%	142
beaf$^{AB\text{-}KO}$*;* mCherry RNAi/MTD	--	--	0
beaf$^{AB\text{-}KO}$*;* CHK2 RNAi/MTD	--	--	0
dRad54$^{AA/RU}$*;* mCherry RNAi/MTD	28%	72%	147
dRad54$^{AA/RU}$*;* CHK2 RNAi/MTD	88%	12%	348

5 Final Discussion and Concluding Remarks

In this work I set out to identify dPDS5 function(s) during oogenesis and to characterize a possible new branch of the meiotic checkpoint (or an altogether parallel pathway) that monitors this protein. In the present section, I will discuss and contextualize the main findings of the work.

5.1 dPDS5 is required for nuclear organization during oogenesis

Characterization of the dPDS5 foci during mid-oogenesis revealed their co-localization with insulator bodies - punctuate nuclear structures that result from the clustering of several chromatin insulators (Gurudatta and Corces, 2009). Insulators have been suggested to organize the eukaryotic genome into epigenetically inheritable states through the mediation of intra- and inter-chromosomal interactions (Gurudatta and Corces, 2009; Phillips and Corces, 2009). The localization of these nuclear foci during oogenesis revealed an altogether unexpected pattern: the foci were detected both in close proximity to the karyosome as well as dispersed in the nucleoplasm. Since insulator bodies are considered to assemble only in association with DNA (Gurudatta and Corces, 2009), this observation suggests the possible existence of additional genomic material in the oocyte nucleus aside from the highly condensed karyosome. On the other hand, the insulator bodies could be assembled before localizing to their specific DNA sequence, in accordance to the DNA-binding protein present. To answer this question, it should be verified if DNA can be precipitated together with the insulator proteins of the oocyte.

Throughout meiosis, chromosomes suffer a series of modifications, both morphological and epigenetic, that are important for successful gametogenesis. (Eun et al., 2010; Ivanovska and Orr-Weaver, 2006; Kimmins and Sassone-Corsi, 2005). Although insulator proteins have not been, so far, described to be involved in gametogenesis, we speculate that, together with dPDS5, they might be active players in this process. The dynamic behaviour observed for these nuclear foci also suggests that the underlying chromatin will likewise undergo reorganization at the same time. In addition, alterations in the chromatin structure of mammalian oocytes have been described to correlate with modifications in the transcriptional status of these cells (De La Fuente and Eppig, 2001). In this work, stage 5 of egg chamber development is shown to correspond to a period of transcriptional quiescence, which is also the stage where in the first dPDS5/insulator foci appear.

Both the cohesin complex and insulator proteins have been suggested to participate in both DNA loop stabilization and/or in higher order-chromatin organization by facilitating the interaction between intra- and inter-chromosomal regions (Dorsett, 2009; Dorsett and Merkenschlager, 2013; Phillips-Cremins and Corces, 2013; Remeseiro and Losada, 2013; Remeseiro et al., 2013; Vogelmann et al., 2011). In addition, at least in mammals the cohesin complex is required for the CTCF insulator to be functional (Nativio et al., 2009; Wendt et al., 2008), contrary to what is accepted to occur in *Drosophila* (Phillips-Cremins and Corces, 2013). However, our data demonstrate that the cohesin accessory protein dPDS5 is required for the proper localization of insulator proteins to the oocyte nucleus. This result would suggest that the cohesin complex itself could be involved in insulator body assembly during mid-oogenesis (Figure 5.1AB). However, when comparing the expression pattern of our dPDS5:tagged transgenes and insulator proteins with that of the

cohesin core transgenes, the latter ones do not co-localize to the nuclear foci observed between stage 5 to 10 of oogenesis. This result opens up the possibility of that dPDS5 interacts directly with the insulator proteins through its protein-protein interacting HEAT domains (Figure 5.1CD), in what would be the first described function for dPDS5 outside of the cohesin complex. This possibility should be addressed in a more direct fashion, first by determining if the insulator proteins are able to co-immunoprecipitate with cohesin core proteins from ovarian extracts and second by performing GST-pulldowns between dPDS5 and CP190.

Another open question is whether dPDS5 is required for both DNA loop stabilization (Figure 5.1AC) and insulator clustering (Figure 5.1BD) or only for insulator clustering. Again dPDS5 could perform either function with or without interacting with the cohesin complex. Taking into consideration the observed increase in size of the CP190 foci upon dPDS5 loss it might be that this latter protein is not required for the stabilization of the DNA loops themselves, but for the clustering of otherwise separated insulators. The best way to address this question would be to visualize the DNA loops themselves, both in the presence and in the absence of dPDS5.

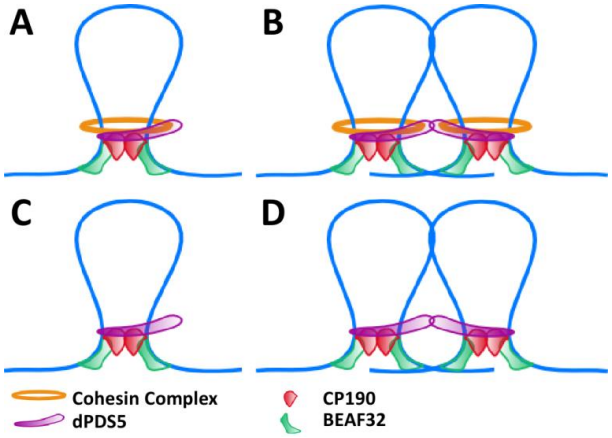

Figure 5.1 – Possible modes of interaction of dPDS5 with the insulator proteins both within a chromatin loop and between chromatin loops. (A-B) dPDS5 interacts both with the cohesin complex and the insulator proteins, both helping to stabilize loop formation (A) and bridging together otherwise separate DNA loops. (C-D) dPDS5 directly interacts with the insulator proteins through its HEAT domains (C) and also participates in the clustering of insulator complexes. DNA is represented in blue.

Our initial evidence suggested that dPDS5 loss, and consequent insulator body disorganization, also affected transcription. However, upon closer inspection, we found that whereas dPDS5 loss is indeed the direct cause for the abnormal localization of the insulator proteins, the same was not true for the observed transcriptional delay. The latter was a consequence of the persistent checkpoint activation observed in these mutants. This result uncouples transcription regulation from alterations in the chromatin structure (insulator body localization), similar to what has been shown in mouse oocytes (De La Fuente et al., 2004). Taken together, our results lead us to propose that dPDS5 is required for proper organization of the oocyte nuclear structure during mid-oogenesis.

5.2 A new meiotic dATM-dependent checkpoint

A potential function for dPDS5 during oogenesis first came to our attention due to the eggshell ventralization and karyosome fragmentation phenotypes of *dPds5* mutant germline clones (Barbosa et al., 2007). Both phenotypes are associated with the persistent activation of the canonical dATR-dependent meiotic checkpoint (Ghabrial and Schüpbach, 1999; Ghabrial et al., 1998; Staeva-Vieira et al., 2003). Interestingly, dATR was shown to not be the transducer kinase that monitors dPDS5 (Barbosa et al., 2007). Thus, an additional transducer kinase may be active during oogenesis, as previously suggested by the Schüpbach lab that found BRCA2 to be required for meiotic checkpoint signalling independently of dATR (Klovstad et al., 2008). Indeed, our data shows that dPDS5 is under dATM surveillance. Moreover, the activation of this kinase converges in the recruitment of the effector kinase dCHK2 that is also a component of the canonical meiotic DDR, hence the appearance of the same phenotypes upon persistent activation of either transducer kinase (Figure 5.2).

The cellular process that is under dATM surveillance is still not known. From the work here presented we know that dATM is monitoring dPDS5 function during oogenesis. Moreover, from work previously published by Barbosa and colleagues (2007), we know that dPDS5 is required upon DSBs, since *dSpo11 dPds5* double mutants rescue the eggshell ventralization phenotype (Barbosa et al., 2007). Moreover, the work here presented, shows that dPDS5 is required during mid-oogenesis for proper insulator protein localization. These results open two possible cellular processes to be under dATM surveillance: 1, completion of DSB repair (Figure 5.2A) and 2, proper high-order chromatin organization of the oocyte nucleus (Figure 5.2B). The work of Klovstad and colleagues (2008) had previously shown that a dATR

independent meiotic DSB signalling pathway is present during *Drosophila* oogenesis. The typical persistent meiotic checkpoint activation phenotypes of eggshell ventralization and karyosome fragmentation are present in *brca2* mutants. These phenotypes are rescued in double mutants between *brca2* and *mei-p22* or *dChk2*, but not in *dAtr;; brca2* (Klovstad et al., 2008), a result similar to the ones presented here for *dPds5* mutants. In addition, it was shown that double mutants *brca2* with other repair mutants (e.g., *dRad51*, *dRad54* and *spnD*) result in a strong rescue of the ventralization and karyosome fragmentation phenotypes (Klovstad et al., 2008). Considering that *dPds5* mutants still maintain γH2Av signalling in region 3 of the germarium (Vítor Barbosa, personal communication) and that dPDS5 is required upon DSBs (Barbosa et al., 2007), it is conceivable that this protein may be required for DSB repair and that this is the function dATM is surveilling. The fact that PDS5 has been shown to be required for meiotic DSB repair in yeast (Jin et al., 2009) further supports this hypothesis. Moreover, H2Av has been shown to be redundantly phosphorylated by dATR and the dATM in *Drosophila* germaria upon DSB induction (Joyce et al., 2011). These results suggest that dATR and dATM can have at least partially redundant functions in DSB repair signalling during oogenesis (Figure 5.2A). For a better understanding of this question, the progression of DSB repair should be monitored in mutants that activate either of the kinases (as discussed in chapter 4). Furthermore, it would be interesting to determine if BRCA2 is also part of the pathway that monitors dPDS5.

Our second hypothesis is that dATM is monitoring the nuclear organization of the oocyte through dPDS5 during mid-oogenesis (Figure 5.2B). The fact that dPDS5 function is not under dATR surveillance could imply that a role other than DSB repair is activating the dATM-dependent DDR. Additionally, previous studies suggest that while dATM is required to restrict the number of occurring DSBs it is not required for the activation and/or maintenance of the canonical

meiotic checkpoint that monitors DSB repair (Joyce et al., 2011). Furthermore, in recent years, additional roles have been proposed for ATM other than DDR activation upon DSB detection, namely in response to genotoxic stresses (*e.g.*, hypoxia, hyperthermia, replication stress and treatments with chloroquine) and even in homeostasis maintenance (Shiloh and Ziv, 2013). Moreover, work by Kaidi and Jackson (2013) shows that phosphorylation of the acetyltransferase KAT5 increases upon DNA damage, which in turn promotes ATM acetylation and thus DDR activation. Interestingly, ATM signalling and KAT5 phosphorylation are also enhanced in the presence of chromatin alterations, and this ATM response appears to be MRN independent. This argues for a possible independence of DSB repair to activate an ATM-dependent response (Kaidi and Jackson, 2013). These studies further underscore our hypothesis of a dATM-dependent DDR in response to improper chromatin organization during mid-oogenesis (Figure 5.2B).

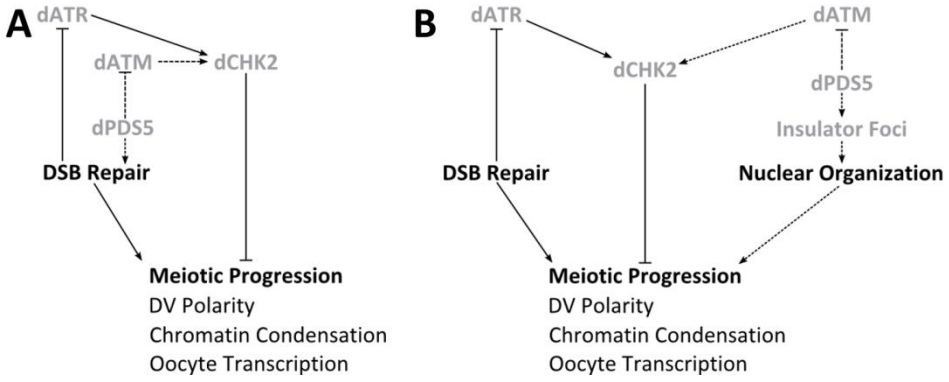

Figure 5.2 – dATR and dATM activate parallel meiotic DDRs during oogenesis. (A) dATR and dATM are both active in the germarium where they have partially redundant functions in response to endogenous DSBs during oogenesis. dATM, but not dATR, monitors dPDS5 function in DSB repair. (B) dATR responds to the endogenous DSBs induced in the germarium, while dATM monitors the oocyte nuclear organization during mid-oogenesis, through the function of dPDS5 in proper assembly of insulator foci. In either case, activation of both kinases converges to the activation of the effector kinase dCHK2 that will arrest meiotic progression, which is required for proper dorsal-ventral polarity of the eggshell, karyosome condensation and initiation of oocyte transcription in stage 7/8.

5.3 Concluding Remarks

This Ph.D. thesis provides new data on chromatin-related requirements for a successful completion of meiosis, as well as on the mechanisms germ cells employ to safeguard chromatin integrity. dPDS5, a cohesin accessory factor, was shown to be required for the proper localization of insulator proteins during *Drosophila* egg development. Until now, cohesin proteins were thought not to be required for insulator function in *Drosophila*. This interaction is not only suggestive of a role for dPDS5 in oocyte chromatin organization, but also of the necessity of a proper nuclear structure for the successful completion of meiosis. Further work will help elucidate if dPDS5 is the only cohesion-related protein involved in this process and if it occurs independently of the cohesin complex. Our preliminary data suggest that a second cohesin accessory protein, NIPPED-B, might also be under checkpoint surveillance in the oocyte.

A great deal of work is necessary to get a more accurate understanding of this dATM-dependent checkpoint. Namely, other proteins required for pathway signalling should be identified to determine how much overlap there is with the dATR pathway and also to elucidate the actual cellular process that is being monitored. The identification of other proteins that could be under dATM surveillance would also facilitate this understanding.

References

Abdu, U., Brodsky, M., and Schüpbach, T. (2002). Activation of a meiotic checkpoint during Drosophila oogenesis regulates the translation of Gurken through Chk2/Mnk. Curr. Biol. *12*, 1645–1651.

Ashburner, M., Golic, K.G., and Hawley, R.S. (2005). Female Meiosis. In Drosophila: A Laboratory Hanbook, M. Ashburner, K.G. Golic, and R.S. Hawley, eds. (New York: Cold Spring Harbour Press), pp. 757–826.

Bakkenist, C.J., and Kastan, M.B. (2003). DNA damage activates ATM through intermolecular autophosphorylation and dimer dissociation. Nature *421*, 499–506.

Barbosa, V., Kimm, N., and Lehmann, R. (2007). A maternal screen for genes regulating Drosophila oocyte polarity uncovers new steps in meiotic progression. Genetics *176*, 1967–1977.

Bartkuhn, M., Straub, T., Herold, M., Herrmann, M., Rathke, C., Saumweber, H., Gilfillan, G.D., Becker, P.B., and Renkawitz, R. (2009). Active promoters and insulators are marked by the centrosomal protein 190. EMBO J. *28*, 877–888.

Baxley, R.M., Soshnev, A.A., Koryakov, D.E., Zhimulev, I.F., and Geyer, P.K. (2011). The role of the Suppressor of Hairy-wing insulator protein in Drosophila oogenesis. Dev. Biol. *356*, 398–410.

Bencokova, Z., Kaufmann, M.R., Pires, I.M., Lecane, P.S., Giaccia, A.J., and Hammond, E.M. (2009). ATM activation and signaling under hypoxic conditions. Mol. Cell. Biol. *29*, 526–537.

Benoit, B., Nemeth, A., Aulner, N., Kühn, U., Simonelig, M., Wahle, E., and Bourbon, H.M. (1999). The Drosophila poly(A)-binding protein II is ubiquitous throughout Drosophila development and has the same function in mRNA polyadenylation as its bovine homolog in vitro. Nucleic Acids Res. *27*, 3771–3778.

Blanton, J., Gaszner, M., and Schedl, P. (2003). Protein:protein interactions and the pairing of boundary elements in vivo. Genes Dev. *17*, 664–675.

Bortle, K. Van, Ramos, E., Takenaka, N., Yang, J., Wahi, J.E., and Corces, V.G. (2012). Drosophila CTCF tandemly aligns with other insulator proteins at the borders of H3K27me3 domains. Genome Res. *22*, 2176–2187.

Van Bortle, K., and Corces, V.G. (2012). Nuclear organization and genome function. Annu. Rev. Cell Dev. Biol. *28*, 163–187.

Van Bortle, K., and Corces, V.G. (2013). The role of chromatin insulators in nuclear architecture and genome function. Curr. Opin. Genet. Dev. *23*, 212–218.

Burgoyne, P.S., Mahadevaiah, S.K., and Turner, J.M. a (2007). The management of DNA double-strand breaks in mitotic G2, and in mammalian meiosis viewed from a mitotic G2 perspective. Bioessays *29*, 974–986.

Butcher, R.D.J., Chodagam, S., Basto, R., Wakefield, J.G., Henderson, D.S., Raff, J.W., and Whitfield, W.G.F. (2004). The Drosophila centrosome-associated protein CP190 is essential for viability but not for cell division. J. Cell Sci. *117*, 1191–1199.

Byrd, K., and Corces, V.G. (2003). Visualization of chromatin domains created by the gypsy insulator of Drosophila. J. Cell Biol. *162*, 565–574.

Carpenter, A.T.C. (1975). Electron Microscopy of Meiosis in Drosophila melanogaster Females I. Structure, Arrangement, and Temporal Change of the Synaptonemal Complex in Wild-type. Chromosoma *182*, 157–182.

Chan, K.-L., Roig, M.B., Hu, B., Beckouët, F., Metson, J., and Nasmyth, K. (2012). Cohesin's DNA exit gate is distinct from its entrance gate and is regulated by acetylation. Cell *150*, 961–974.

Chan, K.-L., Gligoris, T., Upcher, W., Kato, Y., Shirahige, K., Nasmyth, K., and Beckouët, F. (2013). Pds5 promotes and protects cohesin acetylation. Proc. Natl. Acad. Sci. U. S. A. *110*, 13020–13025.

Cooperstock, R.L., and Lipshitz, H.D. (2001). RNA localization and translational regulation during axis specification in the Drosophila oocyte. Int. Rev. Cytol. *203*, 541–566.

Cunningham, M.D., Gause, M., Cheng, Y., Noyes, A., Dorsett, D., Kennison, J. a, and Kassis, J. a (2012). Wapl antagonizes cohesin binding and promotes Polycomb-group silencing in Drosophila. Development *139*, 4172–4179.

Dävring, L., and Sunner, M. (1982). A lampbrush phase in oocytes of Drosophila and its bearing upon mutagen sensitivity data. Hereditas *259*, 247–259.

Dorsett, D. (2009). Cohesin, gene expression and development: lessons from Drosophila. Chromosome Res. *17*, 185–200.

Dorsett, D. (2011). Cohesin: genomic insights into controlling gene transcription and development. Curr. Opin. Genet. Dev. *21*, 199–206.

Dorsett, D., and Merkenschlager, M. (2013). Cohesin at active genes: a unifying theme for cohesin and gene expression from model organisms to humans. Curr. Opin. Cell Biol. *25*, 327–333.

Dorsett, D., and Ström, L. (2012). The ancient and evolving roles of cohesin in gene expression and DNA repair. Curr. Biol. *22*, R240–50.

Dorsett, D., Eissenberg, J.C., Misulovin, Z., Martens, A., Redding, B., and McKim, K. (2005). Effects of sister chromatid cohesion proteins on cut gene expression during wing development in Drosophila. Development *132*, 4743–4753.

Eichinger, C.S., Kurze, A., Oliveira, R.A., and Nasmyth, K. (2013). Disengaging the Smc3/kleisin interface releases cohesin from Drosophila chromosomes during interphase and mitosis. EMBO J. *32*, 656–665.

Eun, S.H., Gan, Q., and Chen, X. (2010). Epigenetic regulation of germ cell differentiation. Curr. Opin. Cell Biol. *22*, 737–743.

Gause, M., Morcillo, P., and Dorsett, D. (2001). Insulation of Enhancer-Promoter Communication by a Gypsy Transposon Insert in the Drosophila cut Gene : Cooperation between Suppressor of Hairy-wing and Modifier of mdg4 Proteins Insulation of Enhancer-Promoter Communication by a Gypsy Transposon Insert i. Mol. Cell. Biol. *21*, 4807–4817.

Gause, M., Webber, H. a, Misulovin, Z., Haller, G., Rollins, R. a, Eissenberg, J.C., Bickel, S.E., and Dorsett, D. (2008). Functional links between Drosophila Nipped-B and cohesin in somatic and meiotic cells. Chromosoma *117*, 51–66.

Gavrieli, Y., Sherman, Y., and Ben-Sasson, S. a (1992). Identification of programmed cell death in situ via specific labeling of nuclear DNA fragmentation. J. Cell Biol. *119*, 493–501.

Gerasimova, T.I., Gdula, D. a, Gerasimov, D. V, Simonova, O., and Corces, V.G. (1995). A Drosophila protein that imparts directionality on a chromatin insulator is an enhancer of position-effect variegation. Cell *82*, 587–597.

Gerasimova, T.I., Lei, E.P., Bushey, A.M., and Corces, V.G. (2007). Coordinated control of dCTCF and gypsy chromatin insulators in Drosophila. Mol. Cell *28*, 761–772.

Ghabrial, A., and Schüpbach, T. (1999). Activation of a meiotic checkpoint regulates translation of Gurken during Drosophila oogenesis. Nat. Cell Biol. *1*, 354–357.

Ghabrial, A., Ray, R.P., and Schüpbach, T. (1998). okra and spindle-B encode components of the RAD52 DNA repair pathway and affect meiosis and patterning in Drosophila oogenesis. Genes Dev. *12*, 2711–2723.

Ghosh, D., Gerasimova, T.I., and Corces, V.G. (2001). Interactions between the Su(Hw) and Mod(mdg4) proteins required for gypsy insulator function. EMBO J. *20*, 2518–2527.

Gospodinov, A., and Herceg, Z. (2013). Shaping chromatin for repair. Mutat. Res. *752*, 45–60.

Gurudatta, B. V, and Corces, V.G. (2009). Chromatin insulators: lessons from the fly. Brief. Funct. Genomic. Proteomic. *8*, 276–282.

Gurudatta, B. V, Yang, J., Van Bortle, K., Donlin-Asp, P.G., and Corces, V.G. (2013). Dynamic changes in the genomic localization of DNA replication-related element binding factor during the cell cycle. Cell Cycle *12*, 1605–1615.

Harper, J.W., and Elledge, S.J. (2007). The DNA damage response: ten years after. Mol. Cell *28*, 739–745.

Heidmann, D., Horn, S., Heidmann, S., Schleiffer, A., Nasmyth, K., and Lehner, C.F. (2004). The Drosophila meiotic kleisin C(2)M functions before the meiotic divisions. Chromosoma *113*, 177–187.

Hou, C., Li, L., Qin, Z.S., and Corces, V.G. (2012). Gene density, transcription, and insulators contribute to the partition of the Drosophila genome into physical domains. Mol. Cell *48*, 471–484.

Ivanovska, I., and Orr-Weaver, T.L. (2006). Histone modifications and the chromatin scaffold for meiotic chromosome architecture. Cell Cycle *5*, 2064–2071.

Jin, H., Guacci, V., and Yu, H.-G. (2009). Pds5 is required for homologue pairing and inhibits synapsis of sister chromatids during yeast meiosis. J. Cell Biol. *186*, 713–725.

Joyce, E.F., and McKim, K.S. (2011). Meiotic checkpoints and the interchromosomal effect on crossing over in Drosophila females. Fly (Austin). *5*, 134–141.

Joyce, E.F., Pedersen, M., Tiong, S., White-Brown, S.K., Paul, A., Campbell, S.D., and McKim, K.S. (2011). Drosophila ATM and ATR have distinct activities in the regulation of meiotic DNA damage and repair. J. Cell Biol. *195*, 359–367.

Kagey, M.H., Newman, J.J., Bilodeau, S., Zhan, Y., Orlando, D. a, van Berkum, N.L., Ebmeier, C.C., Goossens, J., Rahl, P.B., Levine, S.S., et al. (2010). Mediator and cohesin connect gene expression and chromatin architecture. Nature *467*, 430–435.

Kaidi, A., and Jackson, S.P. (2013). KAT5 tyrosine phosphorylation couples chromatin sensing to ATM signalling. Nature *498*, 70–74.

Keeney, S. (2008). Spo11 and the Formation of DNA Double-Strand Breaks in Meiosis. In Recombination and Meiosis: Crossing-Over and Disjunction, R. Egel, and D.-H. Lankenau, eds. (Springer Berlin Heidelberg), pp. 81–123.

Khetani, R.S., and Bickel, S.E. (2007). Regulation of meiotic cohesion and chromosome core morphogenesis during pachytene in Drosophila oocytes. J. Cell Sci. *120*, 3123–3137.

Kimmins, S., and Sassone-Corsi, P. (2005). Chromatin remodelling and epigenetic features of germ cells. Nature *434*, 583–589.

King, R.C. (1970). Ovarian Development in Drosophila melanogaster. (New York: Academic Press).

Klovstad, M., Abdu, U., and Schüpbach, T. (2008). Drosophila brca2 is required for mitotic and meiotic DNA repair and efficient activation of the meiotic recombination checkpoint. PLoS Genet. *4*, e31.

Kruhlak, M., Crouch, E.E., Orlov, M., Montaño, C., Gorski, S. a, Nussenzweig, A., Misteli, T., Phair, R.D., and Casellas, R. (2007). The ATM repair pathway inhibits RNA polymerase I transcription in response to chromosome breaks. Nature *447*, 730–734.

Kueng, S., Hegemann, B., Peters, B.H., Lipp, J.J., Schleiffer, A., Mechtler, K., and Peters, J.-M. (2006). Wapl controls the dynamic association of cohesin with chromatin. Cell *127*, 955–967.

De La Fuente, R., and Eppig, J.J. (2001). Transcriptional activity of the mouse oocyte genome: companion granulosa cells modulate transcription and chromatin remodeling. Dev. Biol. *229*, 224–236.

De La Fuente, R., Viveiros, M.M., Burns, K.H., Adashi, E.Y., Matzuk, M.M., and Eppig, J.J. (2004). Major chromatin remodeling in the germinal vesicle (GV) of mammalian oocytes is dispensable for global transcriptional silencing but required for centromeric heterochromatin function. Dev. Biol. *275*, 447–458.

Lake, C.M., and Hawley, R.S. (2012). The molecular control of meiotic chromosomal behavior: events in early meiotic prophase in Drosophila oocytes. Annu. Rev. Physiol. *74*, 425–451.

Lancaster, O.M., Breuer, M., Cullen, C.F., Ito, T., and Ohkura, H. (2010). The meiotic recombination checkpoint suppresses NHK-1 kinase to prevent reorganisation of the oocyte nucleus in Drosophila. PLoS Genet. *6*, e1001179.

Mahowald, A.P., and Tiefert, M. (1970). Fine Structural Changes in the Drosophila Oocyte Nucleus during a Short Period of RNA Synthesis: An Autoradiographic and Ultrastructural Study of RNA Synthesis in in the Oocyte Nucleus of Drosophila. Wilhelm Roux' Arch. *165*, 8–25.

Manheim, E. a, and McKim, K.S. (2003). The Synaptonemal complex component C(2)M regulates meiotic crossing over in Drosophila. Curr. Biol. *13*, 276–285.

Mehrotra, S., and McKim, K.S. (2006). Temporal analysis of meiotic DNA double-strand break formation and repair in Drosophila females. PLoS Genet. *2*, e200.

Melnikova, L., Juge, F., Gruzdeva, N., Mazur, A., Cavalli, G., and Georgiev, P. (2004). Interaction between the GAGA factor and Mod(mdg4) proteins promotes insulator bypass in Drosophila. Proc. Natl. Acad. Sci. U. S. A. *101*, 14806–14811.

Misulovin, Z., Schwartz, Y.B., Li, X.-Y., Kahn, T.G., Gause, M., MacArthur, S., Fay, J.C., Eisen, M.B., Pirrotta, V., Biggin, M.D., et al. (2008). Association of cohesin and Nipped-B with transcriptionally active regions of the Drosophila melanogaster genome. Chromosoma *117*, 89–102.

Morin, X., Daneman, R., Zavortink, M., and Chia, W. (2001). A protein trap strategy to detect GFP-tagged proteins expressed from their endogenous loci in Drosophila. Proc. Natl. Acad. Sci. U. S. A. *98*, 15050–15055.

Nasmyth, K. (2011). Cohesin: a catenase with separate entry and exit gates? Nat. Cell Biol. *13*, 1170–1177.

Nasmyth, K., and Haering, C.H. (2005). The structure and function of SMC and kleisin complexes. Annu. Rev. Biochem. *74*, 595–648.

Nasmyth, K., and Haering, C.H. (2009). Cohesin: its roles and mechanisms. Annu. Rev. Genet. *43*, 525–558.

Nativio, R., Wendt, K.S., Ito, Y., Huddleston, J.E., Uribe-Lewis, S., Woodfine, K., Krueger, C., Reik, W., Peters, J.-M., and Murrell, A. (2009). Cohesin is required for higher-order chromatin conformation at the imprinted IGF2-H19 locus. PLoS Genet. *5*, e1000739.

Navarro, C., Puthalakath, H., Adams, J.M., Strasser, A., and Lehmann, R. (2004). Egalitarian binds dynein light chain to establish oocyte polarity and maintain oocyte fate. Nat. Cell Biol. *6*, 427–435.

Pai, C.-Y., Lei, E.P., Ghosh, D., and Corces, V.G. (2004). The centrosomal protein CP190 is a component of the gypsy chromatin insulator. Mol. Cell *16*, 737–748.

Pauli, A., Althoff, F., Oliveira, R.A., Heidmann, S., Schuldiner, O., Lehner, C.F., Dickson, B.J., and Nasmyth, K. (2008). Cell-type-specific TEV protease cleavage reveals cohesin functions in Drosophila neurons. Dev. Cell *14*, 239–251.

Perrimon, N., Engstrom, L., and Mahowald, a P. (1985). Developmental genetics of the 2C-D region of the Drosophila X chromosome. Genetics *111*, 23–41.

Petronczki, M., Siomos, M.F., and Nasmyth, K. (2003). Un Ménage à Quatre: The Molecular Biology of Chromosome Segregation in Meiosis. Cell *112*, 423–440.

Phillips, J.E., and Corces, V.G. (2009). CTCF: master weaver of the genome. Cell *137*, 1194–1211.

Phillips-Cremins, J.E., and Corces, V.G. (2013). Chromatin insulators: linking genome organization to cellular function. Mol. Cell *50*, 461–474.

Polo, S.E., and Jackson, S.P. (2011). Dynamics of DNA damage response proteins at DNA breaks: a focus on protein modifications. Genes Dev. *25*, 409–433.

Price, B.D., and D'Andrea, A.D. (2013). Chromatin remodeling at DNA double-strand breaks. Cell *152*, 1344–1354.

Remeseiro, S., and Losada, A. (2013). Cohesin, a chromatin engagement ring. Curr. Opin. Cell Biol. *25*, 63–71.

Remeseiro, S., Cuadrado, A., and Losada, A. (2013). Cohesin in development and disease. Development *140*, 3715–3718.

Rollins, R.A., Morcillo, P., and Dorsett, D. (1999). Nipped-B, a Drosophila Homologue of Chromosomal Adherins, Participates in Activation by Remote Enhancers in the cut and Ultrabithorax Genes Robert. Genetics *152*, 577–593.

Roy, S., Gilbert, M.K., and Hart, C.M. (2007). Characterization of BEAF mutations isolated by homologous recombination in Drosophila. Genetics *176*, 801–813.

Schaaf, C. a, Kwak, H., Koenig, A., Misulovin, Z., Gohara, D.W., Watson, A., Zhou, Y., Lis, J.T., and Dorsett, D. (2013). Genome-wide control of RNA polymerase II activity by cohesin. PLoS Genet. *9*, e1003382.

Sexton, T., Yaffe, E., Kenigsberg, E., Bantignies, F., Leblanc, B., Hoichman, M., Parrinello, H., Tanay, A., and Cavalli, G. (2012). Three-dimensional folding and functional organization principles of the Drosophila genome. Cell *148*, 458–472.

Shanbhag, N.M., Rafalska-Metcalf, I.U., Balane-Bolivar, C., Janicki, S.M., and Greenberg, R. a (2010). ATM-dependent chromatin changes silence transcription in cis to DNA double-strand breaks. Cell *141*, 970–981.

Shiloh, Y., and Ziv, Y. (2013). The ATM protein kinase: regulating the cellular response to genotoxic stress, and more. Nat. Rev. Mol. Cell Biol. *14*, 197–210.

Silva, E., Tiong, S., Pedersen, M., Homola, E., Royou, A., Fasulo, B., Siriaco, G., and Campbell, S.D. (2004). ATM is required for telomere maintenance and chromosome stability during Drosophila development. Curr. Biol. *14*, 1341–1347.

Soutoglou, E., and Misteli, T. (2008). Activation of the cellular DNA damage response in the absence of DNA lesions. Science *320*, 1507–1510.

Spradling, A.C. (1993). Developmental Genetics of Oogenesis. In The Development of Drosophila Melanogaster, M. Bate, and A. Martinez Arias, eds. (Cold Spring Harbour Press), pp. 1–70.

Staeva-Vieira, E., Yoo, S., and Lehmann, R. (2003). An essential role of DmRad51/SpnA in DNA repair and meiotic checkpoint control. EMBO J. *22*, 5863–5874.

Von Stetina, J.R., and Orr-Weaver, T.L. (2011). Developmental control of oocyte maturation and egg activation in metazoan models. Cold Spring Harb. Perspect. Biol. *3*, a005553.

Tsai, J.-H., and McKee, B.D. (2011). Homologous pairing and the role of pairing centers in meiosis. J. Cell Sci. *124*, 1955–1963.

Vaur, S., Feytout, A., Vazquez, S., and Javerzat, J.-P. (2012). Pds5 promotes cohesin acetylation and stable cohesin-chromosome interaction. EMBO Rep. *13*, 645–652.

Vernì, F., Gandhi, R., Goldberg, M.L., and Gatti, M. (2000). Genetic and molecular analysis of wings apart-like (wapl), a gene controlling heterochromatin organization in Drosophila melanogaster. Genetics *154*, 1693–1710.

Vogelmann, J., Valeri, A., Guillou, E., Cuvier, O., and Nollmann, M. (2011). Roles of chromatin insulator proteins in higher-order chromatin organization and transcription regulation. Nucleus *2*, 358–369.

Webber, H. a, Howard, L., and Bickel, S.E. (2004). The cohesion protein ORD is required for homologue bias during meiotic recombination. J. Cell Biol. *164*, 819–829.

Wendt, K.S., Yoshida, K., Itoh, T., Bando, M., Koch, B., Schirghuber, E., Tsutsumi, S., Nagae, G., Ishihara, K., Mishiro, T., et al. (2008). Cohesin mediates transcriptional insulation by CCCTC-binding factor. Nature *451*, 796–801.

White-Cooper, H., and Davidson, I. (2011). Unique aspects of transcription regulation in male germ cells. Cold Spring Harb. Perspect. Biol. *3*, 3:a002626.

Whitfield, W.G., Millar, S.E., Saumweber, H., Frasch, M., and Glover, D.M. (1988). Cloning of a gene encoding an antigen associated with the centrosome in Drosophila. J. Cell Sci. *89*, 467–480.

Wood, J.L., and Chen, J. (2008). DNA-damage checkpoints: location, location, location. Trends Cell Biol. *18*, 451–455.

Yan, R., and McKee, B.D. (2013). The cohesion protein SOLO associates with SMC1 and is required for synapsis, recombination, homolog bias and cohesion and pairing of centromeres in Drosophila Meiosis. PLoS Genet. *9*, e1003637.

Yang, J., Ramos, E., and Corces, V.G. (2012). The BEAF-32 insulator coordinates genome organization and function during the evolution of Drosophila species. Genome Res. *22*, 2199–2207.

Yanowitz, J. (2010). Meiosis: making a break for it. Curr. Opin. Cell Biol. *22*, 744–751.

Abbreviation List

AE, Axial Element

ATM, Ataxia Telangiectasia-Mutated

ATR, Ataxia Telangiectasia-Related

BEAF32, Boundary-Element Associated Factor of 32 kDa

CE, Central Element

CONA, Corona

CP190, Centrosomal Protein 190kDa

CR, Central Region

C(2)M, Crossover Suppressor on 2 of Manheim

C(3)G, Crossover Suppressor on 3 of Gowen

dCTCF, *Drosophila* CCCTC-binding factor

DDR, DNA Damage Response

DSB, Double Strand Break

EGFR, Epidermal Growth Factor Receptor

GAGA/TRL, GAGA factor/Trithorax-like

GC, Germline Cell

GRK, Gurken

FC, Follicule Cell

GSC, Germline Stem Cell

LE, Lateral Element

ORD, Orientation Disruptor

MEI-W68, Meiotic W68

Mod(mdg4), Modifier of Modg4

MRN, MRE11- RAD50-NBS1

NC, Nurse Cell

PI3, Phosphatidylinositol-4,5-bisphosphate 3-kinase

RPA, Replication Protein A

SC, Synaptonemal Complex

SMC, Structural Maintenance Chromosome

SPO11, Sporulation-Specific Protein 11

ssDNA, single stranded DNA

SuHw, Supressor of Hairy-Wing

TF, Transverse Filament

TGF-α, Transforming Growth Factor-α

Zw5, Zeste-White 5